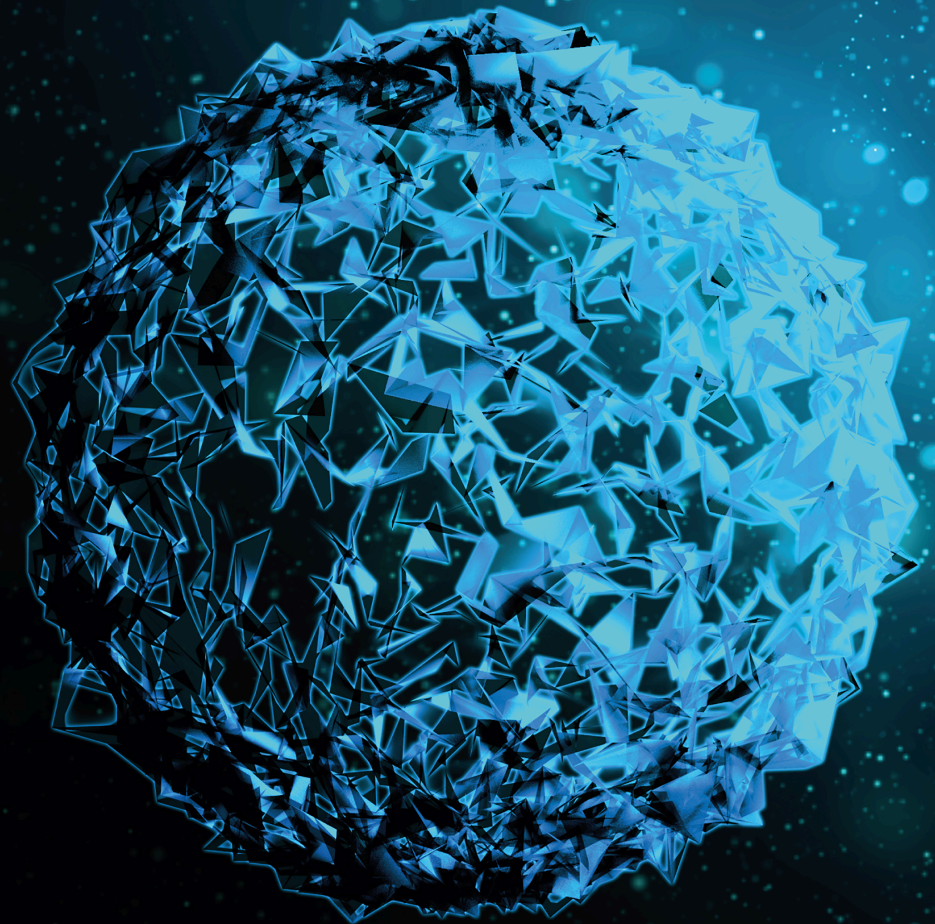


The Threat of Antibiotics and Heavy Metal Pollution to Human Health and Potential Solutions

Lead Guest Editor: Peng Bao

Guest Editors: Xiu-Li Gao and Guo-qi Wen





The Threat of Antibiotics and Heavy Metal Pollution to Human Health and Potential Solutions

BioMed Research International

The Threat of Antibiotics and Heavy Metal Pollution to Human Health and Potential Solutions

Lead Guest Editor: Peng Bao

Guest Editors: Xiu-Li Gao and Guo-qi Wen



Copyright © 2020 Hindawi Limited. All rights reserved.

This is a special issue published in "BioMed Research International." All articles are open access articles distributed under the Creative Commons Attribution License, which permits unrestricted use, distribution, and reproduction in any medium, provided the original work is properly cited.

Editorial Board

Shahrzad Bazargan-Hejazi, PhD, USA

Vance W Berger, USA

Luenda Charles, USA

Reinie Cordier, Australia

Peter P. Egeghy, USA

Antonella Gigantesco, Italy

Kumud K. Kafle, Nepal

Anna Karakatsani, Greece

Sadik A. Khuder, USA

Barthélémy Kuate Defo, Canada

Blanca Laffon, Spain

Xavier Nsabagasani, Uganda

Mangesh S. Pednekar, India

Hynek Pikhart, United Kingdom

Abdelaziz M. Thabet, Palestinian Authority

Komla Tsey, Australia

Contents

The Threat of Antibiotics and Heavy Metal Pollution to Human Health and Potential Solutions

Peng Bao , Xiu-Li Gao, and Guo-Qi Wen 


Editorial (2 pages), Article ID 8730406, Volume 2020 (2020)

Efficacy of Neoadjuvant Chemotherapy with Epirubicin and Cyclophosphamide and Weekly Paclitaxel and Trastuzumab in Human Epidermal Growth Factor Receptor 2-Positive Breast Carcinoma: A Real-World Study

Mengmeng Zhang, Ling Li, Shiyong Zhang, Wenlong Zhu, Senguo Yang, Guangsheng Di, Xiaoxia Ma, and Haisong Yang 




Research Article (9 pages), Article ID 3208391, Volume 2020 (2020)

Alkyl Thiourea Functionalised Silica for the Effective Removal of Heavy Metals from Acanthopanax senticosus Extract

Hong-Li Guo, Shuo Zhang, Christopher North, Min Zhang, Xiao-xia Meng, and Xiu-Li Gao 


Research Article (10 pages), Article ID 9860425, Volume 2020 (2020)

Abundance of Multidrug Resistance Efflux Pumps in the Urinary Metagenome of Kidney Transplant Patients

Asha Rani , Ravi Ranjan , Ahmed A. Metwally, Daniel C. Brennan, Patricia W. Finn, and David L. Perkins 


Research Article (9 pages), Article ID 5421269, Volume 2020 (2020)

Application of Quality Control Circle in Promoting the Use of Rubber Dams in the Root Canal Treatment of Primary Teeth

Fang Jingxian , Liu Yang, Liu Qiong, Qian Hong, Liu Hedi, Zhang Jinglan, Liu Fang, Yang Jing, Wu Xiaoming, and Song Yingying


Research Article (5 pages), Article ID 5397838, Volume 2020 (2020)

Outcome of Gynecologic Laparoendoscopic Single-Site Surgery with a Homemade Device and Conventional Laparoscopic Instruments in a Chinese Teaching Hospital

Xianghui Su, Xiaolong Jin, Canliang Wen, Qiong Xu, Chunfang Cai, Zhuohui Zhong, and Xiang Tang 




Research Article (4 pages), Article ID 5373927, Volume 2020 (2020)

Treatment of Large and Complicated Scalp Defects with Free Flap Transfer

Fanfan Chen, Hongbin Ju, Anfei Huang, Yongjun Yi, Yongfu Cao, Wei Xie, Xinliang Wang , and Guo Fu 

Research Article (6 pages), Article ID 2748219, Volume 2020 (2020)

Cardiac Contractility Modulation Attenuates Chronic Heart Failure in a Rabbit Model via the PI3K/AKT Pathway

Qingqing Hao , Feifei Zhang, Yudan Wang, Yingxiao Li , and Xiaoyong Qi 

Research Article (8 pages), Article ID 1625362, Volume 2020 (2020)

Effect of Metformin on a Preeclampsia-Like Mouse Model Induced by High-Fat Diet

Fuchuan Wang , Guangming Cao, Wei Yi, Li Li, and Xiuzhen Cao

Research Article (8 pages), Article ID 6547019, Volume 2019 (2019)

Editorial

The Threat of Antibiotics and Heavy Metal Pollution to Human Health and Potential Solutions

Peng Bao ¹, Xiu-Li Gao,² and Guo-Qi Wen ³

¹Key Lab of Urban Environment and Health, Institute of Urban Environment, Chinese Academy of Sciences, Xiamen 361021, China

²Guizhou Medical University, Guiyang, China

³Université Laval, Québec, Canada

Correspondence should be addressed to Peng Bao; pbao@iue.ac.cn

Received 4 March 2020; Accepted 5 March 2020; Published 5 May 2020

Copyright © 2020 Peng Bao et al. This is an open access article distributed under the Creative Commons Attribution License, which permits unrestricted use, distribution, and reproduction in any medium, provided the original work is properly cited.

Environment-associated human health problems are getting worldwide attention with the extension of human society. Antibiotics are abused to protect the health of humans and animals that may accelerate the development of antibiotic resistance genes (ARGs) and antibiotic-resistant microorganisms (ARMs) which shade health risks to humans. A wide variety of ARGs have been found in microorganisms distributed in the environment. Heavy metal contamination represents a long-standing selection pressure on the maintenance and spread of ARGs, with both environmental and clinical importance. Therefore, heavy metals have also led to their own concerns over their risks on human health and the environment. In this special issue, we intend to report research studies that focus on adverse effects of antibiotics and heavy metals on the environment and human health and meta-analysis, medicines, and technologies that improve human health. The purpose of this special issue is to report the recent progress of those fields. A brief summary of all accepted papers is provided below.

The paper by Wang et al. reported that metformin significantly improved high blood pressure, proteinuria, and the foetal and placental weights in the HF-M group compared with the HF group. Metformin significantly improved placental labyrinth and foetal vascular development in pre-eclampsia. In addition, metformin effectively increased matrix metalloproteinase-2 (MMP-2) and vascular endothelial growth factor (VEGF) levels in the placenta.

The paper by Zhang et al. reported that HER2+BC patients showed improvement in pCR and DFS after neoad-

juvant trastuzumab treatment. Patients without pCR had prolonged DFS after trastuzumab maintenance.

The paper by Asha et al. reported an increased abundance of antibiotic resistance genes in the kidney transplant subjects. The antibiotic resistance genes identified in the transplant subjects were predominantly composed of multi-drug efflux pumps (MDEPs) which are evolutionarily ancient, are commonly encoded on chromosomes rather than plasmids, and have a low rate of mutation. Since the MDEPs had a low abundance in the healthy subjects, the MDEPs may enhance the fitness of bacteria to survive in the high-stress environment of transplantation that includes multiple stressors including surgery, antibiotics, and immunosuppressive agents.

The paper by Hao et al. found that cardiac contractility modulation (CCM) could elicit positive effects on heart failure (HF) therapy, which was potentially due to the variation in the Pi3k/Akt signaling pathway.

The paper by Guo et al. reported a heavy metal removal process that was optimised by orthogonal experiment with dynamic and static adsorption modes. The method can be used to satisfy the high efficiency of selective removal of harmful elements in *Acanthopanax senticosus* extract and the effective composition of almost no effect, it can be recommended for pretreatment of heavy metals in traditional Chinese medicine extracts, and this way provides a new thought and research technique to decrease the contents of heavy metals.

The paper by Su et al. found that LESS surgery with conventional laparoscopic instruments is feasible and safe

compared with traditional laparoscopy, but postoperative exhaust time is longer than the control group.

The paper by Fang et al. reported that the quality control circle activities played a significant role in promoting the use of rubber dams in the root canal treatment of primary teeth, and it can be used as a method to promote new clinical treatment programs.

The paper by Chen et al. reported that free flap transfer is an ideal method for the reconstruction of large, complicated scalp defects with a one-stage operation. The anterolateral thigh flap is favored because of its durability, adjustability, water tightness, and infection prevention.

Conflicts of Interest

The editors declare that they have no conflict of interest regarding the publication of this Special Issue.

Acknowledgments

We would like to express our gratitude to all authors who made this special issue possible. We hope this collection of articles will be useful to the scientific community.

*Peng Bao
Xiu-Li Gao
Guo-Qi Wen*

Research Article

Efficacy of Neoadjuvant Chemotherapy with Epirubicin and Cyclophosphamide and Weekly Paclitaxel and Trastuzumab in Human Epidermal Growth Factor Receptor 2–Positive Breast Carcinoma: A Real-World Study

Mengmeng Zhang,¹ Ling Li,² Shiyong Zhang,¹ Wenlong Zhu,¹ Senguo Yang,¹ Guangsheng Di,¹ Xiaoxia Ma,¹ and Haisong Yang¹ 

¹Department of Breast Surgery, The Affiliated Hospital of Guizhou Medical University, Guizhou 550004, China

²Department of Neurology, 925 Hospital of PLA Joint Logistics Support Force, Guizhou 550009, China

Correspondence should be addressed to Haisong Yang; yanghaisong@gmc.edu.cn

Received 14 September 2019; Revised 29 December 2019; Accepted 16 January 2020; Published 5 May 2020

Guest Editor: Peng Bao

Copyright © 2020 Mengmeng Zhang et al. This is an open access article distributed under the Creative Commons Attribution License, which permits unrestricted use, distribution, and reproduction in any medium, provided the original work is properly cited.

Background. Trastuzumab has been introduced a decade ago and demonstrated improvement in the prognosis in patients with human epidermal growth factor receptor 2- (HER2-) positive (+) breast carcinoma (BC). This study is aimed at evaluating the efficacy of epirubicin/cyclophosphamide with weekly paclitaxel-trastuzumab as neoadjuvant chemotherapies in HER2+ BC patients. **Methods.** A total of 234 HER2+ BC patients were given neoadjuvant chemotherapy (NAC) between 2010 and 2016. The primary endpoints were pathologic complete response (pCR) and disease-free survival (DFS). Univariate and multivariate analyses of clinical and pathological factors associated with pCR and DFS were conducted. **Results.** The pCR (30.4% vs. 14.8%; $P=0.004$) and DFS ($P=0.036$) showed significant differences between patients administered with neoadjuvant trastuzumab therapy and those who did not. Multivariate logistic regression analysis showed that neoadjuvant trastuzumab treatment was regarded as an independent predictor of pCR. Patients with pCR had prolonged DFS ($P=0.025$). In patients who did not achieve pCR (non-pCR), those who received trastuzumab had more prolonged DFS ($P=0.046$). The luminal B/HER2+ subtypes had prolonged DFS when compared with nonluminal B/HER2+ subtypes ($P=0.010$). The luminal B/HER2+ subgroup also showed improved DFS in non-pCR patients ($P=0.010$). In the subgroup of non-pCR, the luminal B/HER2+ subgroup administered with trastuzumab showed no superior DFS ($P=0.168$). However, a positive result was observed in patients without trastuzumab ($P=0.039$). Multivariate analysis showed cT stage ($P=0.006$) and tumor grade ($P=0.041$), considering them as significant prognostic factors of DFS. **Conclusions.** HER2+ BC patients showed improvement in pCR and DFS after neoadjuvant trastuzumab treatment. Patients without pCR had prolonged DFS after trastuzumab maintenance. Although the prognosis of luminal B/HER2+ BC showed favorable outcomes in the non-pCR subgroup, those receiving trastuzumab showed no survival advantage.

1. Introduction

Breast carcinoma (BC) is the most commonly encountered malignancy in women and the leading cause of mortality in female patients [1]. The human epidermal growth factor receptor 2 (HER2) is overexpressed in 25% to 30% of patients with BC, and this is associated with elevated malignancy potential [2, 3]. Trastuzumab, a humanized monoclonal anti-

body that targets HER2 by binding to its extracellular domain as a single agent, demonstrated modest antitumor activities. It is used for treating both metastatic and early-stage HER2 + BC with high efficacy [4–6]. Randomized studies reported similar survival benefits for particular treatment regimens, regardless of whether the treatment is preoperatively or post-operatively administered. Neoadjuvant chemotherapy (NAC) for early and locally advanced BC is broadly

employed to downstage the primary lesion, allowing a higher rate of breast preservation [7, 8]. In addition, it can be used for testing chemosensitivity *in vivo*, making it possible to assess the efficacy of early systemic therapy and to stop ineffective treatment. The achievement of pathologic complete response (pCR) upon NAC is considered an important surrogate marker to improve the long-term outcomes [8, 9]. It is hypothesized that a regimen that produces higher pCR rates in a neoadjuvant systemic therapy setting also ensues higher rates of long-term cure. Recently, phase II and III clinical studies have intensely assessed the combination of trastuzumab and NAC as neoadjuvant systemic therapy for early and locally advanced HER2+ BC, respectively [10–12]. Also, recent studies showed that NAC when combined with trastuzumab assists in achieving significantly higher pCR rates than NAC alone [10, 11, 13]. Trastuzumab-based therapy has been used over the past decade and demonstrated a favorable impact on survival when compared with the same chemotherapy alone as therapy [14]. For HER2+ BC patients who require neoadjuvant therapy, trastuzumab is generally added to chemotherapy, and the patient receives adjuvant trastuzumab for 1 year.

However, whether the results of randomized controlled trials (RCTs) are applicable to the real-world cases is one of the major issues. The present work is aimed at assessing NAC with epirubicin/cyclophosphamide (EC) and paclitaxel-trastuzumab (PH) in HER2+ BC patients. The study also explored whether the effectiveness of neoadjuvant trastuzumab in association with NAC in the real-world treatment of patients with HER2+ BC was comparable to that observed in RCTs.

2. Materials and Methods

2.1. Patient Population. In this study, 234 cases with operable or locally advanced HER2+ BC who underwent treatment at our hospital between 2010 and 2016 were analyzed. All patients underwent a core biopsy before receiving NAC, followed by surgery or radiotherapy. Before initiating the therapy, all patients underwent staging evaluation, which included a complete history check, physical examination, computed tomography (CT) scan of the chest and liver, and bone scan. Mammography of both breasts was performed, and additional breast and axillary assessment of the tumor site was done by ultrasound. This trial had approval from the Research and Ethics Committee of our hospital, and informed consent was obtained from all patients.

2.2. Treatments. All patients were confirmed with the diagnosis of invasive BC by biopsy before NAC, including breast ultrasonography, breast mammography, and breast magnetic resonance imaging (MRI) to confirm the tumor size; fine needle aspiration was performed to assess metastasis to axillary lymph nodes and chest ultrasonography, abdominal CT, and whole-body bone scan to exclude distant metastases. Patient treatment was based on the National Comprehensive Cancer Network guidelines. Furthermore, 92 patients received dose-dense epirubicin/cyclophosphamide and paclitaxel-trastuzumab (EC-PH) and 142 were

administered with dose-dense EC-P NAC. EC-PH consisted of four cycles of EC (epirubicin/cyclophosphamide (90/600 mg/m²)) on day 1 treatment, administered at 2-week intervals, and paclitaxel (80 mg/m²) once a week for 12 weeks. Trastuzumab 4 mg/kg (loading dose) was administered on day 1 and 2 mg/kg per week for 12 weeks (NAC duration). Also, 92 patients completed trastuzumab therapy for a year. The patients underwent surgery at 1–4 weeks upon NAC completion. Surgical intervention included breast-conserving operation, mastectomy and sentinel node biopsy, or axillary lymph node dissection. Radiation therapy was administered in case of breast-conserving surgery or locally advanced disease. Patients with hormone receptor-positive (HR+) cancer received adjuvant endocrine therapy for 5 years.

2.3. Pathological Assessment. Immunohistochemical (IHC) assessment of human epidermal growth factor receptor 2 (HER2), estrogen receptor (ER), and progesterone receptor (PR) was conducted on pretreatment biopsies and surgical specimens by pathologists. Through IHC detection, HER23+ was considered positive, and 0-1+ was considered negative; 2+ required verification through fluorescence *in situ* hybridization (FISH), in which 2.2 gene copies (per FISH) were considered positive for *HER2* amplification. Nuclear staining $\geq 1\%$ of ER or PR was deemed to be positive. For Ki-67, the positive cells demonstrated light yellow to brown nuclei under 400x light microscopy in 10 randomly selected fields. A total of 500 cells were counted in each field, and the ratio of Ki-67-positive cells to total cells was calculated. A pCR was defined as the absence of invasive residual breast tumor or invasive lesion in ipsilateral axillary nodes (ypT0 ypN0).

2.4. Follow-Up. From day 1 after surgery, all patients were followed up till March 2018, with the follow-up information obtained through outpatient interviews or telephone calls. Disease-free survival (DFS) was determined from day 1 after surgery to the first local relapse.

2.5. Statistical Analysis. The association of clinical characteristics with pCR was determined by Pearson's χ^2 or Fisher's exact test. Univariate analysis was performed, and parameters showing significant associations entered the multivariate logistic models. Multivariate analysis used an unconditional stepwise logistic regression approach. Univariate/multivariate survival analyses were performed using the Cox regression model. The interactions between significant investigation variables were considered when developing the multivariate model. DFS estimation was carried out by Kaplan–Meier analysis, and the log-rank test was used to compare the groups. $P < 0.05$ was considered to be statistically significant. All statistical analyses were performed using SPSS Statistic software 19.

3. Results

3.1. Clinical Characteristics and Response to NAC. From April 2011 to August 2017, 234 patients with HER2+ BC who

underwent surgery were given neoadjuvant trastuzumab combined with dose-dense EC-P. The median age of the patients was 50 years, ranging from 27 to 75 years. A total of 160 patients had T1–T2 tumors (69.2%), and 108 had lymph node metastasis (46.2%). Associations of baseline patient features and therapeutic indexes with pCR in univariate analysis are reported in Table 1. All cases had highly proliferative invasive ductal carcinoma (in which 46.6% showing Ki-67 > 30%). Tumor grades were 1–2 in 53 (22.6%) and 3 in 181 (77.4%) cases. The luminal B/HER2+ (HER2+/ER+ and/or PR+) and nonluminal B/HER2+ (HER2+/ER– and PR–) subtypes were involved in 127 (54.3%) and 107 (45.7%) patients, respectively. The residual invasive breast lesions were found in 185 (79.1%) patients and residual non-invasive tumors in 49 (20.9%) patients. The pCR rate was increased in patients who were given neoadjuvant trastuzumab therapy ($P < 0.05$) (Table 1). Multivariate logistic regression analysis revealed that the use of trastuzumab independently predicted pCR (Table 2).

3.2. Patient Survival. The median follow-up was 32.9 months (range, 5–82 months), and the mean DFS was 32 months. In this study, 25/234 (10.7%) cases showed local relapse or distant metastases. In Kaplan–Meier analysis, survival showed marked differences between cases administered with trastuzumab and the remaining patients ($P = 0.036$, Figure 1). Multivariate logistic regression analysis revealed neoadjuvant trastuzumab administration ($P = 0.004$) as an independent predictive factor for pCR ($P = 0.004$, Table 2). Meanwhile, cases with pCR had prolonged DFS ($P = 0.025$, Figure 2). Among those who did not achieve pCR, patients administered with trastuzumab more likely showed a prolonged DFS ($P = 0.046$, Figure 3). However, a positive result was not observed in patients with pCR (Figure 4). Moreover, patients with luminal B/HER2+ had improved DFS ($P = 0.010$) than those with nonluminal B/HER2+ (Figure 5). The luminal B/HER2+ subtype also showed improvement in the DFS rates in non-pCR cases ($P = 0.010$, Figure 6). In subgroup analyses, patients with luminal B/HER2+ with trastuzumab administration showed no prolonged DFS in non-pCR cases ($P = 0.168$, Figure 7). However, a positive result was observed in patients without trastuzumab ($P = 0.039$, Figure 8). Multivariate analysis revealed cT stage (hazard ratio = 3.80, 95% CI 1.46–9.89; $P = 0.006$) and tumor grade (hazard ratio = 5.17, 95% CI 1.07–24.96; $P = 0.041$) as independent predictive factors for DFS in patients with BC (Table 3).

4. Discussion

Recent studies have focused on the relative value of RCTs to help make a routine clinical decision, as they are the major endpoints of comparative effectiveness research [15, 16]. Although findings of RCTs largely determine the comparison among treatment groups, case selection criteria and the rigidity of protocols do not allow changes easily in dose and toxicity management, making these findings not generalizable to the patient level [17]. Whether the results of these RCTs are applicable to real-world cases and whether patients can

TABLE 1: Associations of clinical characteristics with pCR in univariate analysis.

	Non-pCR (n = 185)		pCR (n = 49)		P value
	n	%	n	%	
Age (year)					0.182
≤35	24	13.0	3	6.1	
>35	161	87.0	46	93.9	
Menopausal status					0.527
Premenopausal	100	54.1	24	49.0	
Postmenopausal	85	45.9	25	51.0	
cT stage					0.389
cT1–2	124	67.0	36	73.5	
cT3–4	61	33.0	13	26.5	
cN stage					0.07
cN0	94	50.8	32	65.3	
cN1–3	91	49.2	17	34.7	
Grade					0.729
G1–2	41	22.2	12	24.5	
G3	144	77.8	37	75.5	
ER					0.472
Positive	105	56.8	25	51.0	
Negative	80	43.2	24	49.0	
PR					0.949
Positive	84	45.4	22	44.9	
Negative	101	54.6	27	55.1	
HR					0.854
Positive	82	44.3	21	42.9	
Negative	103	55.7	28	57.1	
Ki-67					0.791
>30%	87	47.0	22	44.9	
≤30%	98	53.0	27	55.1	
Molecular subtype					0.607
Luminal B/HER2+	102	55.1	25	51.0	
Nonluminal/HER2+	83	44.9	24	49.0	
Trastuzumab					0.004
Yes	64	34.6	28	57.1	
No	121	65.4	21	42.9	

afford these drugs for some special reasons are major issues. Due to economic reasons, especially in resource-limited regions, many patients with HER2+ less likely received trastuzumab-containing treatment. In 2017, the cost of trastuzumab was substantially reduced in China, making it feasible for most of the patients to afford the drug. Accordingly, observational retrospective trials are considered important sources of data on the effectiveness of alternative therapies based on patient and tumor properties. Therefore, the present work is aimed at reporting the effectiveness of neoadjuvant trastuzumab with dose-dense EC-P in 234 cases with operable or locally advanced HER2+ BC. This novel retrospective study compared the effectiveness of EC-PH and

TABLE 2: Predictive factors of pCR according to the multivariate logistic regression model.

	OR	Univariate 95% CI	<i>P</i> value	OR	Multivariate 95% CI	<i>P</i> value
Age (year)			0.193			0.189
≤35	1.000			1.000		
>35	2.286	0.659–7.931		2.438	0.645–9.209	
Menopausal status			0.527			0.727
Premenopausal	1.000			1.000		
Postmenopausal	1.225	0.652–2.303		1.130	0.570–2.237	
cT stage			0.39			0.900
cT1–2	1.000			1.000		
cT3–4	0.734	0.363–1.485		0.951	0.436–2.075	
cN stage			0.073			0.324
cN0	1.000			1.000		
cN1–3	0.549	0.285–1.057		0.698	0.342–1.425	
Grade			0.729			0.453
G1–2	1.000			1.000		
G3	0.878	0.420–1.836		0.738	0.334–1.631	
ER			0.473			0.311
Positive	1.000			1.000		
Negative	1.260	0.670–2.368		2.415	0.439–13.279	
PR			0.949			0.931
Positive	1.000			1.000		
Negative	1.021	0.542–1.922		0.886	0.057–13.698	
HR			0.854			0.906
Positive	1.000			1.000		
Negative	1.061	0.562–2.005		0.843	0.050–14.302	
Ki-67			0.791			0.884
>30%	1.000			1.000		
≤30%	1.090	0.579–2.051		1.051	0.538–2.054	
Molecular subtype			0.607			0.590
Luminal B/HER2+	1.000			1.000		
Nonluminal/HER2+	1.180	0.628–2.216		0.610	0.101–3.678	
Trastuzumab			0.005			0.004
Yes	1.000			1.000		
No	0.397	0.209–0.754		0.361	0.180–0.725	

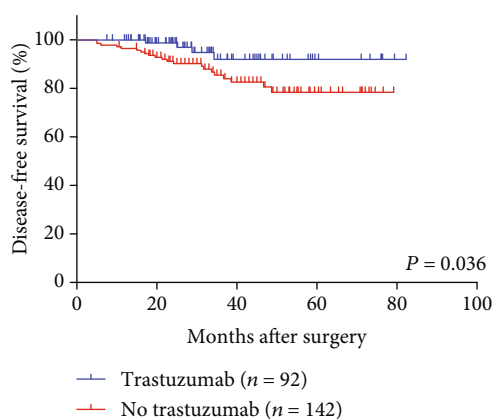


FIGURE 1: Association of trastuzumab use with DFS.

EC-P in HER2+ BC patients. The results showed that (1) pCR was achieved in 30.4% and 14.8% of patients with and without neoadjuvant trastuzumab treatment, respectively; (2) patients with pCR had prolonged DFS; (3) neoadjuvant trastuzumab treatment independently predicted pCR and showed association with improved DFS in all patients and the non-pCR subgroup; (4) the luminal B/HER2+ subtype showed superior DFS in all patients and the non-pCR subgroup; (5) in the non-pCR subgroup, the luminal B/HER2+ subtype without neoadjuvant trastuzumab treatment showed superior DFS; and (6) cT stage and tumor grade were considered independent prognostic factors of DFS.

As expected, the results of this study confirmed that administration of trastuzumab and NAC resulted in elevated pCR rate (30.4%) when compared with the NAC-alone group

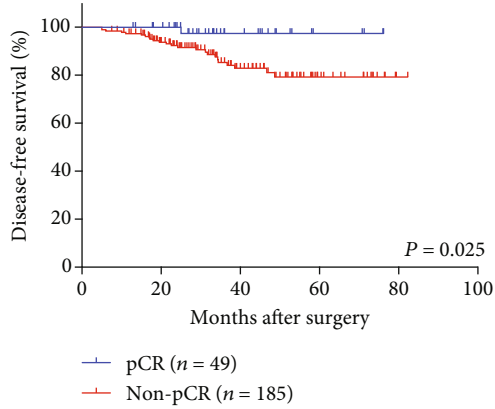


FIGURE 2: DFS in patients with pCR and non-pCR.

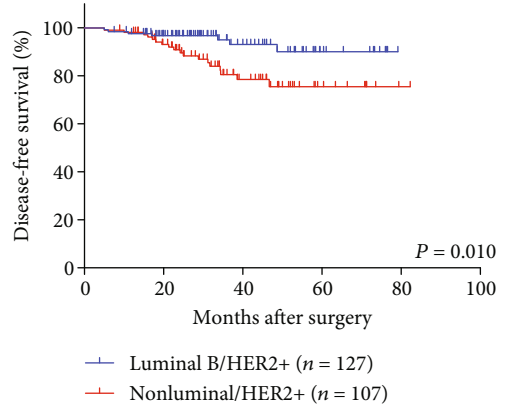


FIGURE 5: DFS curves in luminal B/HER2+ and nonluminal B/HER2+ patients.

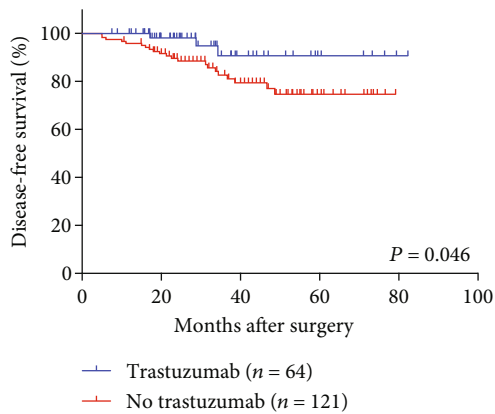


FIGURE 3: Association of trastuzumab use with DFS in non-pCR patients.

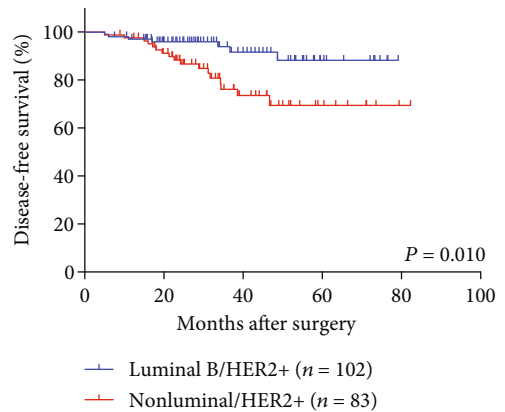


FIGURE 6: DFS curves of luminal B/HER2+ and nonluminal B/HER2+ patients in non-pCR patients.

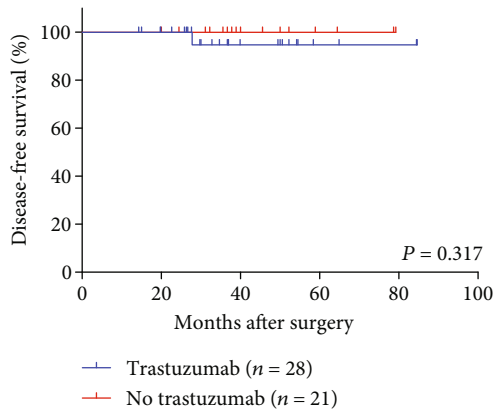


FIGURE 4: Association of trastuzumab use with DFS in pCR patients.

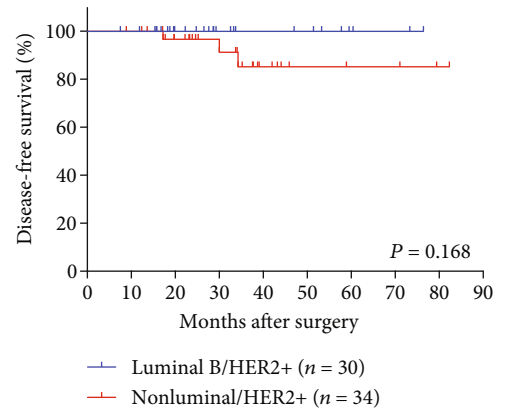


FIGURE 7: DFS curves of luminal B/HER2+ and nonluminal B/HER2+ patients in non-pCR patients administered with trastuzumab.

(14.8%). The previously published pCR rates for NAC and trastuzumab ranged between 32% and 66% [10, 11, 18]. The reasons for the lower rate in this study might be due to its retrospective design and small sample size. In addition, there were more cases with luminal B/HER2+ than the nonluminal B/HER2+ counterpart. Multiple clinical studies have reported marked elevation in the pCR rate in the nonluminal

B/HER2+ molecular subtype when compared with the luminal B/HER2+ molecular subtype [19–21]. More importantly, multivariate analysis also revealed the use of trastuzumab as an independent predictor of pCR. Therefore, trastuzumab plus NAC increased the pCR rate. Recently, many pivotal

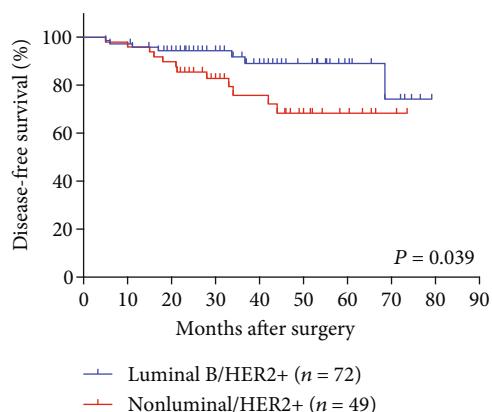


FIGURE 8: DFS curves of luminal B/HER2+ and nonluminal B/HER2+ patients in non-pCR patients without trastuzumab use.

RCTs have confirmed the efficacy and safety of trastuzumab/NAC combination therapy in early and locally advanced HER2+ BC patients [10–12]. This study also revealed that the patients who were treated with trastuzumab plus NAC had prolonged DFS. These results confirmed that the eligibility criteria and treatment outcomes of clinical trials could be translated to the real-world setting.

The most recent view is that luminal B/HER2+ BC represents a distinct subgroup with lower chemotherapy sensitivity and better outcomes when compared with HR-/HER2+ disease [19, 22–24]. In the present study, DFS in the luminal B/HER2+ subtype was better than that in the nonluminal/HER2+ subtype. Moreover, positive results were observed in the non-pCR subgroup. This was due to the use of adjuvant endocrine therapy for patients with the luminal B/HER2+ subtype, which reduced the risk of recurrence. In subgroup analysis, superior DFS was observed in patients with the luminal B/HER2+ subtype without trastuzumab who did not achieve pCR. However, a negative result was observed in patients who had trastuzumab. The role of hormone receptor (HR) status in predicting pCR and prognosis upon trastuzumab-containing NAC administration is subjected to debate, although most of the trials reported positive results. Based on the previous reports, the absence of HR represents a critical predictive factor in pCR and a reliable prognostic index [20–24]. However, a crosstalk is believed to occur between the HER2 and ER pathways in ER+/HER2+ patients, while estrogen-independent ER signaling dominates the classical estrogen-dependent ER signaling pathway [25, 26]. The fact that the upregulation of ER expression and/or activity functions as an escape mechanism, leading to resistance to anti-HER2 treatment in HER2+ and HR+ BC patients [27]. Preclinical studies have shown that ER+ and HER2+ BC cell lines are initially sensitive to lapatinib. After gaining resistance to lapatinib, ER signaling showed significant enhancement, and the resistance can be prevented by simultaneous inhibition of HER2 and ER signals [28, 29]. Researchers have found that the ER functions play a key role in escaping/survival pathway of HER2+/ER+ cells under sustained HER2 inhibition and that a dynamic transition between HER2 and ER activity plays a role in resistance to

regimens containing lapatinib [30]. In addition, recent findings have revealed that PIK3CA-mutated HER2+ BC patients less likely achieved pCR and prolonged DFS upon neoadjuvant anthracycline-taxane chemotherapy when combined with anti-HER2 treatment, and this might explain such discrepancy [31, 32]. Activation of the PI3K/AKT/mTOR signaling pathway is related to oncogenesis and tumor progression and resistance to standard anticancer therapies [33, 34]. The PIK3CA gene that regulates PI3K is one of the most frequently mutated genes in human cancers. Abnormal activation of the PI3K pathway is frequently observed in BC, resulting in uncontrolled tumor cell growth and drug resistance [35]. HER2+ BC carrying PIK3CA mutations is particularly dependent on the PI3K signaling pathway, and it has been shown that activation of this pathway plays a key role in developing resistance to trastuzumab [33, 36].

Whether pCR represents a surrogate marker of DFS and overall survival (OS) in HER2+ BC patients remains to be a largely controversial topic. The present study revealed that patients who achieved pCR had prolonged DFS. Meta-analysis of 6377 cases with primary BC administered with neoadjuvant anthracycline-taxane in 7 randomized studies revealed pCR as a valid substitute of DFS and OS in HER2+ subtypes [37]. In addition, three multicenter retrospective studies on HER2+ BC who underwent treatment with NAC and trastuzumab showed pCR as a surrogate marker for DFS in HR-BC, but the results of the HR+ group were negative [9, 38, 39]. However, researchers confirmed the level of evidence available for supporting a relationship between pCR and OS [40, 41]. Therefore, pCR still cannot be used as a surrogate marker for long-term survival. Subgroup analysis of the present data revealed that trastuzumab use in cases who achieved pCR did not result in favorable survival outcomes. However, our study found that patients who underwent treatment with trastuzumab plus NAC had good DFS for non-pCR responders, indicating that patients who did not achieve pCR should be treated with trastuzumab. To date, phase II and III trials have not been conducted to explore trastuzumab use following trastuzumab plus NAC administration preoperatively in cases who did not achieve pCR. The efficacy of anti-HER2 agents in non-pCR responders also remained controversial [42]. The present study results revealed that these patients gained benefits from using trastuzumab maintenance, although they are less likely to respond to trastuzumab plus NAC.

Multivariate analysis revealed cT stage and tumor grade as significant independent prognostic factors of pCR, which was consistent with the previous studies [9, 39]. The present study was limited due to its relatively small sample size, short follow-up period, and single-institution design. These patients should be followed up in the future to observe the long-term outcomes, and sample size should be enlarged to confirm the current results.

In conclusion, trastuzumab improved the prognosis of patients with HER2+ BC. NAC plus trastuzumab resulted in elevated pCR rate in HER2+ BC patients. The non-pCR cases upon neoadjuvant anti-HER2 treatment plus

TABLE 3: Hazard ratios for DFS prediction in univariate and multivariate analyses.

	HR	Univariate 95% CI	P value	HR	Multivariate 95% CI	P value
Age (year)			0.731			0.917
≤35	1.000			1.000		
>35	0.809	0.242–2.707		0.926	0.216–3.966	
Menopausal status			0.433			0.128
Premenopausal	1.000			1.000		
Postmenopausal	0.726	0.326–1.616		0.475	0.182–1.238	
cT stage			0.004			0.006
cT1–2	1.000			1.000		
cT3–4	3.166	1.433–6.995		3.801	1.460–9.894	
cN stage			0.559			0.242
cN0	1.000			1.000		
cN1–3	1.265	0.576–2.776		0.545	0.197–1.509	
Grade			0.090			0.041
G1–2	1.000			1.000		
G3	3.488	0.822–14.800		5.165	1.069–24.959	
HR			0.056			0.927
Positive	1.000			1.000		
Negative	2.466	0.977–6.127		0.903	0.101–8.084	
Ki-67			0.981			0.607
>30%	1.000			1.000		
≤30%	1.009	0.458–2.227		1.257	0.526–3.007	
Molecular subtype			0.014			0.244
Luminal B/HER2+	1.000			1.000		
Nonluminal/HER2+	2.988	1.248–7.155		3.559	0.421–30.056	
Trastuzumab			0.047			0.190
Yes	1.000			1.000		
No	2.961	1.015–8.632		2.218	0.674–7.297	
Strict pCR			0.055			0.062
Yes	1.000			1.000		
No	7.065	0.955–52.241		0.144	0.019–1.101	
Lymph node involved			0.024			0.074
0	1.000			1.000		
1–3	1.888	0.714–4.992		1.996	0.639–6.237	
≥4	5.296	1.688–16.612		4.855	1.240–19.004	
Endocrine therapy			0.181			0.259
TAM	1.000			1.000		
AI	1.852	0.522–6.563		3.238	0.783–13.398	
No	2.765	0.917–8.342		2.261	0.585–8.737	

chemotherapy followed by trastuzumab maintenance had better long-term outcomes. Although the prognosis of the luminal B/HER2+ subtype demonstrated favorable outcomes in the non-pCR subgroup, luminal B/HER2+ BC patients receiving trastuzumab showed no survival advantage. Hence, more patients and long-term follow-up time are needed for further study. Neoadjuvant treatment with EC-PH might be a suitable alternative regimen for Chinese women who require anthracycline therapy.

Data Availability

The data used to support the findings of this study are available from the corresponding author upon request.

Conflicts of Interest

The authors have no conflict of interest.

Authors' Contributions

Mengmeng Zhang and Ling Li contributed equally to this work.

References

- [1] W. Chen, R. Zheng, P. D. Baade et al., "Cancer statistics in China, 2015," *CA: a Cancer Journal for Clinicians*, vol. 66, no. 2, pp. 115–132, 2016.
- [2] A. Valachis, A. Nearchou, P. Lind, and D. Mauri, "Lapatinib, trastuzumab or the combination added to preoperative chemotherapy for breast cancer: a meta-analysis of randomized evidence," *Breast Cancer Research and Treatment*, vol. 135, no. 3, pp. 655–662, 2012.
- [3] B. Parkinson, R. Viney, M. Haas, S. Goodall, P. Srasuebku, and S. A. Pearson, "Real-world evidence: a comparison of the Australian Herceptin Program and clinical trials of trastuzumab for HER2-positive metastatic breast cancer," *Pharmacoeconomics*, vol. 34, no. 10, pp. 1039–1050, 2016.
- [4] M. J. Piccart-Gebhart, M. Procter, B. Leyland-Jones et al., "Trastuzumab after adjuvant chemotherapy in HER2-positive breast cancer," *The New England Journal of Medicine*, vol. 353, no. 16, pp. 1659–1672, 2005.
- [5] D. Cameron, M. J. Piccart-Gebhart, R. D. Gelber et al., "11 years' follow-up of trastuzumab after adjuvant chemotherapy in HER2-positive early breast cancer: final analysis of the HERceptin Adjuvant (HERA) trial," *The Lancet*, vol. 389, no. 10075, pp. 1195–1205, 2017.
- [6] J. Baselga, X. Carbonell, N.-J. Castañeda-Soto et al., "Phase II study of efficacy, safety, and pharmacokinetics of trastuzumab monotherapy administered on a 3-weekly schedule," *Journal of Clinical Oncology*, vol. 23, no. 10, pp. 2162–2171, 2005.
- [7] D. Mauri, N. Pavlidis, and J. P. Ioannidis, "Neoadjuvant versus adjuvant systemic treatment in breast cancer: a meta-analysis," *Journal of the National Cancer Institute*, vol. 97, no. 3, pp. 188–194, 2005.
- [8] P. Cortazar, L. Zhang, M. Untch et al., "Pathological complete response and long-term clinical benefit in breast cancer: the CTNeoBC pooled analysis," *The Lancet*, vol. 384, no. 9938, pp. 164–172, 2014.
- [9] M. Takada, H. Ishiguro, S. Nagai et al., "Survival of HER2-positive primary breast cancer patients treated by neoadjuvant chemotherapy plus trastuzumab: a multicenter retrospective observational study (JBCRG-C03 study)," *Breast Cancer Research and Treatment*, vol. 145, no. 1, pp. 143–153, 2014.
- [10] M. Untch, P. A. Fasching, G. E. Konecny et al., "Pathologic complete response after neoadjuvant chemotherapy plus trastuzumab predicts favorable survival in human epidermal growth factor receptor 2-overexpressing breast cancer: results from the TECHNO trial of the AGO and GBG study groups," *Journal of Clinical Oncology*, vol. 29, no. 25, pp. 3351–3357, 2011.
- [11] A. U. Buzdar, N. K. Ibrahim, D. Francis et al., "Significantly higher pathologic complete remission rate after neoadjuvant therapy with trastuzumab, paclitaxel, and epirubicin chemotherapy: results of a randomized trial in human epidermal growth factor receptor 2-positive operable breast cancer," *Journal of Clinical Oncology*, vol. 23, no. 16, pp. 3676–3685, 2005.
- [12] L. Gianni, W. Eiermann, V. Semiglazov et al., "Neoadjuvant chemotherapy with trastuzumab followed by adjuvant trastuzumab versus neoadjuvant chemotherapy alone, in patients with HER2-positive locally advanced breast cancer (the NOAH trial): a randomised controlled superiority trial with a parallel HER2-negative cohort," *The Lancet*, vol. 375, no. 9712, pp. 377–384, 2010.
- [13] A. Valachis, D. Mauri, N. P. Polyzos, G. Chlouverakis, D. Mavroudis, and V. Georgoulas, "Trastuzumab combined to neoadjuvant chemotherapy in patients with HER2-positive breast cancer: a systematic review and meta-analysis," *The Breast*, vol. 20, no. 6, pp. 485–490, 2011.
- [14] K. R. Broglio, M. Quintana, M. Foster et al., "Association of pathologic complete response to neoadjuvant therapy in HER2-positive breast cancer with long-term outcomes: a meta-analysis," *JAMA Oncology*, vol. 2, no. 6, pp. 751–760, 2016.
- [15] G. H. Lyman and M. Levine, "Comparative effectiveness research in oncology: an overview," *Journal of Clinical Oncology*, vol. 30, no. 34, pp. 4181–4184, 2012.
- [16] E. L. Korn and B. Freidlin, "Methodology for comparative effectiveness research: potential and limitations," *Journal of Clinical Oncology*, vol. 30, no. 34, pp. 4185–4187, 2012.
- [17] O. M. Hahn and R. L. Schilsky, "Randomized controlled trials and comparative effectiveness research," *Journal of Clinical Oncology*, vol. 30, no. 34, pp. 4194–4201, 2012.
- [18] L. Gianni, W. Eiermann, V. Semiglazov et al., "Neoadjuvant and adjuvant trastuzumab in patients with HER2-positive locally advanced breast cancer (NOAH): follow-up of a randomised controlled superiority trial with a parallel HER2-negative cohort," *The Lancet Oncology*, vol. 15, no. 6, pp. 640–647, 2014.
- [19] R. Costa, G. Kurra, L. Greenberg, and C. Geyer, "Efficacy and cardiac safety of adjuvant trastuzumab-based chemotherapy regimens for HER2-positive early breast cancer," *Annals of Oncology*, vol. 21, no. 11, pp. 2153–2160, 2010.
- [20] L. Gianni, T. Pienkowski, Y.-H. Im et al., "Efficacy and safety of neoadjuvant pertuzumab and trastuzumab in women with locally advanced, inflammatory, or early HER2-positive breast cancer (NeoSphere): a randomised multicentre, open-label, phase 2 trial," *The Lancet Oncology*, vol. 13, no. 1, pp. 25–32, 2012.
- [21] J. Baselga, I. Bradbury, H. Eidtmann et al., "Lapatinib with trastuzumab for HER2-positive early breast cancer (NeoALTTO): a randomised, open-label, multicentre, phase 3 trial," *The Lancet*, vol. 379, no. 9816, pp. 633–640, 2012.
- [22] F. Peintinger, A. U. Buzdar, H. M. Kuerer et al., "Hormone receptor status and pathologic response of HER2-positive breast cancer treated with neoadjuvant chemotherapy and trastuzumab," *Annals of Oncology*, vol. 19, no. 12, pp. 2020–2025, 2008.
- [23] N. Houssami, P. Macaskill, G. von Minckwitz, M. L. Marinovich, and E. Mamounas, "Meta-analysis of the association of breast cancer subtype and pathologic complete response to neoadjuvant chemotherapy," *European Journal of Cancer*, vol. 48, no. 18, pp. 3342–3354, 2012.
- [24] D. Angelucci, N. Tinari, A. Grassadonia et al., "Long-term outcome of neoadjuvant systemic therapy for locally advanced breast cancer in routine clinical practice," *Journal of Cancer Research and Clinical Oncology*, vol. 139, no. 2, pp. 269–280, 2013.
- [25] G. Arpino, H. Weiss, A. V. Lee et al., "Estrogen receptor-positive, progesterone receptor-negative breast cancer: association with growth factor receptor expression and tamoxifen

- resistance,” *Journal of the National Cancer Institute*, vol. 97, no. 17, pp. 1254–1261, 2005.
- [26] J. Shou, S. Massarweh, C. K. Osborne et al., “Mechanisms of tamoxifen resistance: increased estrogen receptor-HER2/neu cross-talk in ER/HER2-positive breast cancer,” *Journal of the National Cancer Institute*, vol. 96, no. 12, pp. 926–935, 2004.
- [27] F. Montemurro, S. Di Cosimo, and G. Arpino, “Human epidermal growth factor receptor 2 (HER2)-positive and hormone receptor-positive breast cancer: new insights into molecular interactions and clinical implications,” *Annals of Oncology*, vol. 24, no. 11, pp. 2715–2724, 2013.
- [28] L. Liu, J. Greger, H. Shi et al., “Novel mechanism of lapatinib resistance in HER2-positive breast tumor cells: activation of AXL,” *Cancer Research*, vol. 69, no. 17, pp. 6871–6878, 2009.
- [29] W. Xia, S. Bacus, P. Hegde et al., “A model of acquired autoreistance to a potent ErbB2 tyrosine kinase inhibitor and a therapeutic strategy to prevent its onset in breast cancer,” *Proceedings of the National Academy of Sciences of the United States of America*, vol. 103, no. 20, pp. 7795–7800, 2006.
- [30] Y. C. Wang, G. Morrison, R. Gillihan et al., “Different mechanisms for resistance to trastuzumab versus lapatinib in HER2-positive breast cancers-role of estrogen receptor and HER2 reactivation,” *Breast Cancer Research*, vol. 13, no. 6, article R121, 2011.
- [31] S. Loibl, G. Von Minckwitz, A. Schneeweiss et al., “PIK3CA mutations are associated with lower rates of pathologic complete response to anti-human epidermal growth factor receptor 2 (her2) therapy in primary HER2-overexpressing breast cancer,” *Journal of Clinical Oncology*, vol. 32, no. 29, pp. 3212–3220, 2014.
- [32] S. Loibl, I. Majewski, V. Guarneri et al., “PIK3CA mutations are associated with reduced pathological complete response rates in primary HER2-positive breast cancer: pooled analysis of 967 patients from five prospective trials investigating lapatinib and trastuzumab[†],” *Annals of Oncology*, vol. 27, no. 8, article S0923753419347350, pp. 1519–1525, 2016.
- [33] K. Berns, H. M. Horlings, B. T. Hennessy et al., “A functional genetic approach identifies the PI3K pathway as a major determinant of trastuzumab resistance in breast cancer,” *Cancer Cell*, vol. 12, no. 4, pp. 395–402, 2007.
- [34] T. W. Miller, B. N. Rexer, J. T. Garrett, and C. L. Arteaga, “Mutations in the phosphatidylinositol 3-kinase pathway: role in tumor progression and therapeutic implications in breast cancer,” *Breast Cancer Research*, vol. 13, no. 6, p. 224, 2011.
- [35] H. Ellis and C. X. Ma, “PI3K inhibitors in breast cancer therapy,” *Current Oncology Reports*, vol. 21, no. 12, p. 110, 2019.
- [36] A. B. Hanker, A. D. Pfefferle, J. M. Balko et al., “Mutant PIK3CA accelerates HER2-driven transgenic mammary tumors and induces resistance to combinations of anti-HER2 therapies,” *Proceedings of the National Academy of Sciences of the United States of America*, vol. 110, no. 35, pp. 14372–14377, 2013.
- [37] G. Von Minckwitz, M. Untch, J. U. Blohmer et al., “Definition and impact of pathologic complete response on prognosis after neoadjuvant chemotherapy in various intrinsic breast cancer subtypes,” *Journal of Clinical Oncology*, vol. 30, no. 15, pp. 1796–1804, 2012.
- [38] M. Kim, P. Allen, A. Gonzalez-Angulo et al., “Pathologic complete response to neoadjuvant chemotherapy with trastuzumab predicts for improved survival in women with HER2-overexpressing breast cancer,” *Annals of Oncology*, vol. 24, no. 8, pp. 1999–2004, 2013.
- [39] M. Tanioka, M. Sasaki, A. Shimomura et al., “Pathologic complete response after neoadjuvant chemotherapy in HER2-overexpressing breast cancer according to hormonal receptor status,” *The Breast*, vol. 23, no. 4, pp. 466–472, 2014.
- [40] E. Korn, M. Sachs, and L. McShane, “Statistical controversies in clinical research: assessing pathologic complete response as a trial-level surrogate end point for early-stage breast cancer,” *Annals of Oncology*, vol. 27, no. 1, pp. 10–15, 2015.
- [41] F. Fiteni and F. Bonnetain, “Surrogate end points for overall survival in breast cancer trials: a review,” *The Breast*, vol. 29, pp. 44–48, 2016.
- [42] R. X. Wang, S. Chen, X. Jin, C. M. Chen, and Z. M. Shao, “Weekly paclitaxel plus carboplatin with or without trastuzumab as neoadjuvant chemotherapy for HER2-positive breast cancer: loss of HER2 amplification and its impact on response and prognosis,” *Breast Cancer Research and Treatment*, vol. 161, no. 2, pp. 259–267, 2017.

Research Article

Alkyl Thiourea Functionalised Silica for the Effective Removal of Heavy Metals from *Acanthopanax senticosus* Extract

Hong-Li Guo,^{1,2} Shuo Zhang,³ Christopher North,⁴ Min Zhang,^{1,5} Xiao-xia Meng,^{1,5} and Xiu-Li Gao ^{1,5}

¹State Key Laboratory of Functions and Applications of Medicinal Plants & School of Pharmacy, Guizhou Medical University, Guiyang 550025, China

²College of Traditional Chinese Medicine and Lab of Traditional Chinese Medicine, Chongqing Medical University, Chongqing 400016, China

³Guizhou Medical University Experimental Animal Center, Guiyang 550025, China

⁴PhosphonicS Ltd., 114 Milton Park, Abingdon, Oxfordshire OX14 4SA, UK

⁵Microbiology and Biochemical Pharmaceutical Engineering Research Center of Guizhou Province College and University, Guizhou Medical University, Guiyang 550004, China

Correspondence should be addressed to Xiu-Li Gao; xiuligao@hotmail.com

Received 7 November 2019; Revised 16 January 2020; Accepted 18 January 2020; Published 26 March 2020

Academic Editor: Raf Dewil

Copyright © 2020 Hong-Li Guo et al. This is an open access article distributed under the Creative Commons Attribution License, which permits unrestricted use, distribution, and reproduction in any medium, provided the original work is properly cited.

Acanthopanax senticosus extract with excessive standard of Pb, Cd, Hg, and Cu was used as the research object, and the alkyl thiourea functionalised silica was used as a new heavy metal removal scavenger. The heavy metal removal process was optimised by orthogonal experiment with dynamic and static adsorption modes. Meanwhile, the content of *Acanthopanax B* and *Acanthopanax E*, the solid content, and the HPLC fingerprint similarity were used as quality monitoring indicators of *Acanthopanax senticosus* heavy metal removal before and after. Then, the technical adaptability of heavy metal removal by alkyl thiourea functionalised silica was evaluated. Under the optimal dynamic adsorption conditions, the average removal rates of Pb, Cd, Hg, and Cu were 91.64%, 93.04%, 81.77%, and 83.11%, respectively. Under the optimal static adsorption conditions, the average removal rates of Pb, Cd, Hg, and Cu were 82.22%, 89.95%, 81.26%, and 82.97%, respectively. During *Acanthopanax senticosus* extract heavy metal removal before and after, the change percentage of *Acanthopanax B* and *Acanthopanax E* was less than 2.00%, the solid content loss rate was only 0.18%, and the fingerprint similarity was over 99.9%. The method can be used to satisfy the high efficiency of selective removal of harmful elements in *Acanthopanax senticosus* extract and the effective composition of almost no effect; the method is simple and easy, so it can be recommended for pretreatment of heavy metals in Traditional Chinese Medicine extracts, and this way provides a new thought and research technique to decrease the contents of heavy metals.

1. Introduction

Heavy metals have obvious harmful effects on the body's metabolism and normal physiological functions. Excessive levels of heavy metals in the human body can lead to various diseases, such as diseases of the nervous system and blood system and even cancer [1, 2]. The content of heavy metals in Traditional Chinese Medicine is one of the important indicators to measure the quality of Traditional Chinese Medicine [3]. Due to the excessive pollution of heavy metals in

Traditional Chinese Medicine, many incidents occurred in developed countries in Europe and the United States and many were detained which has seriously restricted its international development level [4] and has a great negative impact on the international reputation of Traditional Chinese Medicine; hence, it has attracted the attention of the government and medical science and technologist [5, 6]. In order to solve the current drug safety and the emergency situation facing export, to overcome the problem of Traditional Chinese Medicine contaminated by harmful elements, it is

necessary to find a rapid, convenient, and suitable method for large-scale removal of harmful elements in Traditional Chinese Medicine [7], to strengthen the development and application of various removal technologies and adsorption materials, and to remove the harmful element units in the production of Traditional Chinese Medicine, such as extraction, to control the harmful metal content of the finished medicine at a reasonable level [8]. Due to the complexity of the form of harmful metals in Traditional Chinese Medicine, such as complexation or embedding with effective active ingredients and background values, traditional methods for removing harmful metals in recent years, such as alcohol precipitation, molecular imprinting, activated carbon adsorption, ion-exchange resin, and superfluid methods, still have many defects such as low yield, weak adsorption, large dosage, high cost, and loss of active ingredients [9, 10]. At present, it is only in the experimental research stage and is only reported in the literature, but it still lacks the industrial production mode [11]. Therefore, it is urgent to develop new harmful metal removal technologies with high selectivity, strong adsorption, and good industrial application value, which at the same time can protect the amount and efficacy of active ingredients [12].

Alkyl thiourea functionalised silica is a multifunctional polymer-modified silica material with a highly specific coordination group [13]. Currently, the removal of toxic catalysts in the world's synthetic pharmaceutical industry and the recovery of precious metals in the petroleum industry have been extensively applied [14–16], but the application of harmful element removal in Traditional Chinese Medicine extracts has not been reported in domestic and foreign literature. According to literature reports, silica gel loses its adsorption property after it absorbs water by 17%, which is only a carrier (macroporous resin method and activated carbon are difficult to meet this requirement), and the hydroxyl group on the surface can be coordinated by a modified heteroatom containing S and N (can be strongly complexed with heavy metal specificity) [17]. It can be predicted that the kinds of new solid adsorption technology will have broad market prospects in the field of removal of heavy metals in Traditional Chinese Medicine.

Acanthopanax senticosus is a very important Traditional Chinese Medicine. It has the same effect as ginseng. It can regulate the body's function, improve the body, and enhance the body's immunity, especially in the aspects of antifatigue, improving sleep, antioxidation, and filling gas blood, which all have very good effect to the body's health [18]. This study and the British PhosphonicS Ltd. company jointly carried out the use of alkyl thiourea functionalised silica as a model adsorption material, with *Acanthopanax senticosus* extract as a heavy metal pollution research object, to investigate the removal effect of Pb, Cd, Hg, and Cu; meanwhile, the content of *Acanthopanax B* and *Acanthopanax E*, the solid content, and the HPLC fingerprint similarity were used as quality monitoring indicators of *Acanthopanax senticosus* heavy metal removal before and after. Our study is aimed at judging the adaptability of alkyl thiourea functionalised

silica to remove heavy metals under the premise of protecting the active ingredients of Traditional Chinese Medicine. Furthermore, it provides a reference for the feasibility evaluation of this type of material and it resolves the drug safety and international development problems caused by excessive heavy metals in Traditional Chinese Medicine.

2. Materials and Methods

2.1. Materials. The materials used were as follows: Cd/Cu/Pb/Hg standard stock solution (National Nonferrous Metals and Electronic Materials Analysis and Testing Center); ICP-MS tuning fluid (Thermo Ltd.); ICP-MS Mass Calibration Solution (Thermo Ltd.); nitric acid (Suzhou Crystal Rui Chemical Co., Ltd.); hydrogen peroxide (Chongqing Chuanjiang Chemical Reagent Factory); alkyl thiourea functionalised silica (PhosphonicS Ltd., UK); *Acanthopanax senticosus* extract (Shaanxi Tiandiyuan Biotechnology Co., Ltd.); and *Acanthopanax B* and *Acanthopanax E* (Guizhou Dida Biotechnology Co., Ltd.).

2.2. Methods

2.2.1. Preparation of *Acanthopanax senticosus* Extract Solution. Weigh 50 g of *Acanthopanax senticosus* extract in a 200 mL volumetric flask; add about 150 mL of ultrapure water; add 2 mL of Pb, Cd, Hg, and Cu; mix standard solution with a concentration of $100 \mu\text{g}\cdot\text{mL}^{-1}$; perform ultrasound for 15 minutes at room temperature; and then make up to 200 mL with ultrapure water.

2.2.2. Quantitative Analysis of Pb, Cd, Cu, and Hg. Precisely measure 2.0 mL of *Acanthopanax senticosus* solution adsorbed before and after. Add 6 mL of HNO_3 (GR) and 2 mL of H_2O_2 (GR) in a Teflon bottle, shake it and mix it, seal, and predissolve for 10 hours. Digest by microwave digestion instrument, cool to room temperature, volatilize the acid to 1–2 mL liquid at 120°C , transfer it to a 25 mL volumetric flask, dilute to volume with ultrapure water, and determine Pb, Cd, Hg, and Cu simultaneously by ICP-MS.

2.2.3. Optimization of Static Adsorption Method and Condition. Weigh the appropriate amount of alkyl thiourea functionalised silica in a round bottom flask, add the *Acanthopanax senticosus* solution (Section 2.2.1), and put it into the air bath constant temperature oscillator to oscillate. The amount of alkyl thiourea functionalised silica, the oscillation frequency, the oscillation temperature, and the shock time were as a single factor investigated in this study, to determine the optimal range of each factor. On this basis, the orthogonal test of 4 factors and 3 levels was designed; the overall rating of average removal rates of heavy metals was used as the process evaluation index; then, the optimal static adsorption conditions of removal of heavy metals in the *Acanthopanax senticosus* was determined. The method for determination of heavy metals in optimal static process was referred in Section 2.2.2.

(1) *Effect of Alkyl Thiourea Functionalised Silica Dosage.* The amount of medicinal material/adsorbed dose was 30, 50, 80, and 120, respectively. The adsorption conditions (25°C, 260 times·min⁻¹, and 600 min) were used to analyze the effect of the amount of adsorbent on the removal rate.

(2) *Effect of Oscillation Frequency.* The amount of controlled medicinal material/adsorbed dose was 80, at low speed (80 times·min⁻¹), medium speed (160 times·min⁻¹), high speed (260 times·min⁻¹), and super high speed (360 times·min⁻¹) frequencies. Heavy metals in *Acanthopanax senticosus* solution were adsorbed for 600 min at 25°C. The effect of oscillation frequency on the removal rate was analyzed.

(3) *Effect of Adsorption Temperature.* The amount of controlled medicinal material/adsorbed dose was 80, and the heavy metals in the *Acanthopanax senticosus* solution were adsorbed for 600 min at a temperature of 15, 25, 35, and 45°C and 260 times·min⁻¹, respectively. The effect of adsorption temperature on the removal rate was analyzed.

(4) *Effect of Adsorption Time.* The amount of controlled medicinal material/adsorbed dose was 80, 25°C and 260 times·min⁻¹, and the heavy metals in *Acanthopanax senticosus* solution were adsorbed for 10, 30, 60, 120, 200, 400, 600, and 800 min, respectively. The effect of adsorption time on the removal rate was analyzed.

(5) *Orthogonal Test Design.* In order to investigate the interaction of various factors on the removal rate of heavy metals, based on the single-factor experiment, the orthogonal combination test of L9(34) was designed based on four factors: adsorption dosage, adsorption time, oscillation frequency, and adsorption temperature. The residual amount of Pb, Cd, Cu, and Hg in the *Acanthopanax senticosus* solution was determined (refer to Section 2.2.2).

2.2.4. Dynamic Adsorption Method and Condition Optimization. Accurately weigh the alkyl thiourea functionalised silica with the medicinal material/adsorbed dose which was 80, wetly load the column, equilibrate with ultrapure water, collect the liquid solution after passing through the solid adsorption column, and measure the residual amount of Pb, Cd, Cu, and Hg in the sample solution. In order to discuss the optimal dynamic adsorption process, this study evaluated the effects of different 4 factors of aspect ratio, elution speed, temperature, and sample loading on the removal rate. On this basis, the orthogonal test of 4 factors and 3 levels was designed to remove the heavy metals. Comprehensive scores of average removal rates of heavy metals were used as the process evaluation index to determine the optimal dynamic adsorption conditions of removal of heavy metals in the *Acanthopanax senticosus*. The method for determination of heavy metals in optimal dynamic process was referred in Section 2.2.2.

(1) *Influence of the Aspect Ratio.* Select three different adsorption columns (the diameter to height ratios are 1 : 10, 1 : 15, and 1 : 20); the loading is 100 mL, the elution temperature is 25°C, and the elution rate was 5 BV·h⁻¹ (the elution rate of a BV is equivalent to the volume of a solid adsorption

column), and the effect of the aspect ratio on the removal rate was analyzed.

(2) *Effect of the Elution Rate.* Select a column with an aspect ratio of 1 : 20; the loading was 100 mL, the elution temperature was 25°C, and the elution rate was 3, 5, 8, and 10 BV·h⁻¹, respectively. The effect on the removal rate was analyzed.

(3) *Effect of Sample Loading.* Select a column with diameter to column height of 1 : 20. The elution temperature is 25°C, the elution rate is 3 BV·h⁻¹, and the sample loading is 100, 200, 300, and 500 mL, respectively. The effect on the removal rate was analyzed.

(4) *Effect of Elution Temperature.* Select a column with an aspect ratio of 1 : 20, elute at 3 BV·h⁻¹, select 100 mL for sample loading, and analyze the temperature for removal at temperatures of 15, 25, 35, and 45°C, respectively. The effect on the removal rate was analyzed.

(5) *Orthogonal Test Design.* In order to investigate the interaction of various factors on the removal rate of heavy metals, based on the single-factor experiment, this paper will design the orthogonal combination of L9(34) with four factors: aspect ratio, sample loading, elution speed, and temperature. Measure 900 mL of *Acanthopanax senticosus* solution (Section 2.2.1); divide it into 9 parts, each 100 mL of liquid medicine; test according to the orthogonal design method; and determine residual content of Pb, Cd, Cu, and Hg in each sample (refer to Section 2.2.2).

2.2.5. Quality Evaluation of *Acanthopanax senticosus* Heavy Metal Removal Before and After. The content of *Acanthopanax B* and *Acanthopanax E*, the solid content, and the HPLC fingerprint similarity were used as quality monitoring indicators of *Acanthopanax senticosus* heavy metal removal before and after. Then, the technical adaptability of heavy metal removal by alkyl thiourea functionalised silica was evaluated.

(1) *Determination of *Acanthopanax B* and *Acanthopanax E* in Liquid Medicine.*

- (1) Preparation of the Test Solution. Precisely measure 1 mL of *Acanthopanax* solution (25% by mass) where heavy metals were removed before and after to 20 mL volumetric flask, make up to 80% methanol solution (volume), and perform ultrasound for 25 min; a test solution of about 12.5 mg·mL⁻¹ was obtained, the test solution was filtered by 0.22 μm microporous membrane, and then the filtrate was collected for analysis
- (2) Preparation of the Reference Substance *Acanthopanax B* Solution. Accurately weigh 0.48 mg of *Acanthopanax B*, make up to 5 mL (80% methanol solution) (mass concentration 96 μg·mL⁻¹), and perform ultrasound for 5 min
- (3) Preparation of the Reference Substance *Acanthopanax E* Solution. Accurately weigh 0.51 mg of *Acanthopanax E*, make up to 5 mL (80% methanol solution) (mass concentration 102 μg·mL⁻¹), and perform ultrasound for 5 min

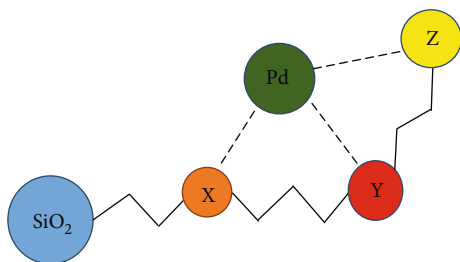


FIGURE 1: Schematic diagram of heavy metal removal.

- (4) Preparation of the Mixed Reference Solution of Acanthopanax B and Acanthopanax E. Accurately weigh 0.53 mg and 0.60 mg of reference substance Acanthopanax B and reference substance Acanthopanax E, make up to 5 mL (80% methanol solution) (concentrations of Acanthopanax B and Acanthopanax E were $106 \mu\text{g}\cdot\text{mL}^{-1}$ and $120 \mu\text{g}\cdot\text{mL}^{-1}$, respectively), and perform ultrasound for 5 min

(2) *Analysis of the Solid Content.* Taking the Acanthopanax senticosus heavy metal removal solution before and after as the research object, weigh 25 mL into the evaporating dish which had been dried to constant weight and evaporate to dryness in a boiling water bath. The drying was continued in a blast-drying oven at 105°C . Weigh it and calculate the solid content and loss rate of the liquid.

(3) *HPLC Fingerprint Similarity Evaluation.* To prepare the test solution, precisely measure 2 mL of the Acanthopanax heavy metal removal solution (25% by mass) before and after to a 10 mL volumetric flask, dilute to the mark with ultrapure water, and perform ultrasound for 25 min. The concentration of test solution was $50 \text{mg}\cdot\text{mL}^{-1}$. Filter with $0.22 \mu\text{m}$ microporous membrane and collect the continuous filtrate for analysis.

2.2.6. Principle of Heavy Metal Removal by the New Kinds of Scavenger. Figure 1 shows that heavy metal (Pd) is present in the Traditional Chinese Medicine freely or chemically bonded to the active ingredient in Traditional Chinese Medicine (e.g., Y or Z). The alkyl thiourea-bonded silica (SiO_2 bonding organic functional group X) used in this study is competitively heavy metal-binding with the active ingredient of the Traditional Chinese Medicine (e.g., Y or Z), thereby performing heavy metal removal, similar to the tug-of-war effect. Hence, the alkyl thiourea-bonded silica forms a chelate with the heavy metal.

3. Results

3.1. Static Adsorption and Condition Optimization Results

3.1.1. Effect of the Amount of Scavenger on the Removal Rate of Heavy Metals. Figure 2 shows that the removal rate of Pb, Cd, Hg, and Cu was close to the maximum when the ratio of medicinal material/adsorbent dose was 80. If the ratio of medicinal material/adsorbent dosage continues to increase, the removal rate of heavy metals was significantly reduced.

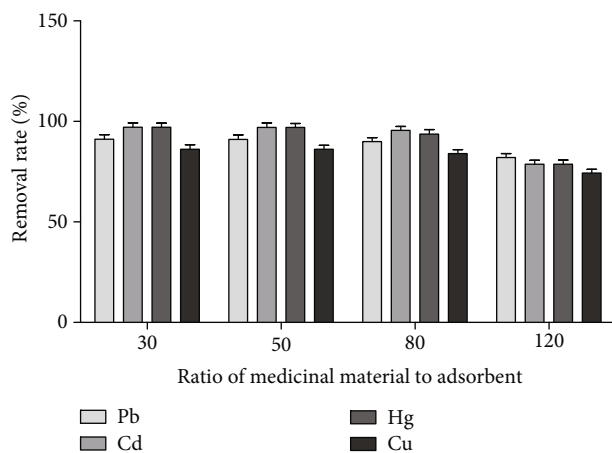


FIGURE 2: Effect of the amount of scavenger on the removal rate of heavy metals ($n = 3$).

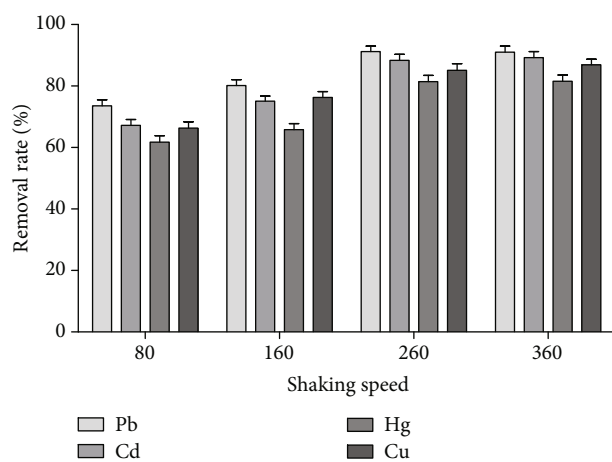


FIGURE 3: The effect of shaking speed on the removal rate of heavy metals ($n = 3$).

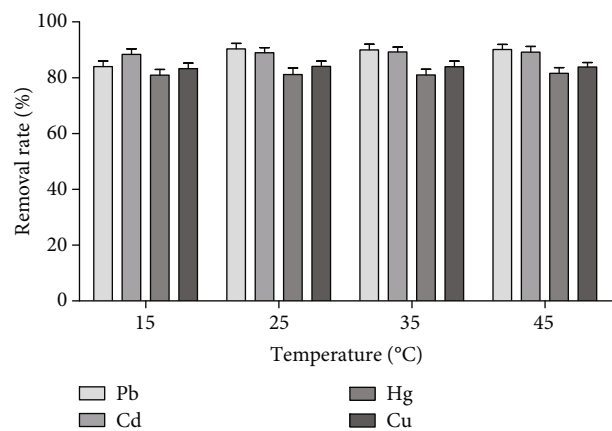


FIGURE 4: The effect of temperature on the removal rate of heavy metals ($n = 3$).

3.1.2. Influence of Oscillation Frequency on the Removal Rate of Heavy Metals. Figure 3 shows that within a certain oscillation frequency range, the removal rate of heavy metals was

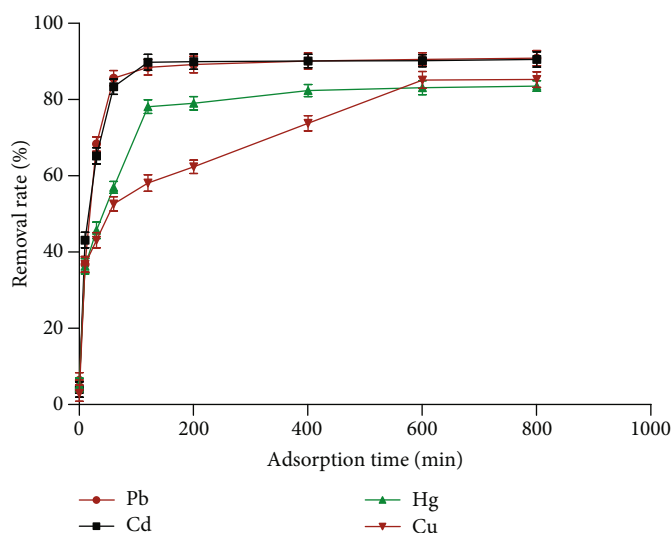


FIGURE 5: The effect of scavenging time on the removal rate of heavy metals ($n = 3$).

TABLE 1: The results of the orthogonal test.

Serial number	A	B	C	D	Results (rate removal of heavy metals (%))				Average rate of removal
					Pb	Cd	Hg	Cu	
1	1	1	1	1	65.66	58.69	43.97	45.97	53.57
2	1	2	2	2	85.63	89.93	81.79	61.69	79.76
3	1	3	3	3	87.37	91.12	82.27	84.97	86.43
4	2	1	2	3	66.12	63.00	49.76	43.03	55.48
5	2	2	3	1	82.19	87.27	76.25	65.37	77.76
6	2	3	1	2	72.34	65.34	59.33	63.14	65.04
7	3	1	3	2	66.31	63.00	46.28	41.26	54.21
8	3	2	1	3	69.37	65.08	62.00	58.08	63.63
9	3	3	2	1	80.06	73.17	63.07	74.25	72.64
K1	73.25	54.42	60.75	67.99					
K2	66.09	73.72	69.23	66.37					
K3	63.49	74.70	72.80	68.51					
R	9.76	20.28	12.05	2.18					

proportional to the oscillation frequency. When the oscillation frequency reached $260 \text{ times} \cdot \text{min}^{-1}$, the removal rate of heavy metals no longer increased significantly.

3.1.3. *Effect of Adsorption Temperature on the Removal Rate of Heavy Metals.* Figure 4 shows that the effect of temperature on the removal rate of heavy metals was not obvious.

3.1.4. *Effect of Adsorption Time on the Removal Rate of Heavy Metals.* Figure 5 shows that the adsorption time was proportional to the removal rate in a certain adsorption time. The removal rates of Pb, Cd, and Hg did not increase significantly after 120 min of adsorption time, but the removal rate of Cu did not increase after 600 min. Pb, Cd, and Hg had a faster removal rate than Cu since the adsorption reaches a short saturation time.

3.1.5. *Orthogonal Test Analysis Results.* From the results of the orthogonal test (Table 1), it can be seen that the influence of four factors on the removal rate of heavy metals was significant. The primary and secondary order was $B > C > A > D$. The D factor with the smallest difference was used as the error term for variance analysis. The analysis results (Table 2) indicated that factor B had a significant difference, which indicated that the adsorption time has a greater impact on the removal rate of heavy metals. According to the analysis results, the optimal static adsorption process conditions for Pb, Cd, Hg, and Cu in the aqueous solution of *Acanthopanax senticosus* extract were $A_1B_3C_3D_3$.

3.1.6. *Verification Test Results for Optimal Process Conditions.* The following optimal adsorption process conditions were

TABLE 2: The results of analysis of variance.

Source of variance	SS	<i>f</i>	MS	<i>F</i>	<i>P</i>
A	153.28	2	19.79	19.00	<0.05
B	784.75	2	101.32	19.00	<0.05
C	230.63	2	29.78	19.00	<0.05
D (errors)	7.75	2	1.00	19.00	

Note: $P < 0.05$ indicates that the difference is statistically significant.

TABLE 3: The test results of the optimal process conditions.

Sample serial number	Rate removal of heavy metals (%)			
	Pb	Cd	Hg	Cu
1	83.31	89.26	82.89	85.17
2	83.29	91.47	83.03	83.12
3	84.27	90.12	80.28	82.26
4	85.34	90.91	81.79	84.53
5	83.27	89.25	82.51	82.64
6	83.43	91.33	80.01	83.39
Average	82.12	89.21	81.27	82.47
RSD	1.27	1.49	1.78	1.34

adopted: the amount of medicinal material/adsorbent was 80, the oscillation frequency was 260 times·min⁻¹, the adsorption time was 600 min, the adsorption temperature was 45°C, and the 6 parallel tests were carried out to verify the process conditions and obtain higher removal. Table 3 shows that the removal rate of heavy metals was more than 81% and the RSD value was all less than 2.00, so this process was reasonable and reliable.

3.2. Dynamic Adsorption and Condition Optimization Results

3.2.1. Effect of Diameter to Column Height on the Removal Rate of Heavy Metals. Figure 6 shows that the removal rate of Pb, Cd, Hg, and Cu was the largest when the effect of diameter to column height was 0.05. The smaller the diameter to column height, the higher the column efficiency and the higher the removal rate of heavy metals, but the greater the resistance and the slower the flow rate. Therefore, the choice of the diameter to column height depends on the viscosity of the sample to be purified.

3.2.2. Effect of the Elution Rate on the Removal Rate of Heavy Metals. Figure 7 shows that in the dynamic adsorption process, the elution rate was directly related to the removal rate of heavy metals. The faster the elution rate, the worse the removal effect was. When the elution rate reached 5 BV·h⁻¹, the purpose of efficiently removing heavy metals can be satisfied.

3.2.3. Effect of Sample Loading on the Removal Rate of Heavy Metals. Figure 8 shows that there was a direct relationship between the amount of sample and the removal rate of heavy metals. The results showed that the removal rate of heavy metals was close to the maximum when the sample volume was 200 mL.

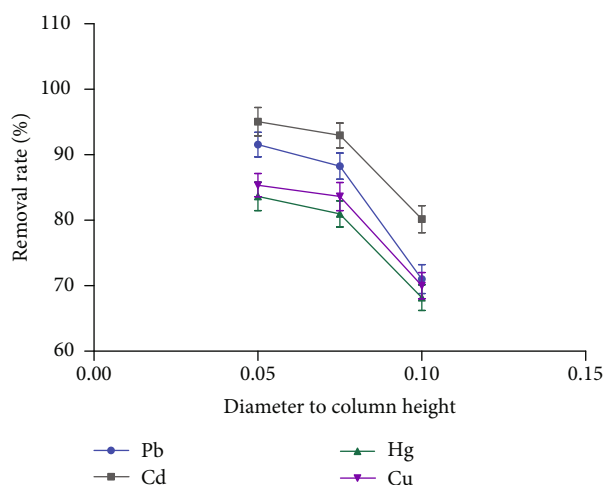


FIGURE 6: The effect of diameter to column height on the removal rate of heavy metals ($n = 3$).

3.2.4. Effect of Elution Temperature on the Removal Rate of Heavy Metals. Figure 9 shows that the effect of temperature on the removal rate of heavy metals was not obvious.

3.2.5. Orthogonal Test Analysis Results. From the results of the orthogonal test (see Table 4), it can be seen that the influence of four factors on the removal rate of heavy metals was significant. The primary and secondary order was $F > G > E > K$, and the K factor with the smallest difference was used as the error term for variance analysis. The results of the analysis of variance (Table 5) indicated that both factors F and G have significant differences and indicated that both the loading and elution rates had a large effect on the removal rate of heavy metals. According to the analysis results, the optimal dynamic adsorption process conditions for removal of Pb, Cd, Hg, and Cu in the aqueous solution of *Acanthopanax senticosus* extract were $E_3F_1G_1K_1$.

3.2.6. Verification Test Results for Optimal Process Conditions. The optimal adsorption process conditions were as follows: the diameter to column height ratio was 1 : 20, the sample loading was 100 mL, the elution rate was 3 BV·h⁻¹, the elution temperature was 15°C, and the 6 parallel tests were performed to verify the process conditions and obtain higher. The metal removal rate and the RSD value were both less than 2.00%. The results are shown in Table 6. So the process of metals removed was reasonable and reliable.

3.3. Result Quality of *Acanthopanax senticosus* Heavy Metal Removal Before and After

3.3.1. The Content of *Acanthopanax B* and *Acanthopanax E* in Sample Liquid. Table 7 shows that active ingredients *Acanthopanax glycosides B* and *E* were not affected by heavy metal removal before and after, and the rate of change was less than 2%.

Figure 10 displays the mixed control and testing sample HPLC chromatogram.

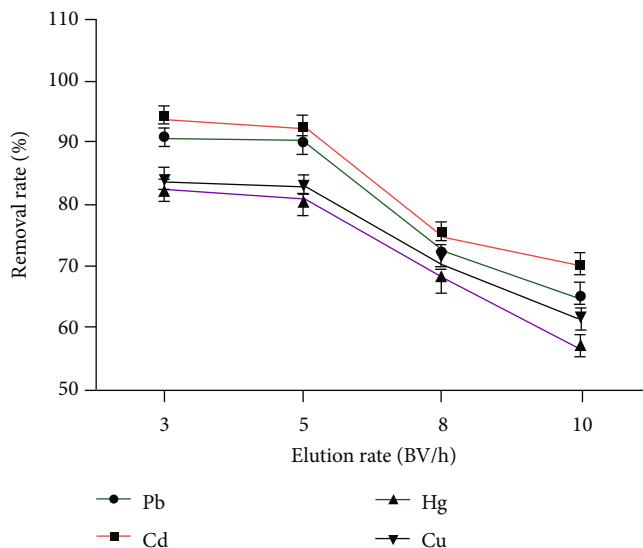


FIGURE 7: The effect of washing speed on the removal rate of heavy metals ($n = 3$).

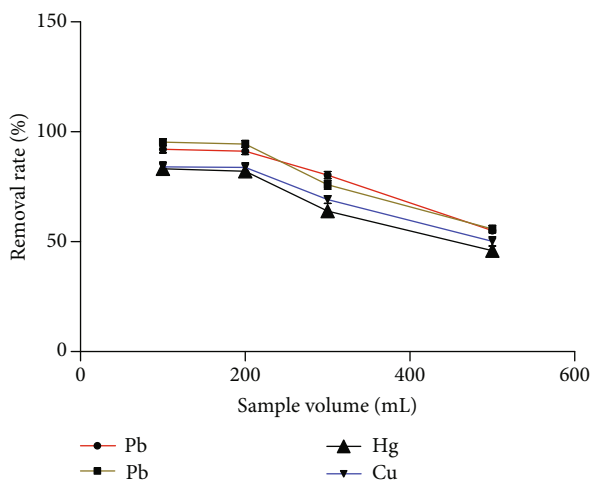


FIGURE 8: The effect of sample volume on the removal rate of heavy metals ($n = 3$).

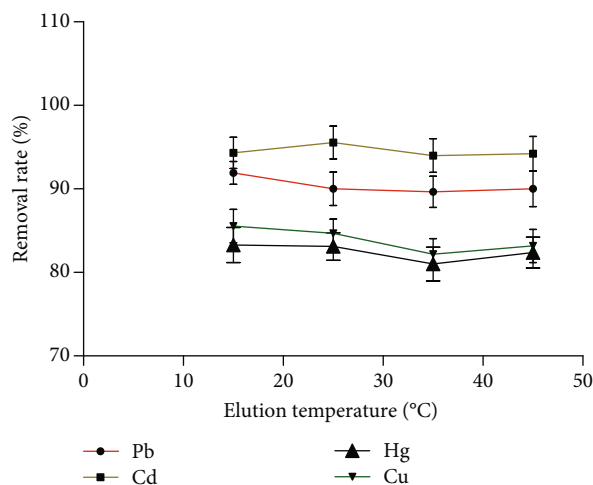


FIGURE 9: The effect of washing temperature on the removal rate of heavy metals ($n = 3$).

3.3.2. *Analysis of Solid Content of the Drug Solution Adsorption Before and After.* The solid content of the liquid before and after removal was $227.38 \text{ mg}\cdot\text{mL}^{-1}$ and $225.62 \text{ mg}\cdot\text{mL}^{-1}$, respectively, and the loss rate was only 0.18%, which indicated that there was no obvious loss of solid content before and after removal of heavy metals by using new solid adsorbent.

3.3.3. *Evaluation Results of HPLC Fingerprint Similarity Adsorption Before and After.* The HPLC fingerprints of *Acanthopanax senticosus* heavy metal adsorption before and after were analyzed. The results showed that the active composition ingredients of *Acanthopanax senticosus* did not change. The “Traditional Chinese Medicine fingerprint similarity evaluation system (version 2.0)” issued by the National Pharmacopoeia Committee was adopted, which

analyzed *Acanthopanax senticosus* after heavy metal removal and obtained the control fingerprint by using the pre-adsorption spectrum as a reference. Based on this, the overall similarity evaluation was performed, and 6 parallel experiments were performed. The chromatographic peaks of the HPLC spectra before and after removal of heavy metals were matched with each other, and the similarity evaluation results were all greater than 99.9%. The results are shown in Figure 11.

4. Conclusion

In this study, the samples of the extracts of Traditional Chinese Medicine to be purified that exceeded the standard of heavy metals were prepared, and the main production operation units involved in the extraction process of

TABLE 4: The results of the orthogonal test.

Serial number	E	F	G	K	Results (rate removal of heavy metals (%))				
					Pb	Cd	Hg	Cu	Average rate of removal
1	1	1	1	1	82.07	85.13	82.31	85.95	83.89
2	1	2	2	2	80.16	79.55	78.00	79.71	79.36
3	1	3	3	3	60.07	63.08	67.33	64.93	63.85
4	2	1	2	3	85.13	89.61	72.14	73.05	80.11
5	2	2	3	1	79.39	82.18	68.66	72.37	75.65
6	2	3	1	2	79.60	73.33	61.76	67.34	70.51
7	3	1	3	2	79.88	85.06	75.64	77.08	79.42
8	3	2	1	3	92.67	95.05	82.17	84.96	88.72
9	3	3	2	1	78.69	84.38	69.12	71.65	75.96
K1	75.70	81.13	81.03	78.42					
K2	75.88	81.09	78.43	76.76					
K3	80.78	70.19	72.89	77.18					
R	5.08	10.91	8.15	1.65					

TABLE 5: The results of analysis of variance.

Source of variance	SS	<i>f</i>	MS	<i>F</i>	<i>P</i>
E	49.85	2	11.237	19.00	
F	237.40	2	53.52	19.00	<0.05
G	103.87	2	23.45	19.00	<0.05
K (errors)	4.46	2	1.00	19.00	

Note: $P < 0.05$ indicated that the difference is statistically significant.

TABLE 6: The test results of the optimal process conditions.

Sample serial number	Rate removal of heavy metals (%)			
	Pb	Cd	Hg	Cu
1	91.10	93.57	80.11	85.21
2	90.21	95.17	82.19	81.47
3	93.17	92.67	83.57	84.15
4	91.24	92.33	80.37	83.64
5	92.16	91.27	82.87	80.78
6	91.76	93.01	81.22	83.17
Average	91.67	93.00	81.76	83.19
RSD	1.26	1.39	1.97	1.99

TABLE 7: Determination results of Eleutheroside B and Eleutheroside E with or without metal removal.

Indicator components	Control	Sample 1	Sample 2	Quality score (%)				Rate of change (%)
				Sample 3	Sample 4	Sample 5	Sample 6	
Acanthopanax B	0.556	0.561	0.563	0.559	0.547	0.566	0.567	1.35
Acanthopanax E	0.957	0.960	0.982	0.969	0.972	0.971	0.978	1.67

Traditional Chinese Medicine, such as stirring extraction and dynamic column, were designed. The static stirring mode and dynamic column mode were used to remove heavy metals. The process research, while examining the single-factor influence removal rate and orthogonal exper-

iment optimization optimal process, obtained a better removal effect; dynamic and static adsorption can achieve more than 80% heavy metal removal rate.

The carrier of the novel solid adsorption bonding material used in the research is silica gel. When the water

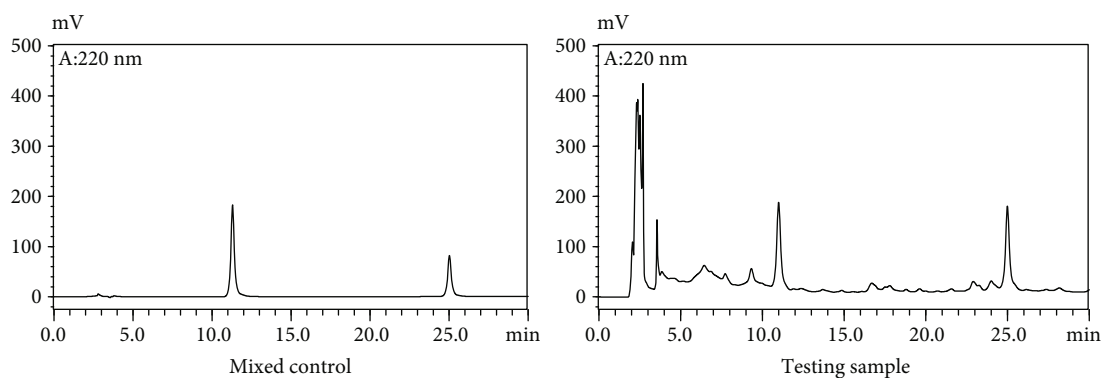


FIGURE 10: HPLC chromatogram.

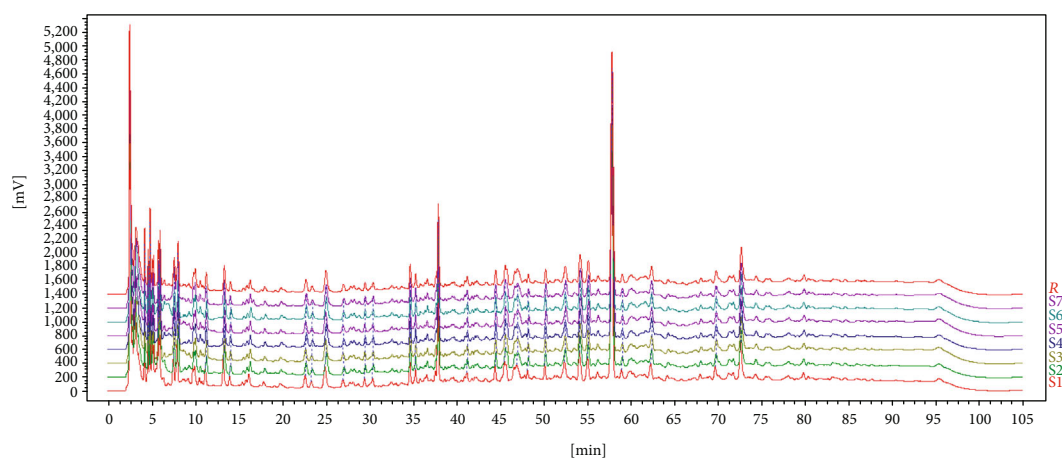


FIGURE 11: Evaluate results of the similarity on fingerprint with or without metal removal.

content of silica gel exceeds 17%, the adsorption property is not suitable. It is especially suitable for Chinese medicine liquid (aqueous liquid or alcohol liquid); that is, the adsorbent is harmful in removing heavy metals. At the same time, the elements do not significantly affect the active ingredients of Traditional Chinese Medicine. By comprehensively analyzing the content of index components, solid content loss rate, and HPLC fingerprint before and after removing heavy metals from *Acanthopanax senticosus* extract aqueous solution, it is further verified that the alkyl thiourea-bonded silica gel removed Pb, Cd, Hg, and Cu. The chemical composition has not changed significantly, and the experimental design purpose of selective and high-efficiency removal of heavy metals under the premise of protecting the active constituents of *Acanthopanax senticosus* extract (unilateral medicinal materials) has been achieved, and it has good industrial application value.

Data Availability

The data sets used and/or analyzed during the current study are available from the corresponding author on reasonable request.

Conflicts of Interest

The authors have declared that there is no conflict of interests regarding the publication of this paper.

Acknowledgments

This work was supported by the Guizhou Traditional Chinese Medicine Modernization Technology Industry (Qian-kehe Chinese characters, 5010).

References

- [1] A. Woźniak, A. Kujawa, M. Seńczuk-Przybyłowska et al., "Physiological metals in the serum, hair and nails of patients with head and neck cancer," *Przegląd Lekarski*, vol. 69, no. 10, pp. 785–797, 2012.
- [2] L. Chang, S. Shen, Z. Zhang, X. Song, and Q. Jiang, "Study on the relationship between age and the concentrations of heavy metal elements in human bone," *Annals of Translational Medicine*, vol. 6, no. 16, p. 320, 2018.
- [3] M. L. Coghlan, G. Maker, E. Crighton et al., "Combined DNA, toxicological and heavy metal analyses provides an auditing toolkit to improve pharmacovigilance of traditional Chinese medicine (TCM)," *Scientific Reports*, vol. 5, no. 1, article 17475, 2015.

- [4] I.-S. Yu, J.-S. Lee, S.-D. Kim et al., "Monitoring heavy metals, residual agricultural chemicals and sulfites in traditional herbal decoctions," *BMC Complementary and Alternative Medicine*, vol. 17, no. 1, p. 154, 2017.
- [5] A. Yu, D. Adelson, and D. Mills, "Chinese herbal medicine versus other interventions in the treatment of type 2 Diabetes," *Journal of Evidence-Based Integrative Medicine*, vol. 23, 2018.
- [6] A. X. Lin, G. Chan, Y. Hu et al., "Internationalization of traditional Chinese medicine: current international market, internationalization challenges and prospective suggestions," *Chinese Medicine*, vol. 13, no. 1, pp. 1–6, 2018.
- [7] W. Xie, C. Peng, H. Wang, and W. Chen, "Health risk assessment of trace metals in various environmental media, crops and human hair from a mining affected area," *International Journal of Environmental Research and Public Health*, vol. 14, no. 12, p. 1595, 2017.
- [8] S. De Jonge, Q. Boldingh, J. Solomkin et al., "Abstracts from the 5th International Conference on Prevention & Infection Control (ICPIC 2019)," *Antimicrobial Resistance and Infection Control*, vol. 8, article 148, S1, 2019.
- [9] M. P. Stewart, R. Langer, and K. F. Jensen, "Intracellular delivery by membrane disruption: mechanisms, strategies, and concepts," *Chemical Reviews*, vol. 118, no. 16, pp. 7409–7531, 2018.
- [10] J. Yang, B. Hou, J. Wang et al., "Nanomaterials for the removal of heavy metals from wastewater," *Nanomaterials*, vol. 9, no. 3, p. 424, 2019.
- [11] M. T. Bankole, A. S. Abdulkareem, I. A. Mohammed et al., "Selected heavy metals removal from electroplating wastewater by purified and polyhydroxybutyrate functionalized carbon nanotubes adsorbents," *Scientific Reports*, vol. 9, no. 1, pp. 1–19, 2019.
- [12] M. Junaid, M. Z. Hashmi, Y. M. Tang, R. N. Malik, and D. S. Pei, "Potential health risk of heavy metals in the leather manufacturing industries in Sialkot, Pakistan," *Scientific Reports*, vol. 7, no. 1, p. 8848, 2017.
- [13] B. Duan, W. Zhang, H. Zheng, C. Wu, Q. Zhang, and Y. Bu, "Disposal situation of sewage sludge from municipal wastewater treatment plants (WWTPs) and assessment of the ecological risk of heavy metals for its land use in Shanxi, China," *International Journal of Environmental Research and Public Health*, vol. 14, no. 7, p. 823, 2017.
- [14] L. C. Sjøberg, R. Winston, M. Viklander, and G. T. Blecken, "Dissolved metal adsorption capacities and fractionation in filter materials for use in stormwater bioretention facilities," *Water Research X*, vol. 4, p. 100032, 2019.
- [15] N. Galaffu, S. P. Man, R. D. Wilkes, and J. R. H. Wilson, "Highly functionalised sulfur-based silica scavengers for the efficient removal of Palladium species from active pharmaceutical ingredients," *Organic Process Research & Development*, vol. 11, no. 3, pp. 406–413, 2007.
- [16] Y. J. Yang, X. W. Liu, X. J. Kong et al., "Preparation and evaluation of oseltamivir molecularly imprinted polymer silica gel as liquid chromatography stationary phase," *Molecules*, vol. 23, no. 8, p. 1881, 2018.
- [17] Y. H. Kim, M. L. Cho, D. B. Kim et al., "The antioxidant activity and their major antioxidant compounds from *Acanthopanax senticosus* and *A. koreanum*," *Molecules*, vol. 20, no. 7, pp. 13281–13295, 2015.
- [18] K. M. Lau, G. G. Yue, Y. Y. Chan et al., "A review on the immunomodulatory activity of *Acanthopanax senticosus* and its active components," *Chinese Medicine*, vol. 14, p. 25, 2019.

Research Article

Abundance of Multidrug Resistance Efflux Pumps in the Urinary Metagenome of Kidney Transplant Patients

Asha Rani ¹, Ravi Ranjan ¹, Ahmed A. Metwally,^{1,2} Daniel C. Brennan,³ Patricia W. Finn,^{2,4,5} and David L. Perkins ^{2,6,7}

¹Department of Medicine, University of Illinois at Chicago, Chicago, IL 60612, USA

²Department of Bioengineering, University of Illinois at Chicago, Chicago, IL 60612, USA

³Department of Medicine, Johns Hopkins School of Medicine, Baltimore, MD 21287, USA

⁴Division of Pulmonary, Critical Care, Sleep, and Allergy, Department of Medicine, University of Illinois at Chicago, Chicago, IL 60612, USA

⁵Department of Microbiology and Immunology, University of Illinois at Chicago, Chicago, IL 60612, USA

⁶Division of Nephrology, Department of Medicine, University of Illinois at Chicago, Chicago, IL 60612, USA

⁷Department of Surgery, University of Illinois at Chicago, Chicago, IL 60612, USA

Correspondence should be addressed to David L. Perkins; perkinsd@uic.edu

Received 29 September 2019; Accepted 23 January 2020; Published 13 March 2020

Guest Editor: Guo-qi Wen

Copyright © 2020 Asha Rani et al. This is an open access article distributed under the Creative Commons Attribution License, which permits unrestricted use, distribution, and reproduction in any medium, provided the original work is properly cited.

Antibiotic resistance including the emergence of multidrug resistant microbes has become a public health crisis. In this study, we analyzed the antibiotic resistance genes (ARGs) in the urinary metagenome of the kidney transplant and healthy subjects using metagenomic shotgun sequencing. Our data suggest an increased abundance of antibiotic resistance genes in the kidney transplant subjects. In addition, the antibiotic resistance genes identified in the transplant subjects were predominantly composed of multidrug efflux pumps (MDEPs) which are evolutionarily ancient, commonly encoded on chromosomes rather than plasmids, and have a low rate of mutation. Since the MDEPs had a low abundance in the healthy subjects, we speculate that the MDEPs may enhance the fitness of bacteria to survive in the high stress environment of transplantation that includes multiple stressors including surgery, antibiotics, and immunosuppressive agents.

1. Introduction

Antibiotic resistance has emerged as a major medical and public health challenge which has been driven, in part, by the misuse of antibiotics in both the clinical and agricultural arenas [1, 2]. Exposure to clinical levels of antibiotics can promote mutations inducing enhanced antibiotic resistance and the emergence of multidrug resistant strains. Following kidney transplantation, infections remain a major complication, and the most common type of acute infection following solid organ transplantation is bacterial [3, 4]. Consequently, subjects are frequently treated with prophylactic antibiotics, for example, sulfamethoxazole-trimethoprim, which we previously reported can induce increased levels of antibiotic resistance genes (ARGs) in the urinary metagenome [5]. Specifically, we reported increased

levels of dihydrofolate synthase/folylpolyglutamate synthase, two enzymes that can increase folate production but are not blocked by sulfamethoxazole-trimethoprim in subjects that developed urinary tract infections following transplantation.

There are multiple mechanisms for the selection and development of ARGs, but the contribution of the various mechanisms has not been clearly elucidated. Based on the genetic analysis of bacterial genomes, it is estimated that there are more than 20,000 antibacterial resistance genes (ARGs) comprising approximately 400 different types [6]. ARGs are evolutionarily ancient and were present before the advent of antibiotics indicating that ARGs have biological functions in addition to inhibiting effects of antibiotics. In vitro studies have shown that ARGs can inhibit transcription and modulate metabolism suggesting important biological functions in natural ecosystems [7]. Thus, the contribution

of antibiotics and resistance to antibiotics is not well understood in terms of resilience or susceptibility to adverse outcomes including infection or graft rejection in kidney transplantation.

One of the most studied types of ARGs is the beta-lactamases that produce resistance to penicillin. Beta-lactamases are usually expressed on plasmids and can generate new specificities of resistance within days due to the accumulation of point mutations. In contrast, another class of ARGs is the multidrug efflux pumps (MDEPs), which are encoded in the bacterial chromosomes, expressed in all members of a species, and mutate slowly, and thus are not selected by exposure to antibiotics. The MDEPs are ancient genes present in prokaryotes, archaeobacteria, and eukaryotes including mammals. An important example in clinical medicine is p-glycoprotein, which can be responsible for resistance to chemotherapy agents. There are five types of MDEPs in bacteria which have diverse functions including quorum sensing and detoxification of heavy metals, bile salts, and bacterial metabolites. Since the MDEPs emerged early in evolution their original functions were not to convey resistance to antibiotics; nevertheless, the efflux pumps are effective mechanisms to generate antibiotic resistance [8, 9].

To investigate the spectrum of ARGs within the kidney transplant and healthy subjects, we employed shotgun metagenomic sequencing (MGS) in the urinary metagenome. In contrast to targeted 16S rRNA amplicon sequencing, MGS sequencing identifies nearly complete genomes that can identify bacterial taxa at the species level and thus annotate the complete array of ARGs. Interestingly, our study identifies major changes in the profile of ARGs in kidney transplant subjects.

2. Material and Methods

2.1. Study Design, Ethics Statement, Metagenome DNA Isolation, and Sequencing. The objective of this study was to investigate the antibiotic resistance genes (ARGs) contributed by the urinary microbiome of kidney transplant recipients and healthy subjects using shotgun metagenomic sequencing. As previously described, urine samples were collected post-transplant from kidney transplant recipients and controls [5] and 17 additional controls described in Table S1. Similar to the DNA isolation method, library preparations were performed and were sequenced on Illumina MiSeq with 301 paired end chemistry. This study was approved by the Washington University School of Medicine Institutional Review Board, St. Louis, Missouri (IRB ID # 201102312, Protocol Number # 07-0430) and by the University of Illinois Institutional Review Board, Chicago, Illinois (IRB # 2014-1227).

2.2. Bioinformatic Analyses and Antibiotic Resistance Gene Annotation. Raw reads from transplant and control samples were quality filtered and trimmed to remove human sequences using CLC genomics workbench default parameters (CLC bio, Qiagen). High quality filtered reads were *de novo* assembled into contigs, and reads were mapped back to

contigs to generate the number of reads per contig. The sequence data was aligned with the antibiotic resistance genes in the ARDB (Antibiotic Resistance Genes Database) using 80% identity and e -value of $1e^{-5}$ over 80% alignment length of the ORF/gene [6]. ARDB allows the search against antibiotic resistance genes, type, organism, and antibiotic class. A csv file format with antibiotic gene, bacterial taxonomy, and antibiotic class associated with each sample was retrieved. The data file was normalized by dividing the number of reads aligned to each resistance gene/total reads used in the analysis and was converted to a square data matrix for further analysis. Data corresponding to both functional and taxonomical distributions were analyzed using MG-RAST SEED database using 80% similarity cutoff [10].

2.3. Statistical Analyses. Principal Coordinate Analysis (PCoA) was performed to find the axis that best explains the variance in the ARGs data set. The PCoA plot was generated using the Bray-Curtis Dissimilarity matrix for ARGs abundance between transplant and control group. In order to test for significant differences in the transplant and control group, a one-way analysis of similarity (ANOSIM) was conducted as described [11]. SIMPER (Similarity Percentage) analysis was performed to find the ARGs which contributed towards the % dissimilarity among the groups. ANOSIM and SIMPER analyses were performed using PAST statistical software v 3.0 [12]. Differences between two groups were assessed using the Mann-Whitney U Test and Wilcoxon Rank Test. A p -value of ≤ 0.05 considered as a significant difference after multiple test corrections with Benjamini-Hochberg false discovery rate (FDR). Data sets that involved more than two groups were assessed by analysis of variance (ANOVA) followed by Tukey's multiple comparison *post hoc* tests. Data were analyzed using GraphPad Prism (GraphPad Software, San Diego, CA, USA) and were considered as statistically significant with $p \leq 0.05$ unless otherwise indicated.

2.4. High-Throughput Sequencing Data Availability. The sequence data for the study has been submitted to the MG-RAST web server under the following accession number provided in Table S2.

3. Results

Transplant subjects are exposed to multiple stressors including surgery, immunosuppression, and antibiotics. We analyzed the abundance of antibiotic resistance genes (ARGs) in the urinary metagenome in kidney transplant recipients versus controls (Table 1). We performed metagenomic shotgun sequencing (MGS) of additional 17 controls for this study, which generated a total of 312×10^6 raw reads. The raw reads were filtered to remove human sequences and were assembled into 1,429,333 contigs (Table S2). We identified ARGs in 10 out of 21 transplants, and 19 out of 25 controls. To compare the metagenomes of the kidney transplant and control subjects, we performed Principal Coordinate Analysis (PCoA) which projected separation of the two groups based on the ARGs identified in each sample with 26.5% of the

TABLE 1: Relative abundance of bacterial genus in Transplant and Control group. Genera are selected on the basis of >1% abundance in each group. Genera identified in both groups are shown in bold font. The significance of the difference among bacterial genera was computed using Students *t*-test ($*p \leq 0.05$).

Transplant		Control	
Genus	% Abundance	Genus	% Abundance
Enterococcus *	28.6	Ralstonia *	33.2
Escherichia **	12.7	Propionibacterium *	10.9
Ralstonia *	9.6	Enterococcus *	7.2
Shigella **	7.4	Neisseria *	7.1
Propionibacterium*	4.8	Bifidobacterium	5.0
Proteus	4.4	Corynebacterium*	3.8
Streptococcus	3.4	Streptococcus	2.5
Lactobacillus	2.9	Lactobacillus	2.3
Bacteroides	2.4	Burkholderia	2.0
Neisseria *	2.2	Cupriavidus	1.7
Salmonella*	1.6	Bacteroides	1.7
Burkholderia	1.3	Prevotella **	1.4
Staphylococcus *	1.2	Pseudomonas	1.1
Citrobacter	1.1	Mobiluncus *	1.1

variance defined by the first principal coordinate (Figure 1). Variance of the control group ARGs profile was primarily encompassed in the first principal coordinate, whereas the variance of the transplant resistome was predominantly within the second principal coordinate.

We compared the relative abundance of the genera of the two groups with the *Wilcoxon* rank test which showed different ranks in the groups ($p \leq 0.05$) (Table 1). Of note, the genus *Enterococcus*, which we previously reported to express genes predicting resistance to sulfamethoxazole-trimethoprim [5] comprised 28.6% of the transplant microbiome, but only 7.2% of the control microbiome. In contrast, the *Propionibacterium* genus comprised 10.9% of the control microbiome, but only 4.8% of the transplant microbiome. Overall, 4 genera were unique to the transplant microbiome and 4 genera were unique to the control microbiome, and 8 genera were detected in both microbiomes (Table 1). We also analyzed the diversity in the ARGs among the groups. The Shannon diversity index (based on ARG abundance) was significantly higher in the transplant group at 2.1 versus 0.4 in the control group ($p \leq 0.001$); similarly, the evenness was greater in the transplant group (Figures 2(a) and 2(b), respectively).

To identify potential differential functions in the transplant and control metagenomes, we employed the SEED database in MG-RAST v2.0 to identify the relative abundance of ARGs. Analysis of level_1 did not detect significant differences; however, analysis of the more specific level_2 of MG-RAST detected increased “Resistance to antibiotics and toxic compounds” in the transplant group (Figure 3). Overall, we detected 29 unique ARGs in the transplant group, 8 unique in the control group, and 7 that were detected in both groups (Figure 4(a)). The mean number of unique ARGs per patient was 16 in the transplant group, but only 2 in the control group (Figure 4(b)). Next, we determined the predicted spectrum of antibiotic resistance genes based on the metagenomes in each group. Analysis of the relative abundance of ARGs indicated a more diverse profile in the transplant subjects compared with control subjects (Figure 5(a)). In addition, a comparison of

the specificity of the resistance profiles showed different profiles in the two groups (Figure 5(b)). For example, the transplant subjects indicated resistance to 16 of the 17 antibiotics class analyzed. In contrast, the control subjects indicated resistance to a subset of the antibiotics that included bacitracin, chloramphenicol, erythromycin, fluoroquinolone, fosmidomycin, penicillin, and tetracycline. In addition to these antibiotics, the transplant subjects were also resistant to aminoglycosides, cephalosporins, fosfomycin, norfloxacin, kasugamycin, lincomycin, macrolides, and polymyxin. Thus, transplant subjects have a broader profile of antibiotic resistance and a greater abundance of antibiotic resistance genes that is often an order of magnitude greater than in the control subjects.

Since we employed MGS sequencing we were able to identify specific genes in the microbiota. Although some ARGs were detected at low levels, we detected a total of 44 ARGs from both groups, 36 were detected in transplant, and 15 in the control group, both groups shared 7 ARGs (Figure 6). Only 3 ARGs were abundant in the control subjects: *ermf* (a methyl transferase), *pbp2b* (beta-lactamase), and *rosa* (efflux pump/potassium antiporter); however, all 3 were identified at extremely low absolute levels in the transplant group. Interestingly, 14 (above 0.1 gene abundance) unique ARGs were identified in the transplant urinary metagenome suggesting a diverse baseline repertoire of ARGs. Since gender can affect susceptibility to urinary tract infections and has been shown to modify the urinary microbiome [13], we also compared the effect of gender in the 2 groups (Figure 7(a)). We detected changes associated with gender in both the transplant and control groups; however, a Principal Coordinate Analysis showed that the strongest association was between transplant versus control (Figure 7(b)). The SIMPER analysis showed that mean rank (based on Bray-Curtis Dissimilarity matrix) was not significantly different among the transplant male and female (ANOSIM $R = 0.02$, $p = 0.38$), or the control male and female (ANOSIM $R = 0.04$, $p = 0.66$). However, the mean rank between the transplant and control groups was significantly

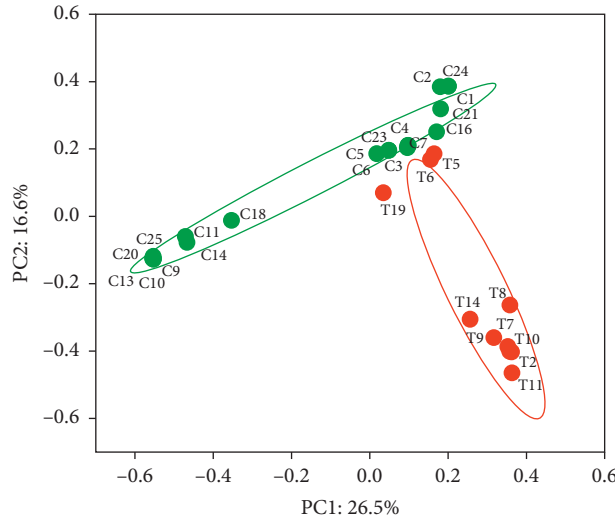


FIGURE 1: Principal Coordinate Analysis. Antibiotic resistance gene (ARG) based profile for each sample is generated based on the Bray-Curtis similarity matrix in kidney transplant and control groups. The first two components (PC1 and PC2) of the PCoA plot explained 26.5 and 16.6% variations, respectively, in transplant and the control group, with a wider range of within-group distribution. Similar direction and magnitude of clustering at 90% CI, indicate a positive association. The percentage of total variance explained by each axis is noted in both the axis labels. Red circles represent the transplant, and green circles represent control group samples. (C: Control, T: Transplant).

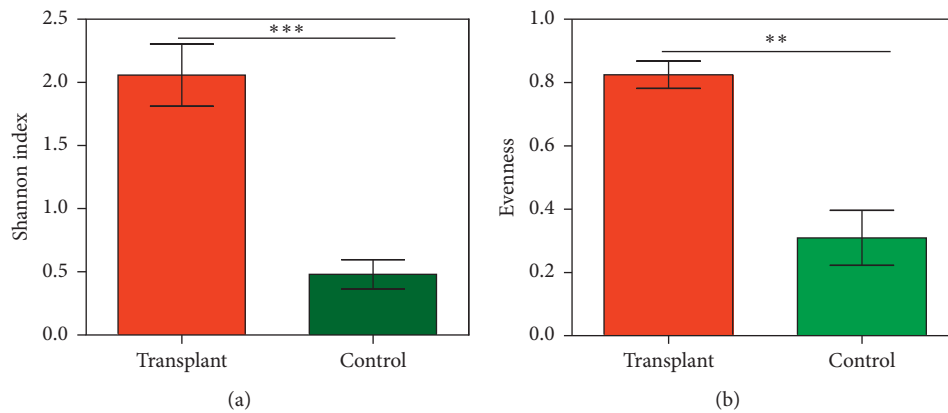


FIGURE 2: Diversity indices for ARG richness and evenness. Diversity indices were compared between the transplant ($n = 21$) and control ($n = 25$) groups using ARG data. (a) Shannon diversity index, (b) Evenness. The significant differences among the groups were computed using Mann-Whitney U Test (** $p \leq 0.001$, *** $p \leq 0.0001$).

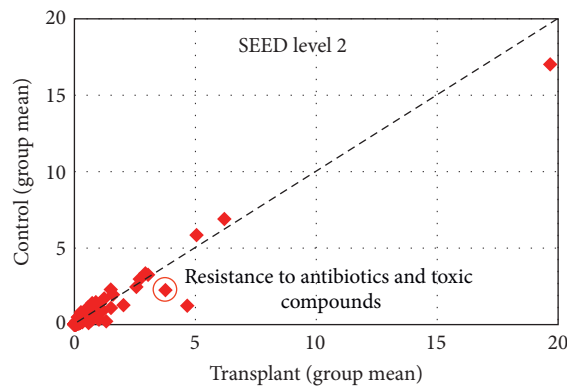


FIGURE 3: Functional analysis using SEED Subsystems at Level 2. Scatter plot was generated using the functions at level 2 among the groups. Pearson correlation between the control group (y-axis) and transplant group (x-axis).

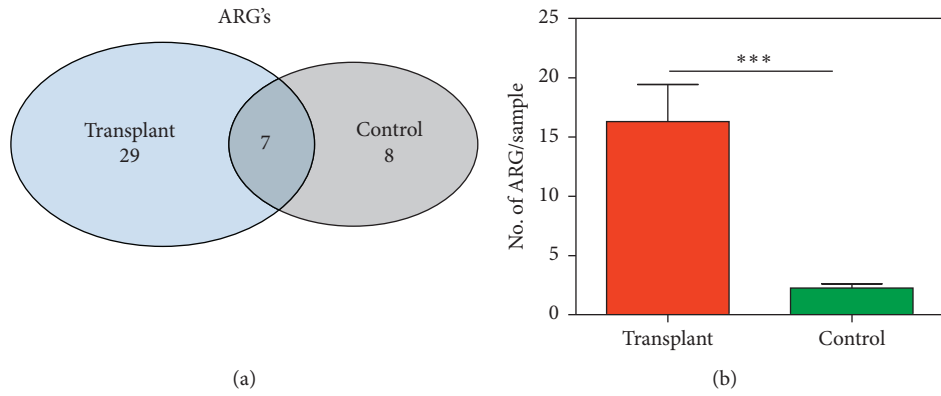


FIGURE 4: Detection of core antibiotic resistance genes (ARGs). (a) Venn diagram of unique and shared ARG between the transplant and control groups. (b) The number of ARG detected per sample is significantly higher in the transplant group compared to controls. Significant differences among the groups were computed using Mann-Whitney *U* Test (** $p \leq 0.0001$).

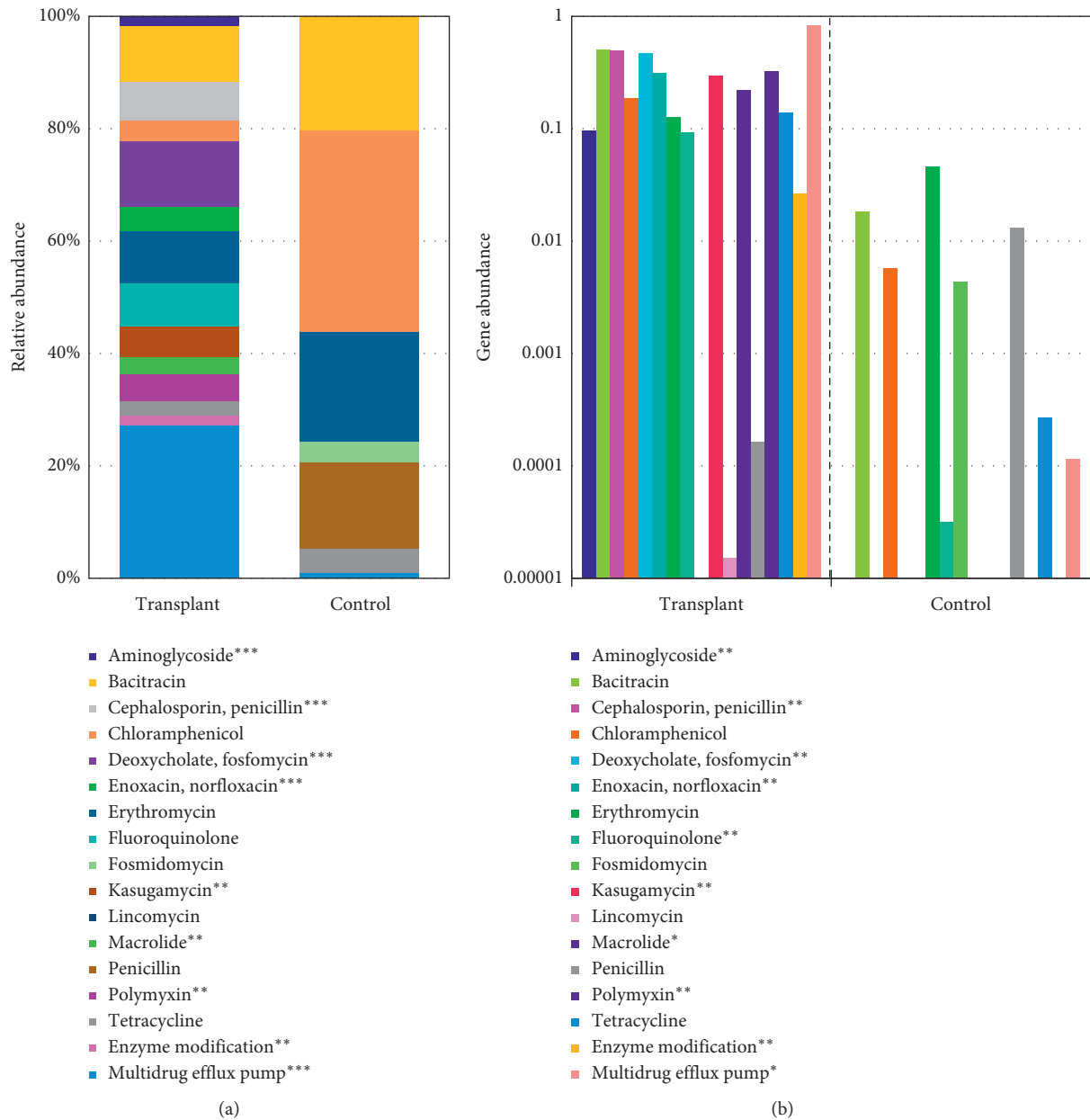


FIGURE 5: Abundance of ARG in transplant and control. (a) Relative abundance of antibiotic class in each group. (b) Absolute count of antibiotic class in each group. The significant differences between the groups were computed using Wilcoxon Rank Test ($p \leq 0.05$).

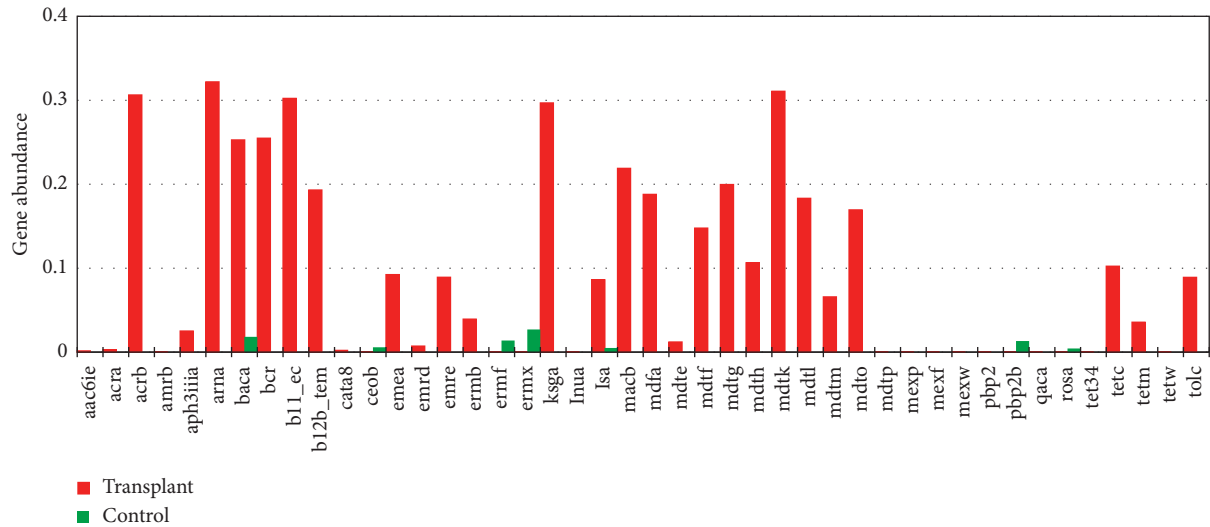


FIGURE 6: Bar chart representation of the ARG in transplant and control. Average abundance of ARG for transplant and control group. ARGs above 0.1% gene abundance are considered highly abundant.

different (ANOSIM $R = 0.59$, $p \leq 0.001$) compared to within-group difference (Figure S1).

An analysis of the type of resistance mechanisms of the ARGs in the transplant subjects indicated that the most common type was a multidrug efflux pump. A SIMPER analysis identified the ARGs which contributed the most differences among the groups, only ARG which contributed above 1% difference are shown (Table 2). In fact, 18 of the 36 ARGs in the transplant group were multidrug efflux pumps (MDEP). The SIMPER analysis showed that MDEPs contributed 65.7% towards the dissimilarity among the groups (Table 2).

There are five major types of MDEPs including ABC (ATP binding cassette), MATE (toxic compound extrusion family), MFS (major facilitator super family), SMR (small multidrug resistance family), and RND (resistance/nodulation division family). Next, we determined which type of efflux pumps were expressed in the transplant subjects (Figure 7(c)). Interestingly, we identified MDEPs from 4 of the 5 types of efflux pumps including 2, 0, 8, 1, and 6 from the ABC, MATE, MFS, SMR, and RND types, respectively. Thus, the MDEPs were derived from multiple diverse types of efflux pumps.

4. Discussion

In this study, we analyzed antibiotic resistance genes in a cohort of kidney transplant subjects compared with controls using metagenome shotgun sequencing (MGS). In a previous report, we showed that bacterial phyla were markedly different in transplant and control subjects [5]. In this study analysis of the bacterial genera showed significantly different abundances of the taxa in the transplant and control groups. For example, the transplant group had increased *Enterococcus* but decreased *Propionibacterium*, *Neisseria*, and *Bacteroides*. In addition, 4 other genera were detected in the transplant group that were absent in the controls (Table 1). In the current study, our analysis of the ARGs by PCoA indicated distinct subsets of ARGs in the transplants and the controls (see Figure 1).

We previously reported that the transplant subjects, who are prophylactically treated with the antibiotic sulfamethoxazole-trimethoprim (Bactrim), developed potential resistance to the antibiotic by increases in dihydrofolate synthase/folylpolyglutamate synthase, two enzymes that can increase folate production but are not blocked by sulfamethoxazole-trimethoprim [5]. Furthermore, our analysis of functions in the SEED database using MG-RAST showed increased “Resistance to antibiotics and toxic compounds” in the transplant group (see Figure 3). Based on these observations, we analyzed antibiotic resistance genes in the transplant and control metagenomes that demonstrated an increased abundance of ARGs as well as more diversity of ARGs in the transplant group (Figure 2). For example, out of 44 different ARGs detected, 29 were unique to the transplant subjects (Figure 4). Also, we detected an average of 16 different ARGs in transplant group versus only 2 in control. Interestingly, the putative specificity of the antibiotic resistance was also different. In the control subjects, resistance was predicted to bactrim, chloramphenicol, erythromycin, fluoroquinolone, fosmidomycin, penicillin, and tetracycline, all antibiotics that are previously or currently used in clinical or agricultural practice. In contrast, the transplant subjects projected resistance to aminoglycosides, cephalosporins, fosfomycin, norfloxacin, kasugamycin, lincomycin, macrolides, and polymyxin antibiotics that are often administered for more serious clinical indications. The most striking observation in our study was the type of ARGs that were detected in the transplant versus control subjects. 18 of the 36 ARGs in the transplant group were classified as multidrug efflux pumps (MDEPs), whereas only 2 were detected at a significant level in the control group. SIMPER analysis showed that MDEPs contributed 65.7% towards dissimilarity among the groups.

The MDEPs differ in the multiple aspects from the other ARGs. There are five major types of MDEPs including ABC (ATP binding cassette), MATE (toxic compound extrusion family), MFS (major facilitator super family), SMR (small multidrug resistance family), and RND (resistance/

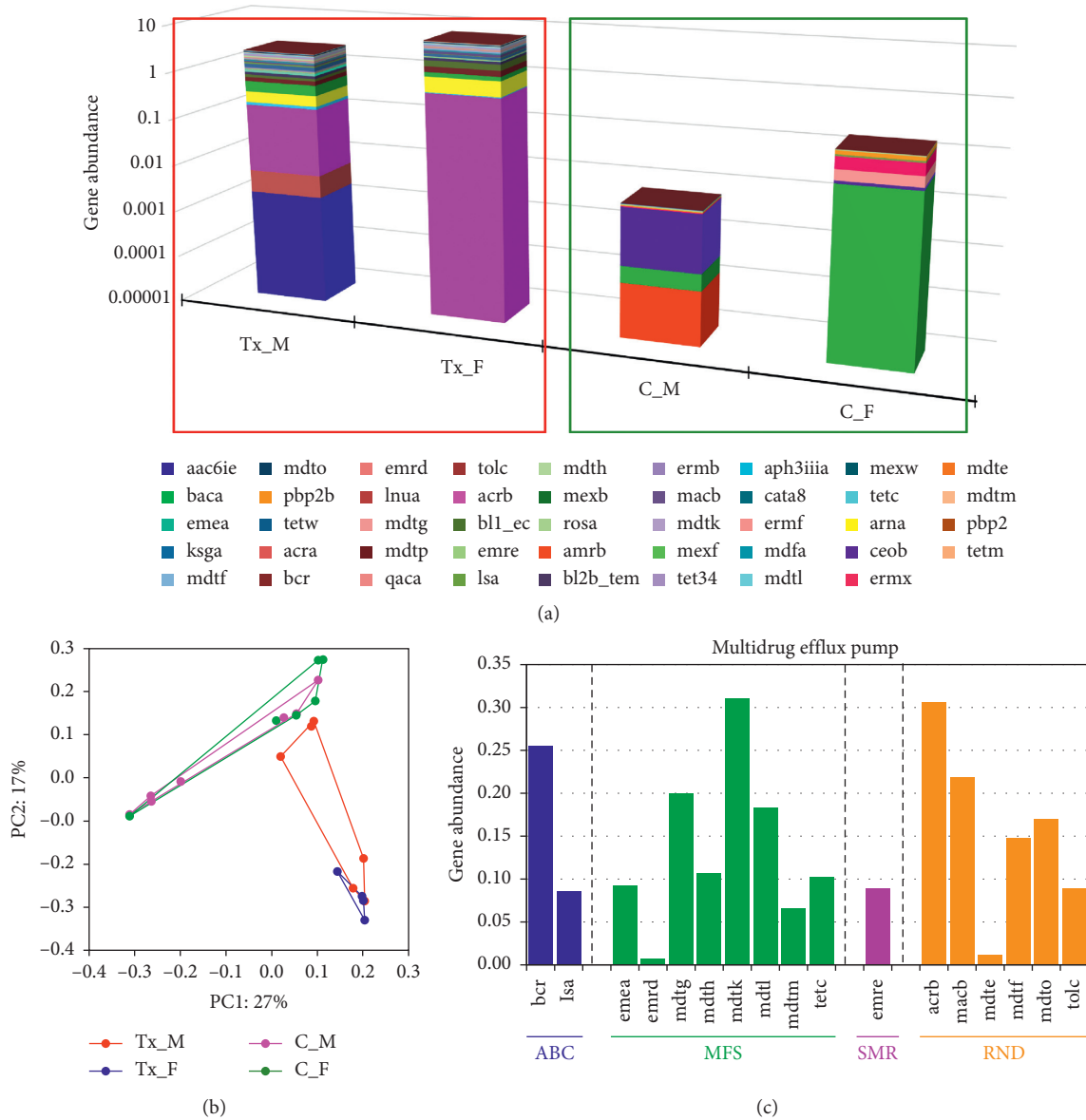


FIGURE 7: (a) Gender based ARG profile among transplant male (Tx_M) vs. females (Tx_F), and control male (C_M) vs. females (C_F). (b) Principal Coordinate Analysis using Bray–Curtis similarity matrix in kidney transplant and control groups. (c) Major types of multidrug efflux pumps (MDEP) identified in the transplant group.

nodulation division family) [8, 9]. We identified MDEPs from 4 of the 5 types of efflux pumps including 2, 0, 8, 1, and 6 from the ABC, MATE, MFS, SMR, and RND types, respectively (Figure 7(c)). Thus, the MDEPs were derived from multiple diverse types of efflux pumps. MFS multidrug efflux pumps genes (*emea*, *emrd*, *mdtg*, *mdth*, *mdtk*, *mdl*, *mdtm*, *tetc*), and RND (*acrb*, *macb*, *mdte*, *mdtf*, *mdto*, *tolc*), were among the abundant antibiotic classes compared to ABC (*bcr*, *isa*) and SMR (*emre*). Of note *mdtk*, *acrb*, and *bcr* were highly abundant among the MFS, RND, and ABC, respectively (Table 2, Figure 7(c)). The MDEPs are ancient elements present in prokaryotes, archaeobacteria, and eukaryotes that exert important biological functions unrelated to antibiotic resistance including quorum sensing, virulence,

detoxification, and biofilm formation. In cancer subjects, the MDEPs can promote resistance to chemotherapy agents. In bacteria, the MDEPs can promote resistance to antibiotics. The MDEP genes are commonly encoded within the genome and structural components are highly conserved in all members of a given bacterial species and subject to low rates of mutation. A single MDEP can convey resistance to multiple antibiotics. Since the MDEPs are ancient genes it is likely that antibiotic resistance by MDEPs is an emergent property not dependent on recent mutations suggesting that MDEPs are not selected due to exposure to antibiotics. In contrast, the development of resistance to higher concentrations or new structures in plasmid encoded ARGs is rapid and can occur within hours to days [14].

TABLE 2: SIMPER (Similarity percentage analysis) for the transplant and control group. Contribution % towards dissimilarity in both groups is shown above 1%.

Antibiotic class	Gene	Target	Transplant (mean abundance)	Control (mean abundance)	Contribution (%)
Erythromycin	lsa	ABC	0.18	0.01	5.5
Bacitracin	bcr	ABC	0.54	0.00	3.9
Tetracycline	tetc	EF	0.22	0.00	2.1
Macrolide	macb	MEP	0.46	0.00	2.9
Fluoroquinolone	emea	MEP	0.19	0.00	7.5
Multidrug efflux pump	acrb	MEP	0.64	0.00	7.3
Deoxycholate, fosfomycin	mdtf	MEP	0.31	0.00	4.6
Enoxacin, norfloxacin	mdtk	MEP	0.65	0.00	4.2
Chloramphenicol	mdtl	MEP	0.39	0.00	3.4
Chloramphenicol	ceob	MEP	0.00	0.01	3.1
Multidrug efflux pump	mdfa	MEP	0.40	0.00	3.1
Deoxycholate, fosfomycin	mdth	MEP	0.22	0.00	2.9
Deoxycholate, fosfomycin	mdtg	MEP	0.42	0.00	2.8
Multidrug efflux pump	mdto	MEP	0.36	0.00	2.8
Multidrug efflux pump	mexb	MEP	0.00	0.00	2.8
Multidrug efflux pump	tolc	MEP	0.19	0.00	1.5
Multidrug efflux pump	emre	MEP	0.19	0.00	1.4
Multidrug efflux pump	amrb	MEP	0.00	0.00	1.2
Multidrug efflux pump	mdtm	MEP	0.14	0.00	1.2
Multidrug efflux pump	aph3iiaa	Phosphorylation	0.05	0.00	1.5
<i>Sum</i>			5.55	0.02	65.7
Erythromycin	ermb	23S rRNA	0.08	0.00	4.1
Erythromycin	ermx	23S rRNA	0.00	0.03	1.4
Kasugamycin	ksga	30S	0.62	0.00	5.2
Polymyxin	arna	Arabinose	0.68	0.00	4.9
Cephalosporin, penicillin	bl1_ec	β -Lactam	0.64	0.00	4.7
Cephalosporin, penicillin	bl2b_tem	β -Lactam	0.41	0.00	2.2
Penicillin	pbp2b	Glycosylase	0.00	0.02	1.2
Bacitracin	baca	Phosphatase	0.53	0.02	7.9
<i>Sum</i>			2.96	0.07	31.6

Our data support the hypothesis that bacteria with diverse abundant MDEPs have increased fitness to colonize and survive in a high stress environment in a transplant host. Transplantation produces multiple stressors including ischemia/reperfusion, exposure to antibiotics, and immunosuppressive agents. Thus, microbiota with relevant MDEPs may have increased fitness and provide the bacteria with a selective advantage in a stressed environment such as induced by transplantation. This could guide the specific changes in the microbiome we documented following transplantation. Further delineation of the effects of high levels of MDEPs in transplant subjects' merits further investigation.

Data Availability

The sequence data for the study have been submitted to the MG-RAST web server under the following accession number provided in Table S2.

Disclosure

Asha Rani and Ravi Ranjan contributed equally and should be considered co-first authors. Patricia W. Finn and David L. Perkins contributed equally and should be considered co-last authors. The current address of Asha Rani is the Department of Food Science, University of Massachusetts,

Amherst, MA 01003, USA. The current address of Ravi Ranjan is Genomics Resource Laboratory, Institute for Applied Life Sciences (IALS), University of Massachusetts, Amherst, MA 01003, USA.

Conflicts of Interest

All authors declare that they have no conflicts of interest.

Authors' Contributions

DLP, PWF, AR, and RR designed the study; AR, RR, AAM, and DCB performed the data analysis; DLP, PWF, AR, and RR wrote the manuscript; DCB provided the materials.

Acknowledgments

This work was supported in part by R01AI053878 and U01AI132898 to PWF and DLP and K24DK02886 and P30DK079333 to DCB.

Supplementary Materials

Figure S1: ANOSIM statistics distance plots. (a) Transplant male vs. female, (b) control male vs. female, (c) transplant group vs. control group. Table S1: demographics of transplant and control subjects. Transplant samples (T1–T21) and

control samples (C1–C8) have been previously analyzed [5]. Table S2: sequencing statistics and accession numbers. Table S3: taxonomic and functional annotation in transplant and control groups. (*Supplementary Materials*)

References

- [1] M. D. Surette and G. D. Wright, “Lessons from the environmental antibiotic resistome,” *Annual Review of Microbiology*, vol. 71, no. 1, pp. 309–329, 2017.
- [2] N. Wagglechner and G. D. Wright, “Antibiotic resistance: it’s bad, but why isn’t it worse?” *BMC Biology*, vol. 15, no. 1, p. 84, 2017.
- [3] S. Ahmad and J. S. Bromberg, “Current status of the microbiome in renal transplantation,” *Current Opinion in Nephrology and Hypertension*, vol. 25, no. 6, pp. 570–576, 2016.
- [4] K. A. Kline and A. L. Lewis, “Gram-positive uropathogens, polymicrobial urinary tract infection, and the emerging microbiota of the urinary tract,” *Microbiology Spectrum*, vol. 4, no. 2, 2016.
- [5] A. Rani, R. Ranjan, H. S. McGee et al., “Urinary microbiome of kidney transplant patients reveals dysbiosis with potential for antibiotic resistance,” *Translational Research*, vol. 181, pp. 59–70, 2017.
- [6] B. Liu and M. Pop, “ARDB—antibiotic resistance genes database,” *Nucleic Acids Research*, vol. 37, no. 1, pp. D443–D447, 2009.
- [7] J. M. Munita and C. A. Arias, “Mechanisms of antibiotic resistance,” *Microbiology Spectrum*, vol. 4, no. 2, 2016.
- [8] M. Alcalde-Rico, S. Hernando-Amado, P. Blanco, and J. L. Martinez, “Multidrug efflux pumps at the crossroad between antibiotic resistance and bacterial virulence,” *Frontiers in Microbiology*, vol. 7, p. 1483, 2016.
- [9] P. Blanco, S. Hernando-Amado, J. A. Reales-Calderon et al., “Bacterial multidrug efflux pumps: much more than antibiotic resistance determinants,” *Microorganisms*, vol. 4, no. 1, p. 14, 2016.
- [10] K. P. Keegan, E. M. Glass, and F. Meyer, “MG-RAST, a metagenomics service for analysis of microbial community structure and function,” *Microbial Environmental Genomics (MEG)*, vol. 1399, pp. 207–233, 2016.
- [11] A. Janssen, S. Kaiser, K. Meissner, N. Brenke, L. Menot, and P. Martinez Arbizu, “A reverse taxonomic approach to assess macrofaunal distribution patterns in abyssal Pacific polymetallic nodule fields,” *PLoS One*, vol. 10, no. 2, Article ID e0117790, 2015.
- [12] O. Hammer, D. Haper, and P. Ryan, “PAST: paleontological statistics software package for education and data analysis,” *Palaeontologia Electronica*, vol. 4, no. 1, pp. 4–9, 2001.
- [13] C. Gottschick, Z.-L. Deng, M. Vital et al., “The urinary microbiota of men and women and its changes in women during bacterial vaginosis and antibiotic treatment,” *Microbiome*, vol. 5, no. 1, p. 99, 2017.
- [14] M. Baym, T. D. Lieberman, E. D. Kelsic et al., “Spatiotemporal microbial evolution on antibiotic landscapes,” *Science*, vol. 353, no. 6304, pp. 1147–1151, 2016.

Research Article

Application of Quality Control Circle in Promoting the Use of Rubber Dams in the Root Canal Treatment of Primary Teeth

Fang Jingxian , Liu Yang, Liu Qiong, Qian Hong, Liu Hedi, Zhang Jinglan, Liu Fang, Yang Jing, Wu Xiaoming, and Song Yingying

Department of Pediatric Dentistry, Stomatological Hospital, Southern Medical University, Guangzhou 510280, China

Correspondence should be addressed to Fang Jingxian; jfangpedo@smu.edu.cn

Received 13 November 2019; Revised 22 January 2020; Accepted 13 February 2020; Published 26 February 2020

Guest Editor: Peng Bao

Copyright © 2020 Fang Jingxian et al. This is an open access article distributed under the Creative Commons Attribution License, which permits unrestricted use, distribution, and reproduction in any medium, provided the original work is properly cited.

Objective. Study the effect of quality control circle (QCC) in promoting the usage of rubber dams (RD) in root canal treatment of chronic pulpitis in primary teeth. **Methods.** Set up a quality control group to increase the amount of rubber dams used in the treatment of chronic pulpitis in primary teeth. Monthly monitoring results of the usage amount were counted by the outpatient computer system. Relevant data were collected through questionnaires, and causes of low utilization were analyzed, and the improvement measurements were formulated and implemented. Quality control circle activity was evaluated. **Results.** Through the quality control circle activity, the consumption of rubber dams in the root canal treatment of chronic pulpitis was significantly improved, children in treatment became more cooperative, and operation time of root canal treatment has also been shortened. **Conclusion.** The quality control circle activities played a significant role in promoting the use of rubber dams in the root canal treatment of primary teeth, and it can be used as a method to promote new clinical treatment programs.

1. Introduction

There are many advantages of using rubber dam (RD) in root canal treatment of chronic pulpitis of deciduous teeth [1], such as improving infection control quality, safety, and therapeutic effects [2, 3]. Therefore, it should be vigorously promoted and applied. However, the utilization rate of rubber dam in deciduous teeth in China is not high in clinical practice [4]. Quality control circle (QCC) is a group of workers who do the same or similar work, who meet regularly to identify, analyze, and solve work-related problems [5]. They are problem solving teams which use simple statistical methods to research and decide on solutions to workshop problems [6]. And they follow the “PDCA” (plan-do-check-act) process [7]. In order to find out the reason why usage of rubber dam was so low in the treatment of chronic pulpitis and to further solve the problem, the following work has been carried out. It has been monitored the usage of rubber dam in root canal treatment of chronic pulpitis of deciduous teeth in the Department of Pediatric Dentistry, Stomatological Hospital of Southern Medical University for twelve months.

Through applying quality control circle, the consumption and using techniques of rubber dam has been improved when compared with the previous year. And the quality control circle activity can be used as a method to promote new clinical treatment programs. The details are reported below.

2. Materials and Methods

2.1. General Information. Our department is the outpatient of Pediatric Dentistry Department in the Tertiary Stomatological Hospital. There are 9 pedodontists, 20 nurses, and 8 dental residents during the year of 2018.

2.2. Methods

2.2.1. QCC. Set up a quality control circle group which consists of 11 members, including 10 dentists and 1 nurse.

2.2.2. Topic Selection. The theme of QCC activity is to increase the usage of rubber dam in root canal treatment of chronic pulpitis of deciduous teeth. The event was held from January 2018 to December 2018.

TABLE 1: Houpt's behavioral rating scale for rubber dam treatment.

Score	Description
1	Aborted, no treatment rendered
2	Poor treatment interrupted, only partial treatment completed
3	Fair treatment interrupted, but eventually all completed
4	Few treatment interrupted, but eventually all completed
5	Very good, some limited crying or movement (e.g., during anesthesia or mouth prop insertion)
6	Excellent, treatment completed

2.2.3. *Reason Analysis.* Through literature review, brainstorming, and questionnaire, the QCC team analyzed the main reasons for low usage of rubber dam in the treatment of chronic pulpitis of milk teeth as several aspects, and finally determined the improvement measurement as scheduled and improves the operation.

2.2.4. *Setting Target.* Value of the goal setting formula = current situation value + (improvement value × improvement focus × circle capacity), the amount of rubber dam used before improvement was 20 pieces/(month · dental chair), the circle capacity was assessed and calculated by all circle members as 83.08%, and the target value after improvement was 34 pieces/(month · dental chair), with an improvement range of 66.46%.

2.2.5. Countermeasures Formulation and Implementation

- (1) Videos about advantages and disadvantages of using rubber dams were played in the waiting room; operating procedures were shown as well
- (2) Using children's language
- (3) Normalizing the practice. The rubber dam was placed by means of wing method. According to the tooth position, the rubber dam was drilled, fixed on the rubber dam clamp, and then extended with the rubber dam clamp, and then placed on the tooth neck together with the rubber cloth. During the process, attention was paid to the protection of oral soft tissue, and fingers were used to guide the rubber dam into position [8]
- (4) Internal and external experience exchanges. Experiences were shared among dentists to face those special tooth conditions
- (5) Local anesthesia
- (6) Questionnaire. Survey was conducted to confirm, review, and improve the implementation status and effect
- (7) Data analysis. Theme progress of rubber dams at each dental chair was counted, and the children in rubber dam group (experimental group) and without rubber dam group (control group) were scored

TABLE 2: Comparison of Houpt's score and clinical operation time between the two groups.

	Houpt's score (points)	Chairside operation time (min)
Experimental group	5.80 ± 0.52	13.20 ± 1.81
Control group	5.05 ± 1.01	18.58 ± 2.27

$P < 0.01$ ($\bar{x} \pm s$).

according to Houpt's evaluation scale (Table 1) [9], and the chairside operation time as well as the complications before and after treatment were analyzed

2.3. *Statistical Analyses SPSS20.0 Software Was Used for Statistical Analysis.* The whole process score of Houpt's score and the operation time beside the chair were compared by t test, the monthly amount of rubber dam, and the numbers of intraoperative and postoperative complications were compared by chi-square test, and $P < 0.05$ was considered statistically significant.

3. Results

3.1. *Monthly Consumption of Rubber Dam for Milk Teeth in Root Canal Treatment of Chronic Pulpitis Is Promoted by QCC Activities.* The activity of quality control circle increased the use of rubber dam in root canal treatment of chronic pulpitis of deciduous teeth in our department. After improvement, consumption of rubber dam was 91pieces per month. Target rate = (improved-base)/(target-present) × 100% = (91-20)/(34-20) × 100% = 507.14%. Meanwhile, when we compare the patient's amount each month, data shows a similar trend while compared with the year of 2017.

3.2. *Using Rubber Dam Can Improve the Cooperation Degree and Reduce the Operation Time beside the Chair.* The Houpt scores of children in both the experimental group and the control group during the whole process of treatment were assessed, and the chairside operation time were counted too (Table 2). Those results were statistically analyzed, and the difference was statistically significant ($P < 0.05$). The children in the experimental group had a higher degree of cooperation in the treatment, and the use of rubber dam shortened the total treatment time.

3.3. *Complications of Using Rubber Dam.* Intraoperative and postoperative complications of the root canal treatment in both the experimental group and the control group were evaluated by questionnaires and statistical analysis. There were statistical differences on discomfort and gingival bleeding between two groups and mucosal bleeding caused by intraoperative saliva suction could be found in the control group, suggesting that painless anesthesia and pain control techniques should be further improved before root canal treatment (Table 3).

4. Discussion

Rubber dam for milk teeth was introduced into our department to use since 2017, but usage amount and frequency

TABLE 3: The comparison of intraoperative and postoperative complications between two groups.

	Experimental group (%)	Control group (%)
Intraoperative discomfort	10.00	0
Gingival bleeding caused by clamp	30.00	0
Mucosal bleeding caused by saliva suction	0	35.00
Provoke or vomiting	0	55.00
Postoperative discomfort	5.00	5.00

$P < 0.01$.

was much lower than that for permanent teeth. Based on the fact that the clinical pathway of hospital information management has been included in the treatment of chronic pulpitis of deciduous teeth, the theme of QCC activity is to increase the usage of rubber dam in root canal treatment of chronic pulpitis of deciduous teeth.

Rubber dam in root canal treatment has been recognized as a standard treatment procedure internationally [10]. In developed countries, rubber dams have been widely used in children's oral treatment. A questionnaire survey study among dentists from China and Japan [11] analyzed the application of rubber dam in the treatment of pulp disease of deciduous teeth. The comparative analysis showed that 81.3% of dentists in the Japanese group routinely used rubber dam in the treatment of pulp disease of deciduous teeth, while 38.1% of dentists in the Chinese group used rubber dam, which was significantly lower than that in the Japanese group. Pediatric dentistry in China started late as an independent specialty, with uneven development in different regions. Meanwhile, China has a large population and insufficient resources in specialized hospitals. Dentists in general hospitals also undertake a large number of children's dental diagnosis and treatment. Statistics show that [4] the utilization rate of rubber dam in the affiliated dental hospital is significantly higher compared with the dental department of the tertiary general hospital. In the tertiary general hospital, the use of rubber dam was not popular. Applying dental dam in deciduous teeth root canal therapy has unique advantages [2, 3]. First, children have more saliva and small mouth angle. Compared with the conventional cotton isolation, application of dental dam leads operating space to be relatively clean and dry. It also reduces chances of infection, so as to improve the quality and efficiency of the root canal treatment [12]. Second, the oral mucosa of children is more vulnerable to be impaired than that of adults. Rubber dams can reduce the stimulation and injury of oral soft tissues caused by the dental instruments and medications during root canal treatment. However, there are many reasons for the low utilization rate of rubber dam in the treatment of milk teeth in China [13]. Old dentists were unfamiliar with the rubber dam system and children were afraid of needle injection or rubber dam clamping [14]. In the process of root canal treatment of deciduous teeth without rubber dam, selection of lotion and treatment will be affected to certain extent. Moreover, children with low degree of coordination are likely to swallow or inhale dental instrument materials [15], which will cause unnecessary medical disputes. In Table 3, it has been shown that rubber clamp itself may cause intraoperative

discomfort and bleeding during operation. The suitability between the crown and the rubber dam of the baby teeth still needs further improvement. Therefore, the use of milk teeth rubber dam requires the joint efforts of child, parents, dentists, and nurses [16]. In addition to communication and technical training for both dentists and nurses, the advantages and values of using rubber dams must be emphasized and routine usage should be encouraged. Besides, more suitable rubber dam clamp for Chinese children should be developed.

In order to improve the application, several methods have been used, such as (1) dental education (videos about advantages and disadvantages of using rubber dams were played in the waiting room, operating procedures were shown as well). So that children and their parents could learn about rubber dams when waiting for medical treatment. This would deepen their knowledge on dental treatment and eliminate fear; [2] using children's language through the whole treatment [17]. To improve their comprehension and cooperation, nurses or dentists try to use some right age words to explain those steps, such as the word "umbrella or raincoat," instead of "dam," or "give tooth a shower" instead of "drill the tooth" [18]; [3] normalizing the practice: concentrated on learning the indications, contraindications, and standard operating methods for the rubber dams and conducted model exercises before clinical operation to enhance operating confidence; [4] experience sharing; and [5] local anesthesia. Many Chinese were contradicted to the anesthesia. In order to provide a pain-free comfortable treatment, guardian should sign the treatment informed consent and perform topical anesthesia or STA (single tooth anesthesia), so that the operation could be done thoroughly. When local anesthesia was rejected, topical anesthesia was also provided, by which discomfort could be relieved. Besides, some more new methods may be tried in future works [19].

Juntgen et al. [17] found that factors that hinder the application of new treatment methods in children's oral clinic include legality, parents' acceptance of changes, and limited resources. Through quality control circle activities, training of medical staff has been strengthened and popular dental education of children and parents has been enhanced. Besides, communication between medical staff and children and parents during diagnosis has strengthened, parents' acceptances of rubber dam application have been improved, and consumption of rubber dam has been effectively increased in root canal treatment of chronic pulpitis of deciduous teeth. Treating children usually involves a one-to-two relationship between doctors, children, and parents, that is,

the pediatric dentistry treatment triangle [20]. After carrying out quality control circle activities, staff, parents, and children communicate more in details. And more communication makes the parents feel cherished, which may shorten the distance between medical staff and children and parents, may enhance mutual trust, and may improve children's obedience and the degree of satisfaction [21]. Children and parents in routine practice play a positive role in promotion of new technology project [22].

Our department has achieved the target value through quality control circle activity, but there is still a gap between the usage of rubber dam in root canal treatment of deciduous teeth and that of permanent teeth. Compared with the 100% incidence rate of permanent root canal treatment, the incidence rate of pulpitis root canal treatment was only 67.35% (the specific data were not shown). This is mainly due to the treatment of young children with low degree of cooperation. When the defect of the child's teeth is too large (two walls are subgingival), or the child's head movement was too big, it is unable to spend a long time in the treatment of the child's teeth to pile up the tooth wall, which leads some doctors to give up the use of the rubber dam of the baby teeth. In order to promote the standardization of the entire activity results in production and normalized quality management, several ways have been tried to improve the rubber dam consumption. Different ring set have been used to fit special shape tooth, and in the second phase of circle activity, different brands of subgingival clamps or the small clips have been tried. The QCC group published monthly statistics, continued to carry out relevant training activities such as skills contest regularly, and summarized the work and the quarterly results into the department medical treatment appraisal system.

Children's personality, parents' appropriate preparation for the clinic, and excellent communication skills of medical staff are several key factors for the success of oral therapy [16]. For children who failed to accept the rubber dam after the first root canal treatment, parents should be instructed to provide effective comfort and communication to the children at home, and try to convey the information to the children and their parents through behavior management in the next visit [18], so as to improve the use of rubber dam of milk teeth. Besides, through the Houpt score evaluation system, it has been shown the children in treatment became more cooperative; in order to eliminate the possibility that children and parents who are willing to accept RD have a character of more cooperative and willingness to obey, in the further research, more questionnaires on parents and patients should be taken.

Organizing and carrying out quality control circle activity not only improves work efficiency and causes economic benefits but also reduces medical risks and the working pressure of medical staff. As a way to improve the quality of clinical treatment, the effect of quality control circle activity is satisfactory. Through this quality control circle activity, the ability of medical staff in our department in finding, analyzing, and improving problems was enhanced. Through discussion, preparation, and implementation of corresponding countermeasures, the usage of rubber dam in root canal treatment of

chronic pulpitis of deciduous teeth was greatly improved. The scientific research awareness and ability of the circle members have also been improved in the process of carrying out this quality control circle activity, which provides certain practical basis and experience guidance for the next quality control circle activities of our department.

Data Availability

The data used to support the findings of this study are available from the corresponding author upon request.

Conflicts of Interest

The authors declare that they have no conflicts of interest.

References

- [1] I. A. Ahmad, "Rubber dam usage for endodontic treatment: a review," *International Endodontic Journal*, vol. 42, no. 11, pp. 963–972, 2009.
- [2] Y. Wang, C. Li, H. Yuan et al., "Rubber dam isolation for restorative treatment in dental patients," *Cochrane Database of Systematic Reviews*, vol. 9, article CD009858, 2016.
- [3] W. Keys and S. J. Carson, "Rubber dam may increase the survival time of dental restorations," *Evidence-Based Dentistry*, vol. 18, no. 1, pp. 19–20, 2017.
- [4] J. J. Zheng, X. Yang, S. Zhang, and L. H. Ge, "The situation of treatment of pulpitis in primary dentition among some dentists in China," *Journal of Modern Stomatology*, vol. 31, no. 3, pp. 144–146, 2017.
- [5] L. Tingfang, "Review of QCC of Chinese Hospital," *Journal of Chinese Research Hospitals*, vol. 2, no. 4, pp. 24–29, 2015.
- [6] H. Feng, G. Li, C. Xu, C. Ju, and P. Suo, "A quality control circle process to improve implementation effect of prevention measures for high-risk patients," *International Wound Journal*, vol. 14, no. 6, pp. 1094–1099, 2017.
- [7] P. Chen, T. Yuan, Q. Sun et al., "Role of quality control circle in sustained improvement of hand hygiene compliance: an observational study in a stomatology hospital in Shandong, China," *Antimicrobial Resistance and Infection Control*, vol. 5, no. 1, 2016.
- [8] Q. Liu, H. Qian, F. Ren, J. X. Fang, H. D. Liu, and X. M. Wu, "Clinical value of children rubber dam during root canal treatment in primary teeth (in Chinese)," *Journal of Oral Science Research*, vol. 34, no. 7, pp. 756–758, 2018.
- [9] G. Zhang and K. Wan, *Handbook of Clinical Dental Sedation (Manuscript/Book in Chinese)*, pp. 20–21, 2010.
- [10] H. M. A. Ahmed, S. Cohen, G. Lévy, L. Steier, and F. Bukiet, "Rubber dam application in endodontic practice: an update on critical educational and ethical dilemmas," *Australian Dental Journal*, vol. 59, no. 4, pp. 457–463, 2014.
- [11] Z. X. C. Jiajia, Z. Sun, and G. Lihong, "Investigation of pulpotomy in primary teeth between Chinese and Japanese dentists," *Journal of Peking University Health Science*, vol. 47, no. 6, pp. 1050–1052, 2015.
- [12] X. X. Chen, B. C. Lin, J. Zhong, and L. H. Ge, "Degradation evaluation and success of pulpectomy with a modified primary root canal filling in primary molars," *Journal of Peking University Health Science*, vol. 47, no. 3, 2015.

- [13] P. Y. Lin, S. H. Huang, H. J. Chang, and L. Y. Chi, "The effect of rubber dam usage on the survival rate of teeth receiving initial root canal treatment: a nationwide population-based study," *Journal of Endodontia*, vol. 40, no. 11, pp. 1733–1737, 2014.
- [14] S. Muhanad, D. M. Alhareky, M. Finkelman, J. Alhumaid, and C. Loo, "Efficiency and patient satisfaction with the Isolite system versus rubber dam for sealant placement in pediatric patients," *Pediatric Dentistry*, vol. 36, no. 5, pp. 400–404, 2014.
- [15] Q. Yang, "Accidental foreign body ingestion in dental practice," *Kou Qiang Ji Bing Fang Zhi*, vol. 24, no. 6, pp. 321–325, 2016.
- [16] D. A. Nash, "Engaging children's cooperation in the dental environment through effective communication," *Pediatric Dentistry*, vol. 28, no. 5, pp. 455–459, 2006.
- [17] L. M. Juntgen, B. J. Sanders, L. A. Walker et al., "Factors influencing behavior guidance: a survey of practicing pediatric dentists," *Pediatric Dentistry*, vol. 35, no. 7, pp. 539–545, 2015.
- [18] J. A. Dean, *McDonald and Avery's Dentistry for the Child and Adolescent*, Elsevier, 10th edition, 2018.
- [19] L. M. Wambier, J. T. Demogalski, D. B. Puja et al., "Efficacy of a new light-cured anesthetic gel for clamp placement before rubber dam isolation in children: a triple-blinded randomized controlled clinical trial," *American Journal of Dentistry*, vol. 31, no. 3, pp. 126–130, 2018.
- [20] G. Z. Wright and A. Kupietzky, *Behavior management in dentistry for children*, I. Ames, Ed., Wiley Blackwell, 2nd edition, 2014.
- [21] M. Maslamani and A. K. Mitra, "Factors associated with patients' satisfaction of rubber dam use during root canal treatment," *Indian Journal of Dental Research*, vol. 29, no. 2, pp. 144–149, 2018.
- [22] H. Gao, X. Q. Wang, J. X. Zhu, and J. Li, "The influencing factors of the cooperation behaviors of patients in department of pediatric dentistry," *Kou Qiang Ji Bing Fang Zhi*, vol. 24, no. 10, pp. 617–620, 2016.

Research Article

Outcome of Gynecologic Laparoendoscopic Single-Site Surgery with a Homemade Device and Conventional Laparoscopic Instruments in a Chinese Teaching Hospital

Xianghui Su, Xiaolong Jin, Canliang Wen, Qiong Xu, Chunfang Cai, Zhuohui Zhong, and Xiang Tang 

Department of Minimal Invasive Gynecology, Guangzhou Women and Children's Hospital, Guangzhou Medical University, Guangzhou, China

Correspondence should be addressed to Xiang Tang; jacktang14@hotmail.com

Received 13 November 2019; Accepted 20 December 2019; Published 22 January 2020

Guest Editor: Peng Bao

Copyright © 2020 Xianghui Su et al. This is an open access article distributed under the Creative Commons Attribution License, which permits unrestricted use, distribution, and reproduction in any medium, provided the original work is properly cited.

Objective. To demonstrate various benign gynecologic diseases that can be performed by laparoendoscopic single-site surgery (LESS) with conventional laparoscopic instruments. **Method.** Patients with benign gynecologic diseases that need ovarian cystectomy, fallopian tube resection, or myomectomy were divided into experimental group and control group, and perioperative outcomes of these patients were analyzed. **Results.** From November 2017 to May 2018, 65 LESS gynecological surgeries were performed, among which there were 25 ovarian cystectomies, 28 unilateral fallopian tube resections, and 12 myomectomies. All the surgeries were completed smoothly, and only one surgery needed one more additional port. No patients have severe complications. Operative time, intraoperative blood loss, and perioperative complications have no difference between the two groups. The LESS laparoscopy group had less postoperative pain scores and longer bowel recovering time, compared with the conventional laparoscopy group (<0.05). **Conclusion.** Compared with traditional laparoscopy, LESS surgery with conventional laparoscopic instruments is feasible and safe, but postoperative exhaust time is longer than the control group.

1. Introduction

As one type of the laparoscopic surgery, the laparoendoscopic single-site (LESS) surgery has been developed in an attempt to further reduce the morbidity and scarring associated with surgical intervention [1, 2]. Single-site gynecologic Surgery is widely carried out all over the world during the recent years. More and more gynecological endoscopic surgeries use this single-site technology, especially transumbilical single-port. Many research studies have indicated advantages of it, such as less postoperative pain, quick recovery, and less skin scar. Some results are conflicting [3–10]. The advantages of LESS are still uncertain. In this study, we analyzed perioperative and postoperative data of single-site laparoscopic surgery and multihole laparoscopic surgery to explore the difference in clinical efficacy between the two groups.

2. Methods

This study was a retrospective study performed in Guangzhou women and children's Hospital, from November 2017 to May 2018. The study was approved by the hospital's ethics committee. All the patients signed the informed consent. The patients who have a history of previous abdominal surgery or BMI >30 were excluded. All the operations were performed by the same doctor who had completed more than 20 LESS surgeries before the research. Similar cases in the research period through conventional laparoscopy were involved into the control group.

2–3 cm longitudinal umbilical incision was measured by a sterile ruler and single-port access by sequence incision to the peritoneum through the periumbilical incision. We inserted the inner ring of the wound retractor and fixed a 6½ size surgical glove on the outer ring of the retractor. One

10 mm trocar and two 5 mm trocars were inserted into the glove fingers and fixed by silk thread. The 10 mm rigid 30° Karl Storz laparoscopy was inserted into the abdominal cavity through the 10 mm trocar, and the conventional laparoscopic instruments were inserted through the other two trocars (Figure 1).

We reviewed all the medical records including the operation time, blood loss, length of hospital stay, bowel recovering time, and postoperative Visual Analog Scale (VAS) score. The VAS was used to score incisional pain on a 10-point scale ranging from 0 (no pain) to 10 (worst possible pain). All the perioperative outcomes of LESS surgery group were compared with the traditional multiport laparoscopic surgery groups.

3. Statistical Analyses

The parametric variables were expressed as mean \pm standard deviation (SD), minimum and maximum, and were compared with a *t*-test. Categorical variables were compared with a Chi-squared test. We used SPSS 22.0 for statistical analyses. The level of statistical significance was set at $p < 0.05$.

4. Results

25 ovarian cystectomies, 12 myomectomies, and 28 unilateral fallopian tube resections have been involved in the LESS group.

In our study, there was no significant difference from the general clinical data between the two groups of patients whether performing adnexal surgery, salpingectomy, or myomectomy. The differences of hospital stays and bowel recovering time between the two groups are significant for the ovarian cystectomies, and the LESS group needed longer time for bowel recovering (Table 1).

For the myomectomies, there is a significant difference of bowel recovering time between the two groups, and the LESS group needs longer time for bowel recovering compared with the conventional laparoscopy group. The difference of 24 h pain between the two groups is significant, and the LESS group has less 24 h VAS compared with the conventional laparoscopy group (Table 2).

For the salpingectomy, there is a significant difference of VAS between the two groups. We did not find differences of other items between the two groups (Table 3).

5. Discussion

Laparoendoscopic single-site surgery (LESS) is a single-port technique through the umbilicus, in the past 10 years, and it has emerged as a potentially less-invasive alternative to multiport laparoscopy. It has enhanced the cosmetic benefit of minimally invasive surgery. At the beginning, a homemade single port is easier to get, low cost and has a good socioeconomic performance, especially for the countryside hospitals. YH Park was the first person who reported that he use a homemade single port device to perform laparoendoscopic single-site nephrectomy [11]. Several meta-



FIGURE 1: Homemade single-port device made of one retractor and one glove.

TABLE 1: Clinical characteristics and operative data of ovarian cystectomy ($N = 50$).

Variable	LESS	ConventionalLS	<i>p</i> value
Patient age	32.35 \pm 5.32	33.29 \pm 4.89	>0.05
BMI	21.43 \pm 3.15	21.04 \pm 1.70	>0.05
Operating time	114.64 \pm 27.75	106.07 \pm 33.43	>0.05
Blood loss	28.24 \pm 15.78	32.35 \pm 51.56	>0.05
Pain score 24 h	1.29 \pm 0.54	2.88 \pm 0.42	>0.05
Bowel recovering time	1.65 \pm 0.54	1.41 \pm 0.48	<0.05
Hospital stay in days	3.64 \pm 1.26	3.24 \pm 0.92	<0.05

analysis researches have been published on the safety and efficacy of LESS in recent years [9, 12–14]. However, it has been unclear whether LESS offers benefits over multiport LH. Sandberg et al. [15] reported that potential benefits were cosmetic satisfaction and less postoperative pain, but the small differences for these outcomes appear not to be of clinical relevance in their systematic review and meta-analysis report. In our study, most items we observed have no difference between two groups.

In the application of any new technique, the safety of the patients is always the most important. In our study, all the surgeries were successfully performed. After a median follow-up period of 3 months, there is no complaint of the LESS surgery. All the LESS group patients were fully satisfied with the appearance of the incisions.

Operating time is routinely considered as a parameter to estimate the surgical learning curve. In our study, there is no difference for adnexal surgery, salpingectomy, or myomectomy. We considered there are different possible reasons for it. (1) Regarding salpingectomy, it is relatively simple for a doctor who passed the learning curve of LESS. (2) For myomectomy, although the surgeon faced additional challenges such as crossing or collision of

TABLE 2: Clinical Characteristics and Operative Data of myomectomy (N=24).

Variable	LESS	Conventional LS	p-value
Patient age	38.82 ± 6.52	38.27 ± 4.36	>0.05
BMI	22.20 ± 3.42	23.20 ± 2.00	>0.05
Operating time	116.36 ± 59.12	128.64 ± 68.72	>0.05
Blood loss	79.09 ± 92.46	64.54 ± 85.60	>0.05
Pain score 24 h	1.36 ± 1.03	2.0 ± 0.97	<0.05
Bowel recovering time	1.71 ± 0.51	1.36 ± 0.50	<0.05
Hospital stay in days	4.81 ± 1.79	4.82 ± 1.17	>0.05

TABLE 3: Clinical characteristics and operative data of salpingectomy (N=56).

Variable	LESS	Conventional LS	p-value
Patient age	31.17 ± 3.13	31.52 ± 4.35	>0.05
BMI	20.85 ± 2.50	21.08 ± 2.18	>0.05
Operating time	61.26 ± 30.68	50.81 ± 14.19	>0.05
Blood loss	20.70 ± 56.27	18.18 ± 37.19	>0.05
Pain score 24 h	1.26 ± 0.71	2.44 ± 0.70	<0.05
Bowel recovering time	1.55 ± 0.50	1.07 ± 0.26	>0.05
Hospital stay in days	3.22 ± 2.43	3.14 ± 1.38	>0.05

instruments, lack of triangulation and inline vision in the LESS group, it will take longer to get the myoma out from abdominal through uterine circumcisor in the conventional laparoscopy group. But when considering patients with peritoneal adhesions or previous abdominal surgery history, LESS surgery is supposed to be more difficult and longer OR time is needed.

We find VAS score was slightly lower in the LESS group at postoperative 24 hours for the salpingectomy, and this difference has statistical significance. Sangnier et al.'s [16] retrospective study involving 87 patients who underwent adnexal surgery indicated that there was no difference in pain scores at 2 or 24 hours after surgery. Jeong Eom's prospective case-control study which included 399 women indicated that the pain score was significantly lower in the LESS group compared with the conventional laparoscopic surgery group only at 2 hours after surgery, but no differences in VAS score at 48 and 72 hours after surgery [17]. They suspected that patient-controlled analgesia narrowed the difference in pain of the two groups. In our study, the result of postoperative pain is similar to Eom's research.

The homemade single-port has some advantages and disadvantages [18, 19]. Advantages are (1) because each trocar is not fixed on the single port, the space between the trocars is more flexible and (2) it is much cheaper than the made-up single port. The disadvantages are (1) the glove is easily broken and (2) it is not very convenient to assemble. According to our experience, after the learning curve, the conventional instruments are up to most of the surgeries.

The present study has several limitations. First, the number of patients was small, and follow-up was over the short term. Second, the differences between the preoperative and postoperative results were minimal and may have resulted from a type II error.

6. Conclusion

LESS surgery is less invasive, suitable and safe for gynecological surgery. The homemade single-port device is cheap and suitable to spread especially in the developing region.

Data Availability

The data (tables) used to support the findings of this study are included within the article and available from the corresponding author upon request.

Conflicts of Interest

The authors declare that they have no conflicts of interest.

Acknowledgments

This research was supported by the Guangdong Natural Science Fund (no. 2015A030310105) and the Guangdong Medical Science and Technology Research Fund.

References

- [1] X. Fan, K. Xu, T. Lin et al., "Comparison of transperitoneal and retroperitoneal laparoscopic nephrectomy for renal cell carcinoma: a systematic review and meta-analysis," *BJU International*, vol. 111, no. 4, pp. 611–621, 2013.
- [2] R. Autorino, J. A. Cadeddu, M. M. Desai et al., "Laparoscopic single-site and natural orifice transluminal endoscopic surgery in urology: a critical analysis of the literature," *European Urology*, vol. 59, no. 1, pp. 26–45, 2011.
- [3] D. Bansal, E. Riachy, W. R. DeFoor et al., "Pediatric varicocele: a comparative study of conventional laparoscopic and laparoendoscopic single-site approaches," *Journal of Endourology*, vol. 28, no. 5, pp. 513–516, 2014.
- [4] F. Friedersdorff, S. J. Aghdassi, P. Werthemann et al., "Laparoscopic single-site (LESS) varicocele with reusable components: comparison with the conventional laparoscopic technique," *Surgical Endoscopy*, vol. 27, no. 10, pp. 3646–3652, 2013.
- [5] S. W. Lee, J. Y. Lee, K. H. Kim, and U.-S. Ha, "Laparoscopic single-site surgery versus conventional laparoscopic varicocele ligation in men with palpable varicocele: a randomized, clinical study," *Surgical Endoscopy*, vol. 26, no. 4, pp. 1056–1062, 2012.
- [6] A. Marte, L. Pintozzi, P. Parmeggiani, and S. Cavaiuolo, "Single-incision laparoscopic surgery and conventional laparoscopic treatment of varicocele in adolescents: comparison between two techniques," *African Journal of Paediatric Surgery*, vol. 11, no. 3, pp. 201–205, 2014.
- [7] J. Wang, B. Xue, Y.-x. Shan et al., "Laparoscopic single-site surgery with a single channel versus conventional laparoscopic varicocele ligation: a prospective randomized study," *Journal of Endourology*, vol. 28, no. 2, pp. 159–164, 2014.
- [8] T. Youssef and E. Abdalla, "Single incision transumbilical laparoscopic varicocele versus the conventional laparoscopic technique: a randomized clinical study," *International Journal of Surgery*, vol. 18, pp. 178–183, 2015.
- [9] M. L. Gasparri, M. D. Mueller, K. Taghavi, and A. Papadia, "Conventional versus single port laparoscopy for the surgical treatment of ectopic pregnancy: a meta-analysis," *Gynecologic and Obstetric Investigation*, vol. 83, no. 4, pp. 329–337, 2018.

- [10] G. Demirayak, İ. A. Özdemir, C. Comba et al., "Comparison of laparoendoscopic single-site (LESS) surgery and conventional multiport laparoscopic (CMPL) surgery for hysterectomy: long-term outcomes of abdominal incisional scar," *Journal of Obstetrics and Gynaecology*, pp. 1–5, 2019.
- [11] Y. H. Park, M. Y. Kang, M. S. Jeong, H. Choi, and H. H. Kim, "Laparoendoscopic single-site nephrectomy using a home-made single-port device for single-system ectopic ureter in a child: initial case report," *Journal of Endourology*, vol. 23, no. 5, pp. 833–835, 2009.
- [12] A. Schmitt, P. Crochet, S. Knight, C. Tourette, A. Loundou, and A. Agostini, "Single-port laparoscopy vs conventional laparoscopy in benign adnexal diseases: a systematic review and meta-analysis," *Journal of Minimally Invasive Gynecology*, vol. 24, no. 7, pp. 1083–1095, 2017.
- [13] W. Xie, D. Cao, J. Yang, M. Yu, K. Shen, and L. Zhao, "Single-port vs multiport laparoscopic hysterectomy: a meta-analysis of randomized controlled trials," *Journal of Minimally Invasive Gynecology*, vol. 23, no. 7, pp. 1049–1056, 2016.
- [14] L. Yang, J. Gao, L. Zeng, Z. Weng, and S. Luo, "Systematic review and meta-analysis of single-port versus conventional laparoscopic hysterectomy," *International Journal of Gynecology & Obstetrics*, vol. 133, no. 1, pp. 9–16, 2016.
- [15] E. M. Sandberg, C. F. la Chapelle, M. M. van den Tweel, J. W. Schoones, and F. W. Jansen, "Laparoendoscopic single-site surgery versus conventional laparoscopy for hysterectomy: a systematic review and meta-analysis," *Archives of Gynecology and Obstetrics*, vol. 295, no. 5, pp. 1089–1103, 2017.
- [16] E. Sangnier, M. Lallemand, M. Gnofam et al., "Single port laparoscopy (SPL): retrospective study evaluating postoperative pain in comparison with conventional laparoscopy (CL)," *Journal of Gynecology Obstetrics and Human Reproduction*, vol. 47, no. 8, pp. 365–369, 2018.
- [17] J. M. Eom, J. S. Choi, W. J. Choi, Y. H. Kim, and J. H. Lee, "Does single-port laparoscopic surgery reduce postoperative pain in women with benign gynecologic disease?," *Journal of Laparoendoscopic and Advanced Surgical Techniques*, vol. 23, no. 12, pp. 999–1005, 2013.
- [18] L. F. Cepedal, M. P. Calvo, H. M. Ortega et al., "Glove port, how do we do it? A low-cost alternative to the single-port approach," *Surgical Endoscopy*, vol. 30, no. 11, pp. 5136–5137, 2016.
- [19] J. Y. Lee, D. H. Kang, J. H. Chung, J. K. Jo, and S. W. Lee, "Laparoendoscopic single-site surgery for benign urologic disease with a homemade single port device: design and tips for beginners," *Korean Journal of Urology*, vol. 53, no. 3, pp. 165–170, 2012.

Research Article

Treatment of Large and Complicated Scalp Defects with Free Flap Transfer

Fanfan Chen,¹ Hongbin Ju,² Anfei Huang,³ Yongjun Yi,² Yongfu Cao,² Wei Xie,² Xinliang Wang ² and Guo Fu ³

¹Department of Neurosurgery, The Second People's Hospital of Shenzhen, Shenzhen, Guangdong 518035, China

²Department of Orthopaedics, Guangzhou First People's Hospital, Guangzhou, Guangdong 510180, China

³Department of Spine and Orthopedic Trauma, The First Affiliated Hospital of Jinan University, Guangzhou, Guangdong 510630, China

Correspondence should be addressed to Xinliang Wang; wxl_371543582@qq.com and Guo Fu; drfuguo@hotmail.com

Received 14 November 2019; Accepted 18 December 2019; Published 10 January 2020

Guest Editor: Peng Bao

Copyright © 2020 Fanfan Chen et al. This is an open access article distributed under the Creative Commons Attribution License, which permits unrestricted use, distribution, and reproduction in any medium, provided the original work is properly cited.

Background. Large scalp defects, especially those complicated by calvarial defects, titanium mesh exposure, or cerebrospinal fluid (CSF) leak, pose a challenge for the neurosurgeon and plastic surgeon. Here, we describe our experience of reconstructing the complex scalp defect with free flap transfer. **Methods.** From October 2012 to September 2017, 8 patients underwent free flap transfer for the reconstruction of the scalp or complicated scalp and calvarial defects. Five patients presented with scalp tumor and the other 3 patients with scalp necrosis or ulceration (2 patients with titanium plate exposure). Seven anterolateral thigh flaps and one radial forearm flap were harvested and employed. The clinical data, including defect characteristics, flap type, complications, and outcomes, were recorded and analyzed. **Results.** Five patients were pathologically diagnosed with malignant tumor, and 3 of them were given further radiotherapy. For the 2 patients with exposure of titanium plate, no titanium plate was removed. For the patient with scalp necrosis after decompressive craniectomy accompanied by CSF leakage, the CSF leak was stopped after reconstruction. The size of the flaps ranged from 3 to 14 cm in width and 4 to 18 cm in length. No flap failure occurred in these cases. From follow-up to the present, no ulceration or necrosis occurred. **Conclusions.** Free flap transfer is an ideal method for the reconstruction of large, complicated scalp defects with a one-stage operation. The anterolateral thigh flap is favored because of its durability, adjustability, water tightness, and infection prevention.

1. Introduction

Large scalp defects are usually secondary to a variety of diseases, such as tumor resection, trauma, infection, and congenital lesions [1, 2]. Reconstruction of the defects should take a comprehensive consideration of size, location, radiation history, and potential for hairline distortion [3]. When the scalp defect is accompanied by a calvarial or dural defect, for example, from scalp and skull bone excision due to tumor invasion, scalp necrosis after decompression surgery, scalp atrophy, or necrosis after titanium plate implant, more related factors affect the therapeutic strategy. The soft tissue coverage of the defect areas, maintaining the enclosed space for the intracranial contents, sealing the

leakage of the cerebrospinal fluid (CSF), and endurance to radiation are all common concerns. This is a challenge for neurosurgeons and plastic surgeons and requires close collaboration between them.

The reconstructive ladder of scalp defects includes primary closure, split-thickness skin graft, local flap, rotated local flap and skin graft, and free flaps. For the large size of soft tissue defects on the scalp, reconstruction with local flap is restricted to the inelasticity and rotation angle. Free flap is the only available method to cover the defect. Currently, there is a lack of consensus regarding which procedure is superior in large and complicated scalp reconstruction. In this retrospective study, we present our experience with the reconstruction of scalp defects with free flap transfer. The

patients and defect conditions, reconstructive options, advantages of free flap transfer, and complications are described and discussed.

2. Materials and Methods

2.1. Patient Data. This retrospective study was approved by the ethics committee of Guangzhou First People's Hospital. All the patients provided written informed consent for the use and publication of data for research purposes. Eight patients with scalp defect underwent free flap reconstruction in Guangzhou First People's Hospital from October 2012 to September 2017 (Table 1). Four men and 4 women were enrolled in this research. The patients' ages ranged from 27 to 70 years (mean, 50 years; median, 51 years). Five patients were diagnosed with scalp tumor (Figures 1(a) and 2(a)). Two patients presented with ulcer of the scalp with titanium plate exposure (Figure 2(d)). The remaining 1 patient had scalp necrosis after decompressive craniectomy accompanied by CSF leakage. The area of the defect was located in the forehead region (1 case), the frontoparietal region (1 case), the frontal region (1 case), the lateral occipital region (1 case), the parietal to occipital region (2 cases), and the temporal region (2 cases).

2.2. Surgical Technique. All the patients received a routine preoperative examination. No signs of general or local infection were found. For the patients with scalp malignancies, tumor infiltration of the periosteum or skull was evaluated, and excision of the skull bone was performed accordingly. For the cases of titanium mesh exposure or scalp necrosis, thorough debridement and excision of the nonvascularized tissue were accomplished. All the reconstructive procedures were performed by the same surgeon. An anterolateral thigh (ALT) fasciocutaneous flap was employed in 7 patients (Figures 2(b) and 2(c)) and a radial forearm flap was used in 1 patient (Figures 2(e) and 2(f)). The facial artery and facial vein were anastomosed with the vessel pedicle of the flap passing through the subcutaneous tunnel in 6 cases. Branches of the external carotid artery and superficial temporal artery were used as the recipient artery in 1 case. The muscular component was not harvested in most cases. When elimination of "dead space" was necessary, proper bulk of muscle was preserved (Figure 1(c), arrow). The superficial temporal artery and vein were used in 1 case. The follow-up period was 3 to 36 months.

3. Results

The pathology of 5 cases diagnosed as malignant scalp tumor included squamous cell carcinoma (2 cases), basal cell carcinoma (2 cases), and adenocarcinoma (1 case). Two patients underwent partial calvarial excision and titanium mesh implantation, as the skull was invaded by the tumor. Three patients (including the 2 patients with titanium mesh) were treated with further radiotherapy, and the other 2 patients refused radiotherapy. The ALT flaps were used in 7 patients, and the radial forearm flap was employed in 1 case. The size of the flaps ranged from 3 to 14 cm in width and 4 to

18 cm in length. Fasciocutaneous flaps were harvested for reconstruction. The remaining 3 patients, 2 patients with titanium mesh exposure and 1 patient with scalp necrosis and CSF leak after decompressive craniectomy (Figure 3(a)), were reconstructed with fasciocutaneous flap as well. The patients were followed-up from 3 to 36 months. No major complications such as flap failure, vascular pedicle thrombosis, necrosis, or ulceration after radiation occurred. The survival rate of the flaps was 100%. Wound dehiscence was found in 2 cases, and the incisions healed after local resuturing. The patient with CSF leak had resolution of the leak after flap reconstruction. No secondary infection occurred. Neither CSF leakage nor extradural effusion was found. The donor site defects of 6 patients were primarily closed, and 2 patients received split-thickness skin grafting.

3.1. Case 1. A 62-year-old woman was diagnosed with adenocarcinoma with tumor invasion of the right mastoid and occiput (Figure 1(a)). An extensive excision of the tumor, underlying the skull bone and regional lymph node, was performed with titanium mesh implantation (Figure 1(b)). An ALT flap (13 × 15 cm) was used to cover the scalp defect (Figures 1(c) and 1(d)). The patient subsequently underwent radiotherapy, and within the 12-month follow-up period, no tumor relapse or flap abnormality were found (Figure 1(e)).

3.2. Case 2. A 54-year-old woman in a persistent vegetative state had scalp necrosis at the incision of a previous decompressive surgery (Figure 3(a)). A CSF leak was found along the lesion, but no general or local infection was found. A thorough debridement of the lesion was performed before an ALT flap (7 × 12 cm) was used to reconstruct the defect (Figure 3(b)). The CSF leak was stopped postoperatively, and the condition of the flap was uneventful in the 9-month follow-up period (Figure 3(c)).

4. Discussion

Large full-thickness scalp defects are a refractory problem for treatment due to the low elasticity of the scalp. Primary closure or local flap transposition is insufficient for reconstruction of large defects or is prone to subsequent atrophy and ulceration due to improper tension. The detailed conditions of each patient should be taken into consideration [3]. For example, the condition of the adjacent scalp of the defect, concomitant scalp and calvarial defects, scalp defects with previous foreign material implantation, the possibility of subsequent radiotherapy, and the general condition of the patient are all closely related to the reconstructive choice. The 2 cases presented in detail were especially difficult. Of the 5 patients diagnosed with scalp tumor (including squamous cell carcinoma, basal cell carcinoma, adenocarcinoma, and dermatosarcoma), 3 of them were treated with further radiotherapy (Figures 2(a)–2(c)), and 2 of these 3 patients underwent titanium plate implantation, as the skull was invaded by the tumor. The ideal reconstructive method should be enough to cover the defect with proper tension, require the least operative time, and be durable for any

TABLE 1: Clinical data of patients.

Patient	Age	Sex	Etiology	Location	Treatment and flap	Flap size (width * length, cm)	Follow-up (months)
1	27	Male	Ulcer with titanium plate exposure	Forehead	RF flap transfer	3 * 4	3
2	64	Male	Malignant tumor	Parietal-occipital	ALT flap transfer	10 * 12	36
3	70	Female	Malignant tumor	Frontoparietal	ALT flap transfer	7 * 9	6
4	54	Male	Malignant tumor	Parietal-occipital lateral	ALT flap transfer, titanium mesh implantation	12 * 18	12
5	58	Female	Malignant tumor	occipital	ALT flap transfer, titanium mesh implantation	13 * 15	12
6	47	Female	Necrosis after decompressive craniectomy, CSF leak	Temporal	ALT flap transfer	7 * 12	9
7	38	Female	Ulcer with titanium plate exposure	Temporal	ALT flap transfer	9 * 13	12
8	41	Male	Malignant tumor	Frontal	ALT flap transfer, titanium mesh implantation	14 * 18	6

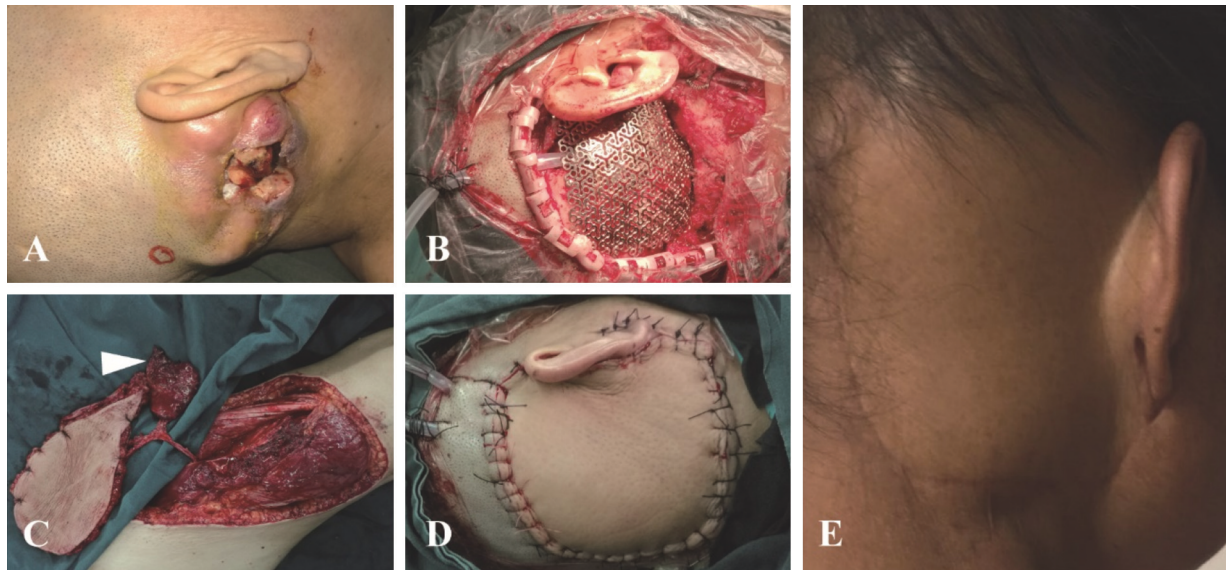


FIGURE 1: An anterolateral thigh (ALT) flap was adopted to reconstruct the complicated scalp defects of a 62-year-old female patient. (a) The lesion was located at right lateral occipital region. (b) A radical excision of the lesion, skull bone, and relevant lymph nodes was performed with a titanium mesh implanted. (c) An ALT flap was harvested with part of quadriceps to fill the dead space. (d) The postoperative image of the patient. (e) The patient received radiotherapy and the flap maintained scalp contour at 12-month follow-up.

subsequent radiotherapy. The remaining 3 patients had brain hemorrhage or brain injury followed by at least two cranial surgeries before the necrosis or ulceration of the scalp. Two patients presented with exposure of the titanium mesh (Figure 2(d)). For the patient who had not had a cranioplasty, CSF leakage occurred. This particular patient was in a persistent vegetative state and had malnutrition. Fortunately, no intracranial infection was observed in this patient. Based on all these adverse factors, reconstructive procedures must be well vascularized, watertight, and able to prevent infection [4]. Although small forehead defects can be effectively repaired by reversed temporal island flap [5], the condition of surrounding scalp, temporalis, and superficial temporal artery should be in good condition. Our patient bearing the forehead

scalp defect had previously experienced times of surgeries which resulted in a vulnerable blood supply and poor condition of nearby scalp (Figure 2(d)). Under this situation, free flap transfer offered a more stable coverage.

The microsurgical free flap transfer for the reconstruction of the scalp has developed ever since it was first performed by McLean and Buncke [6]. In its first application, an omental flap was used to reconstruct a large scalp defect. Although the omental flap was not accepted by later surgeons because of the creation of the laparotomy, the concept of free tissue transfer impressed surgeons. Various donor sites for free flap transfer were achieved and described in articles, including the latissimus dorsi musculocutaneous flap, the radial forearm flap, and the rectus abdominis

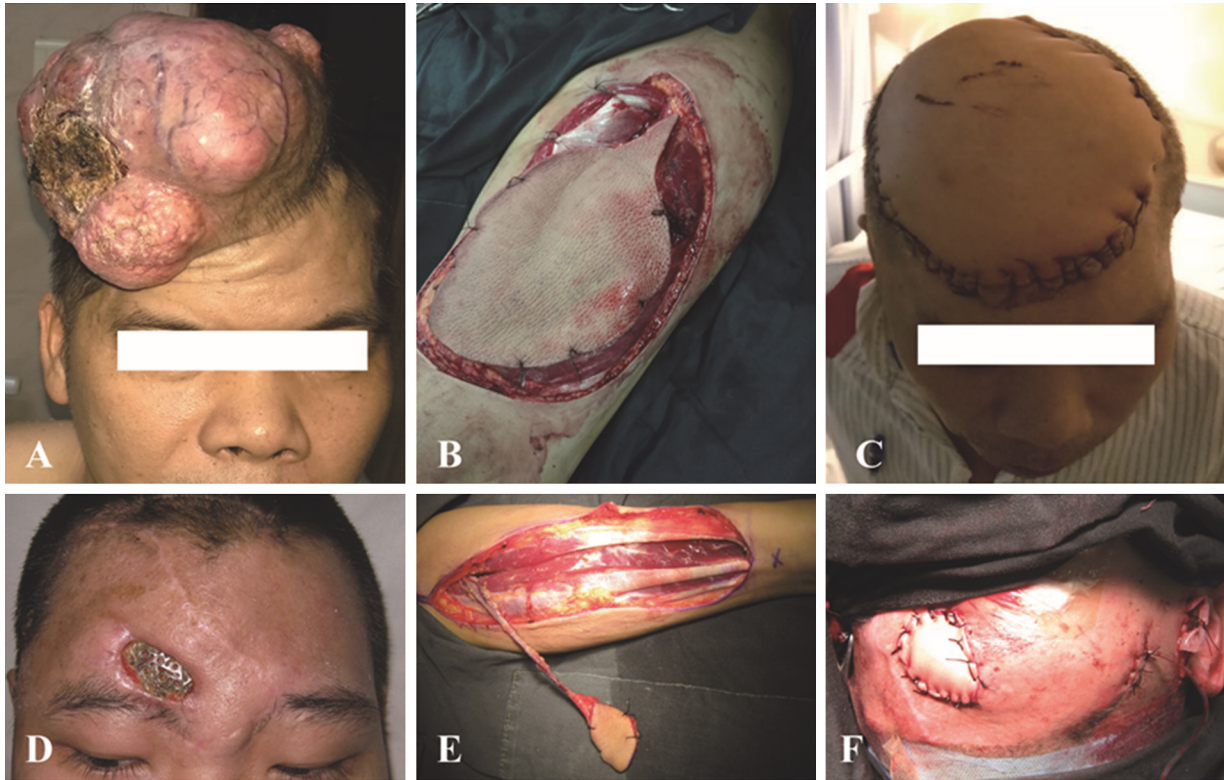


FIGURE 2: Typical cases of free flap transfer in the reconstruction of the complicated scalp and calvarial defects. (a) A patient presented with giant scalp tumor and the tumor with the invaded skull bone was resected. (b) An ALT flap was adopted to reconstruct the scalp defect (a titanium mesh was used to reconstruct the skull defect). (c) The flap maintained the scalp contour with durable coverage of the defect. (d) A patient presented scalp defect and titanium exposure. The patients experienced several operations and the situation of adjacent scalp was poor. (e) A radial forearm flap was harvested for the reconstruction. (f) The vessels of the flap were anastomosed to the right superficial temporal vessels.



FIGURE 3: An ALT flap was used to reconstruct the complicated scalp and calvarial defects of a female patient after decompressive craniectomy. (a) The patient presented with scalp necrosis and cerebrospinal fluid leak. (b) An ALT flap was used to reconstruct the defect. (c) The situation of the flap at 9-month follow-up without CSF leak.

myocutaneous flap, to name a few [7–10]. The latissimus dorsi musculocutaneous flap and radial forearm flap were popularly used before 2000, and the ALT was more frequently adopted later [11]. Skin graft and posture change during surgery are the disadvantages of the latissimus dorsi flap. As for the radial forearm flap, inadequate size for large defects is the major limitation. The rectus abdominis muscle flap was a commonly used flap, whereas donor site complications are a major shortcoming. The ALT flap has gained more attention for tissue defect reconstruction after the description of Song et al. [12], after which this type of flap was technically refined and advocated by surgeons and

widely used for reconstructive surgeries [13–16]. The advantages of the ALT flap include no requirement of position change during surgery, a long vascular pedicle with suitable size for microsurgical anastomosis, enough wide and long cutaneous area, usually direct closure of the donor-site defect, and acceptable morbidity. Moreover, the adequately vascularized fascia component of the flap is helpful to prevent CSF leakage and secondary infection [17].

Nowadays, the reconstruction of scalp defects still remains challenging. Limited sources of local or regional flaps due to the inelasticity of the scalp restrict the practice of primary closure or local flap transposition in most situations

of large scalp defects. Moreover, the compromised blood supply and quality of the adjacent scalp affected by previous surgeries limit the application of a local flap. When closing defects accompanied by titanium exposure or CSF leak, multiple-stage procedures (e.g., removing the titanium mesh and replacing it after wound healing) increase the suffering of the patient. Based on all these factors and our experience, free flap transfer is the most reliable and preferred choice in a one-stage operation.

In our study, the ALT flap was chosen in 7 of 8 cases. One patient with small defects was given a radial forearm flap (Figure 2(e) and 2(f)). The relative thinness and adjustable thickness compared with the dorsi latissimus flap are important merits that make the ALT flap adaptable for different defect depth, either a superficial scalp defect due to cranioplasty or a relatively deep defect without cranioplasty. As mentioned previously, avoiding postoperative infection from foreign matter and CSF leak are also major concerns. The ALT flap offers adequate vascularization both for the dura and the scalp, which is more effective for the prevention of infection than skin grafts or local flaps. The watertight fascia layer of the ALT fasciocutaneous flap is an ideal autologous material for sealing the CSF leak [4, 18, 19].

The complication of free flap transposition includes flap failure, vascular pedicle thrombosis, donor site hematoma, calvarial osteomyelitis, and wound dehiscence. Of our patients, no flap failure or vascular pedicle thrombosis occurred. In addition, no intracranial complications or CSF leak occurred postoperatively. Wound dehiscence occurred in 2 patients, and the wounds healed after local revision.

The limitations of this study are that the sample size is relatively small and the experience results from a single medical center. A further multicenter study may offer more powerful evidence and experience of the reconstruction of the complex scalp defects.

5. Conclusions

In summary, free tissue transfer is an excellent method for reconstruction of scalp defects, especially in complicated situations such as calvarial defects, titanium plate exposure, or CSF leakage. The ALT flap is ideal for large scalp reconstruction with the advantages of durability, adaptability, infection prevention, and watertightness.

Abbreviations

CSF: Cerebrospinal fluid

ALT: Anterolateral thigh.

Data Availability

The data supporting the findings of this study are available from Guangzhou First People's Hospital, but restrictions apply to the availability of these data, which were used under license for the current study and are not publicly available. However, the data are available from the authors upon reasonable request and with permission from Guangzhou First People's Hospital.

Ethical Approval

This retrospective study was approved by the ethics committee of Guangzhou First People's Hospital and conforms to the principles expressed in the Declaration of Helsinki.

Consent

All the patients provided written informed consent for the use and publication of data for research purposes.

Conflicts of Interest

The authors declare that they have no conflicts of interest.

Authors' Contributions

FC and HJ contributed equally to this article. XW, GF, FC, and HJ conceived and designed the work. XW, YY, YC, AH, and WX contributed to performing surgeries and the data collection. FC and HJ drafted the manuscript. XW and GF revised the manuscript critically for important intellectual content and provided comments on the structure, details, and grammar of the article. All authors read and approved the final manuscript.

Acknowledgments

This work was supported by grants from the Science and Technology Plan Projects of Guangdong Province (2016ZC0051), the Fundamental Research Funds for the Central Universities (21619419), and Health and Family Planning Commission of Guangdong Province (A2017475).

References

- [1] B. Lee, K. Bickel, and S. Levin, "Microsurgical reconstruction of extensive scalp defects," *Journal of Reconstructive Microsurgery*, vol. 15, no. 4, pp. 255–262, 1999.
- [2] N. J. P. Beasley, R. W. Gilbert, P. J. Gullane, D. H. Brown, J. C. Irish, and P. C. Neligan, "Scalp and forehead reconstruction using free revascularized tissue transfer," *Archives of Facial Plastic Surgery*, vol. 6, no. 1, pp. 16–20, 2004.
- [3] S. C. Desai, J. P. Sand, J. D. Sharon, G. Branham, and B. Nussenbaum, "Scalp reconstruction," *JAMA Facial Plastic Surgery*, vol. 17, no. 1, pp. 56–66, 2015.
- [4] F. Heller, C.-M. Hsu, C.-C. Chuang, K.-C. Wei, and F.-C. Wei, "Anterolateral thigh fasciocutaneous flap for simultaneous reconstruction of refractory scalp and dural defects," *Journal of Neurosurgery*, vol. 100, no. 6, pp. 1094–1097, 2004.
- [5] J. Zhao, G. Song, X. Zong et al., "Using the reversed temporal island flap to cover small forehead defects from titanium mesh exposure after cranial reconstruction," *World Neurosurgery*, vol. 112, pp. e514–e519, 2018.
- [6] D. H. McLean and H. J. Buncke Jr., "Autotransplant of omentum to a large scalp defect, with microsurgical revascularization," *Plastic and Reconstructive Surgery*, vol. 49, no. 3, pp. 268–274, 1972.
- [7] H. Kaplan, M. R. Wexler, M. Fiensod, and H. Kaplan, "Free groin flap for the reconstruction of the scalp following tumor resection," *Annals of Plastic Surgery*, vol. 2, no. 5, pp. 445–447, 1979.

- [8] Y. Tanaka, K. Miki, S. Tajima, J. Akamatsu, Y. Tsukazaki, and T. Inomoto, "Reconstruction of an extensive scalp defect using the split latissimus dorsi flap in combination with the serratus anterior musculo-osseous flap," *British Journal of Plastic Surgery*, vol. 51, no. 3, pp. 250–254, 1998.
- [9] E. Santamaria, M. Granados, and J. L. Barrera-Franco, "Radial forearm free tissue transfer for head and neck reconstruction: versatility and reliability of a single donor site," *Microsurgery*, vol. 20, no. 4, pp. 195–201, 2000.
- [10] H. Furnas, W. C. Lineaweaver, B. S. Alpert, and H. J. Buncke, "Scalp reconstruction by microvascular free tissue transfer," *Annals of Plastic Surgery*, vol. 24, no. 5, pp. 431–444, 1990.
- [11] K. P. Chang, C. H. Lai, C. H. Chang, C. L. Lin, C. S. Lai, and S. D. Lin, "Free flap options for reconstruction of complicated scalp and calvarial defects: report of a series of cases and literature review," *Microsurgery*, vol. 30, no. 30, pp. 13–18, 2010.
- [12] Y.-g. Song, G.-z. Chen, and Y.-l. Song, "The free thigh flap: a new free flap concept based on the septocutaneous artery," *British Journal of Plastic Surgery*, vol. 37, no. 2, pp. 149–159, 1984.
- [13] Y. Zhan, G. Fu, X. Zhou et al., "Emergency repair of upper extremity large soft tissue and vascular injuries with flow-through anterolateral thigh free flaps," *International Journal of Surgery*, vol. 48, pp. 53–58, 2017.
- [14] X. Zheng, C. Zheng, B. Wang et al., "Reconstruction of complex soft-tissue defects in the extremities with chimeric anterolateral thigh perforator flap," *International Journal of Surgery*, vol. 26, pp. 25–31, 2016.
- [15] F. Simunovic, S. U. Eisenhardt, V. Penna, J. R. Thiele, G. B. Stark, and H. Bannasch, "Microsurgical reconstruction of oncological scalp defects in the elderly," *Journal of Plastic, Reconstructive & Aesthetic Surgery*, vol. 69, no. 7, pp. 912–919, 2016.
- [16] D. Horn, R. Jonas, M. Engel, K. Freier, J. Hoffmann, and C. Freudlsperger, "A comparison of free anterolateral thigh and latissimus dorsi flaps in soft tissue reconstruction of extensive defects in the head and neck region," *Journal of Cranio-Maxillofacial Surgery*, vol. 42, no. 8, pp. 1551–1556, 2014.
- [17] G. T. Çalikapan, S. Yildirim, and T. Aköz, "One-stage reconstruction of large scalp defects: anterolateral thigh flap," *Microsurgery*, vol. 26, no. 3, pp. 155–159, 2006.
- [18] I. Koshima, H. Fukuda, H. Yamamoto, T. Moriguchi, S. Soeda, and S. Ohta, "Free anterolateral thigh flaps for reconstruction of head and neck defects," *Plastic and Reconstructive Surgery*, vol. 92, no. 3, pp. 421–428, 1993.
- [19] Ö. Özkan, O. K. Coşkunfirat, and H. E. Özgentaş, "An ideal and versatile material for soft-tissue coverage: experiences with most modifications of the anterolateral thigh flap," *Journal of Reconstructive Microsurgery*, vol. 20, no. 5, pp. 377–383, 2004.

Research Article

Cardiac Contractility Modulation Attenuates Chronic Heart Failure in a Rabbit Model via the PI3K/AKT Pathway

Qingqing Hao ^{1,2}, Feifei Zhang,² Yudan Wang,¹ Yingxiao Li ² and Xiaoyong Qi ^{1,2}

¹School of Graduate, Hebei Medical University, Shijiazhuang, 050017, Hebei, China

²Department of Cardiology Center, Hebei General Hospital, Shijiazhuang, 050051, Hebei, China

Correspondence should be addressed to Xiaoyong Qi; hbgxiaoyong_q@126.com

Received 15 October 2019; Accepted 27 November 2019; Published 9 January 2020

Guest Editor: Guo-qi Wen

Copyright © 2020 Qingqing Hao et al. This is an open access article distributed under the Creative Commons Attribution License, which permits unrestricted use, distribution, and reproduction in any medium, provided the original work is properly cited.

The Akt plays an important role in regulating cardiac growth, myocardial angiogenesis, and cell death in cardiac myocytes. However, there are few studies to focus on the responses of the Akt pathway to cardiac contractility modulation (CCM) in a chronic heart failure (HF) model. In this study, the effects of CCM on the treatment of HF in a rabbit model were investigated. Thirty six-month-old rabbits were randomly separated into control, HF, and CCM groups. The rabbits in HF and CCM groups were pressure uploaded, which can cause an aortic constriction. Then, CCM was gradually injected to the myocardium of rabbits in the CCM group, and this process lasted for four weeks with six hours per day. Rabbit body weight, heart weight, and heart beating rates were recorded during the experiment. To assess the CCM impacts, rabbit myocardial histology was examined as well. Additionally, western blot analysis was employed to measure the protein levels of Akt, FOXO3, Beclin, Pi3k, mTOR, GSK-3 β , and TORC2 in the myocardial histology of rabbits. Results showed that the body and heart weight of rabbits decreased significantly after suffering HF when compared with those in the control group. However, they gradually recovered after CCM application. The CCM significantly decreased collagen volume fraction in myocardial histology of HF rabbits, indicating that CCM therapy attenuated myocardial fibrosis and collagen deposition. The levels of Akt, FOXO3, Beclin, mTOR, GSK-3 β , and TORC2 were significantly downregulated, but Pi3k concentration was greatly upregulated after CCM utilization. Based on these findings, it was concluded that CCM could elicit positive effects on HF therapy, which was potentially due to the variation in the Pi3k/Akt signaling pathway.

1. Introduction

Chronic heart failure (CHF) is the terminal stage of various structural and functional cardiac diseases [1]. This disease can cause a progressive reduction in cardiac output since it depresses the cardiac contractility and influences the conduction pathways as well by causing a delay in the onset of right or left ventricular systole [2,3]. Although many efforts have already been attempted to treat the CHF in the past decades, such as beta-blockers of metoprolol, bisoprolol, bucindolol, nebivolol, atenolol, and carvedilol [4,5], it still is one of the most common and a complex disease to tackle, and as a result, approximately 30 percent of patients are suffering from this disease worldwide [6].

It is well known that the pathological cardiac dysfunction is contributed to myocardial hypertrophy and cell apoptosis [7], which is influenced by the Akt, a serine/threonine protein kinase, also known as protein kinase B [8]. The Akt is the effector of Pi3k and is essential during postnatal cardiac development that is achieved predominantly by hypertrophy rather than hyperplasia of individual cardiomyocytes [9]. It suggested that increasing Akt expression in cells could promote their hypertrophy and hyperplasia. The Akt also plays an important role in T-lymphocytes and prostate cells to promote lymphoma and prostate cancer [10]. Therefore, it is critical to investigate the variation in protein levels in a CHF model and then develop potential methods to prevent this disease from becoming worse.

Cardiac contractility modulation (CCM) is a series of nonexcitatory signals which can be applied during the absolute refractory period to enhance the strength of left ventricular contraction without increasing myocardial oxygen consumption [11,12]. The process of contraction force increasing is mediated by reversing the molecular remodeling and restoring the expression of several calcium-handling proteins in myocardial hypertrophy with heart failure (HF) [13]. Also, it was reported that CCM could significantly alter the cytoskeleton proteins and matrix metalloproteinases [14]. The Pi3k/Akt signaling pathway was activated by a series of internal- and external-cellular proteins via the phosphorylation at Thr 308 and Ser 473 [8]. Therefore, the effects of CCM on attenuating the CHF are possibly contributed to the variation in Akt pathway signals and related proteins. Until now, there are few studies to focus on the responses of the Akt pathway proteins to the CCM in a rabbit model with HF. In this study, the effects of CCM application in rabbits with HF on their body and heart weight, heart beating rate, collagen volume fraction, Akt, FOXO3, Beclin, pi3k, mTOR, GSK-3 β , and TORC2 expression in cardiac myocytes were investigated.

2. Materials and Methods

2.1. Animals. Thirty six-month-old healthy New Zealand white rabbits (2.5–3.5 kg) were obtained from the Experimental Animal Center of Hebei Medical University (HMU) and housed with 12-hour dark/light cycle for free access to food. This study complied with standards for the Care and Use of Experimental Animals of HMU and the Guide for the Care and Use of Laboratory Animals published by the US National Institutes of Health. All experimental procedures were approved by the Ethics Review of Lab Animal Use Application of Hebei Medical University.

2.2. Experimental Design and Management. The rabbits were randomly separated into three groups, namely, control, HF, and CCM groups, and each group contained 10 rabbits. The rabbits in the control group only received thoracotomy. The HF is characterized by the transition from an initial compensatory response to decompensation, which can be partially mimicked by transverse aortic constriction in rodent models [15]. Therefore, in the HF group, rabbits were treated by thoracotomy and ascending aortic cerclage. The rabbits in the CCM group suffered from thoracotomy, ascending aortic cerclage, and CCM application with a period of 4 weeks after HF occurred.

The rabbits in HF and CCM groups were anesthetized via the ear vein with 3% sodium pentobarbital at 1 ml/kg body weight, and their thoracic cavities were opened. Subsequently, their ascending aorta was dissected until the aorta circumference was constricted up to 60%. After 12 weeks, symptoms of heart failure occurred in the rabbits, including appetite reduction, breathing acceleration, and fewer activities. The HF model was thought to be successfully established while the left ventricular ejection fraction reached 40%.

Before the experiment, an electrode was used to deliver CCM. Specifically, one end of the electrode was sutured to the left ventricular anterior wall of rabbits, and the other end was punctured subcutaneously to the neck. Then, a cardiac stimulator (EPS320, BARD Micro-Pace, Inc., USA) was used to deliver CCM signals to the heart by sensed R-wave at the absolute refractory period. These signals consisted of biphasic square-wave pulses with phase duration of 2 ms, stimulus amplitude of 7 V, and 30 ms delay after R-wave sensing [16]. The CCM signals lasted 6 hours per day for a consecutive 4 weeks.

2.3. Sample Collection and Analysis

2.3.1. Histology and Immunohistochemistry. At the end of the experiment, all rabbits were anesthetized with 0.5 mg/g tribromoethanol. Then, the hearts were fixed in 4% paraformaldehyde solution before storage for 10 min at -20°C . The hearts were sectioned transversely across myocardial papillary muscle before completely covered by paraffin. Myocardial histologic sections (5 μm thickness) were slightly cut from the paraffin blocks and stained with 1% hematoxylin and eosin (H&E) and Masson's trichrome for 10 min at 37°C for histopathological analysis of myocardial fibrosis [17]. Afterward, all slices were fixed with 4% paraformaldehyde and photographed with a high-resolution digital microscope ($\times 400$; BX-51; Olympus, Tokyo, Japan). The collagen volume fraction (CVF) was calculated as the connective tissue areas divided by the total area of connective tissue and muscle [17].

2.3.2. Western Blot Analysis. The total protein was obtained from left ventricular myocardial tissues after extraction with the RIPA lysis buffer (P0013B, Beyotime, China). Protein concentration was measured by the Pierce™ BCA Protein Assay Kit (Thermo Scientific, USA). A total of 60 μg total protein was electrophoresed and separated with 10% SDS-PAGE and transferred onto nitrocellulose membranes (Millipore, US). After blocking with 5% fat-free milk at room temperature for 2 h, the membrane was incubated overnight at 4°C with primary antibody raised in mice against Akt (1 : 1000), FOXO3 (1 : 1000), Beclin (1 : 1000), Actin (1 : 1000), pi3k (1 : 1000), mTOR (1 : 1000), p-Akt (Ser473, 1 : 1000), GSK-3 β (1 : 1000), and TORC2 (1 : 1000). All antibodies were purchased from Cell Signaling Technology (USA). Then, the membranes were incubated with HRP-conjugated secondary antibodies (1 : 2000; Cell Signaling Technology, USA) at room temperature for two hours. The immunoreactive bands were visualized using the enhanced chemiluminescence kit (ECL Millipore Corp., Bedford, MA, USA) in a western blotting detection system (Bio-Rad, CA, USA). Developed films were scanned and Image-ProPlus 5.1 was used for quantitative analysis. In this experiment, β -actin (1 : 1500, Bioss, Beijing, China) was used as the standard and the results were expressed as density values normalized to β -actin.

2.3.3. Statistical Analysis. Data were presented as mean \pm standard deviation. The main effect of treatment was analyzed by using Mixed proc in the SAS software (SAS 9.4 version, SAS institute, USA), and the differences among groups were analyzed using the LSD test. For the heart rate, the sampling dates were treated as a repeated measurement. Shapiro–Wilk was used to test the normality assumption on the residuals of each model, while residual plots were used to verify the homogeneity of variances. When the normality assumption was not met, response variables were transformed using the Box-Cox transformation. All analyses were performed using the Mixed procedure of SAS (SAS software, version 9.4, Cary, NC, USA) at a significant level of $p < 0.05$.

3. Results

3.1. Rabbits Survival and Healthy Conditions. At the end of this experiment, 27 rabbits survived (i.e., 9 rabbits in each experimental group), which met the criteria of HF. Their weight, including body and heart weight, significantly decreased for HF rabbits when compared with those in the control group and they progressively increased after CCM application (Table 1). The CCM signals significantly decreased the heart rate of HF rabbits, and similar heart beat rates were observed between rabbits in control and CCM groups (Table 1).

3.2. Effects of CCM Utilization on Histological Changes. Regarding the heart tissue section photomicrographs of different treatments stained with H&E, we observed the slightly disordered arrangement of myocardial cells, partial myocardial necrosis, and fibrous tissue proliferation and inflammatory cells infiltration in the HF group while compared with those in the control group. These pathological variations were partly recovered after the CCM application (Figure 1(a)).

To assess the changes in cardiac interstitial fibrosis, histological sections of the heart were stained with Masson's trichrome, and the CVF were also examined. Heart tissue in the HF group rabbits presented a massive and intensive collagen accumulation when compared with those in the control group (Figure 1(b)). But, the fibrotic heart tissue area greatly decreased after CCM application. Similar results were observed for the CVF, which indicated that it significantly increased after obtaining HF and then decreased obviously after CCM signals were applied (Figure 1(c)).

3.3. Effect of CCM on Heart Tissue Protein Expressions. In this study, three isoforms of Akt, including Akt1, Akt2, and Akt3, were investigated and they showed similar tendency after CCM application (Figure 2). Results of western blot analysis showed that CCM application and HF disease significantly increased the Akt levels, which suggested that HF and CCM upregulated Akt expressions in the rabbit model (Figure 2).

Compared with the control group, the expressions of FOXO3 and Beclin increased more significantly in the HF group and their concentrations markedly decreased after

TABLE 1: Effects of cardiac contractility modulation (CCM) on the experimental rabbit body weight, heart weight, and heart rate ($n = 27$).

Group	Body weight (kg)	Heart weight (g)	Heart rate (bpm)
Control	3.2 \pm 0.4 ^{a†}	121 \pm 14 ^a	228 \pm 6 ^a
HF	2.5 \pm 0.2 ^c	86 \pm 9 ^b	258 \pm 11 ^b
CCM	2.9 \pm 0.1 ^b	111 \pm 20 ^a	240 \pm 19 ^a
ANOVA			
Treatment [‡]	0.021	0.001	0.011

Data are presented as mean \pm SEM and analyzed by Mixed Proc with SAS software. HF; heart failure. [†]Different letters in each column shows the significant differences at $p < 0.05$. [‡]Treatment included control, heart failure, and cardiac contractility modulation groups.

CCM treatment (Figures 3(a), 3(b), and 3(e)). Contrarily, Pi3k concentrations greatly decreased in rabbits of the HF group as compared with the control group, and it was significantly upregulated while the CCM signals were used to the HF rabbits (Figures 3(c)–3(e)). Compared with the control group, the mTOR, GSK-3 β , and TORC2 expressions were sharply upregulated in the HF group and then significantly downregulated after CCM was used (Figure 4).

4. Discussion

The Akt family of serine-threonine kinases participates in diverse cellular processes, including the promotion of cell survival, glucose metabolism, and cellular protein synthesis in cardiac myocytes [8]. Generally, Akt contains three isoforms of Akt1, Akt2, and Akt3. In the heart, short-term Akt1 activation promotes cardiac growth [18], whereas long-term Akt1 activation induces pathological hypertrophy [19] because overexpression of the myristoylated form of Akt1 gene induces hypertrophy, leading to heart failure [20]. Similar to Akt1, Akt3 overexpression in the heart results in progression from adaptive to maladaptive hypertrophy [21]. In the rabbit model of our study, CCM operation significantly decreased the Akt1 and Akt3 levels, which are significantly lower than those in the HF group and higher than those in the control group (Figures 2(a) and 2(c)). Additionally, our results were supported by [22] reporting that Akt2 overexpression enhanced the murine sensitivity to cardiomyocyte apoptosis in response to ischemic injury. In our results, CCM application slightly decreased the Akt2 expression when compared with the HF group (Figure 2(b)), which could be potentially beneficial for the rabbits to partly recover from HF.

FOXOs are key transcription factors involved in multiple aspects of cardiac diseases. Generally, mammalian cells contain four FOXO isoforms of FOXO1, FOXO3, FOXO4, and FOXO6, and FOXO3 is the most abundant isoform expressed in hearts [23] and its metabolism in tissues was closely related to the Akt because Akt could control FOXO3 expression in the heart [24]. Thus, cardiac regeneration may be promoted by proper control of FOXO3 activity. Overexpression of Beclin, a proautophagy protein, stimulates

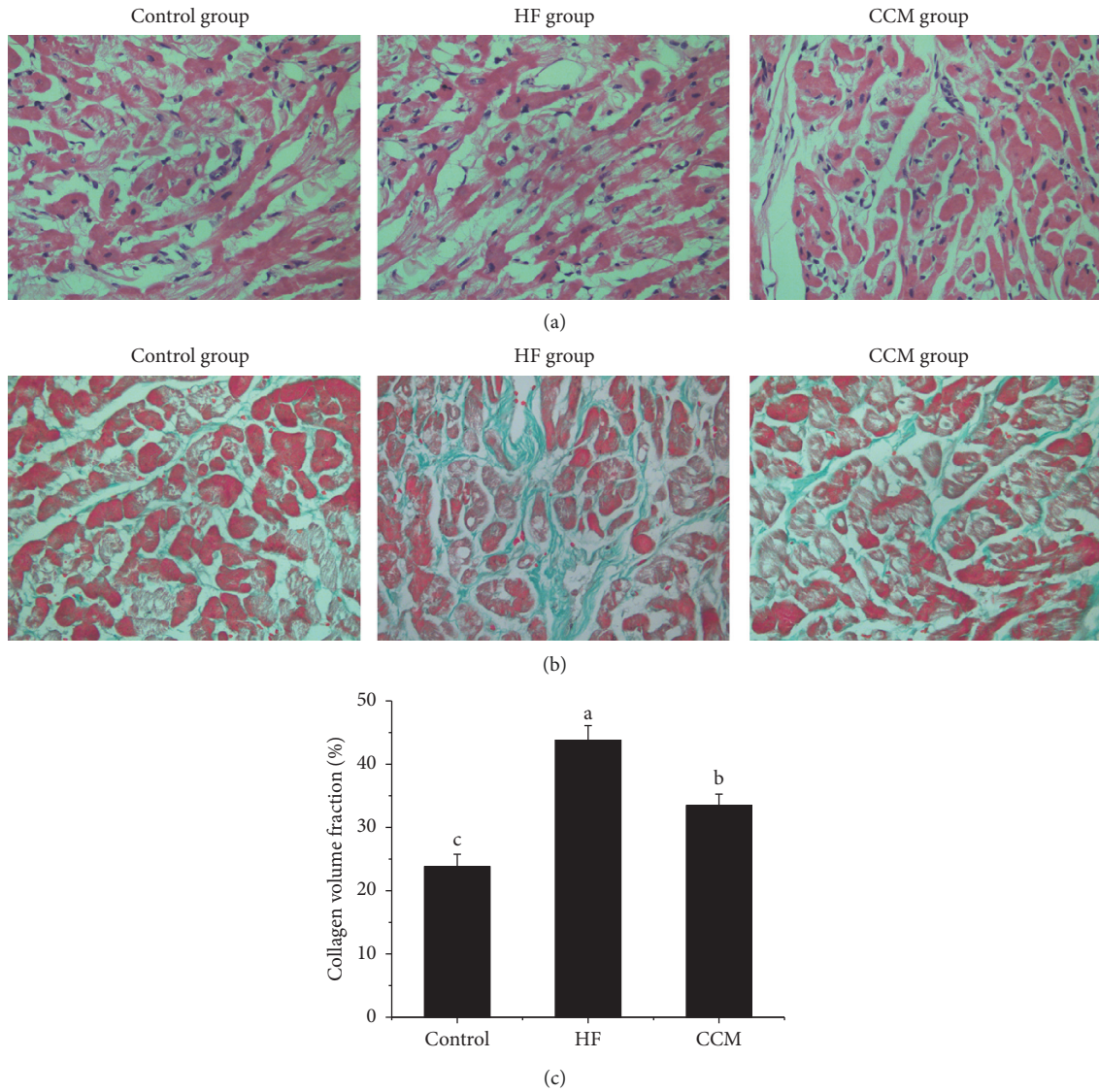


FIGURE 1: Effects of cardiac contractility modulation (CCM) on myocardial histological changes (a) and (b) microphotography (400x) of myocardial samples from experimental rabbits. (c) Collagen volume fraction of rabbit myocardial tissues with different treatments. HF, heart failure. Different letters above each boxplot showed the significant differences at $p < 0.05$.

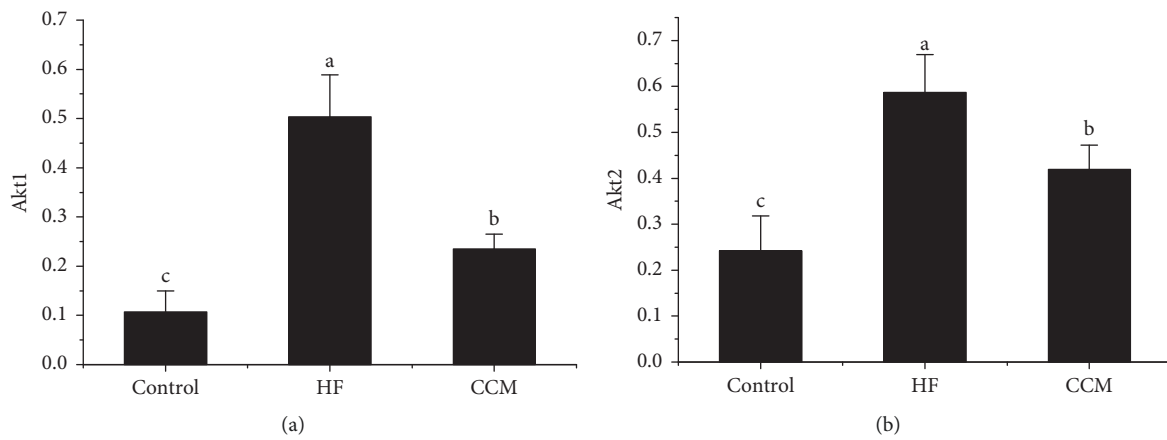


FIGURE 2: Continued.

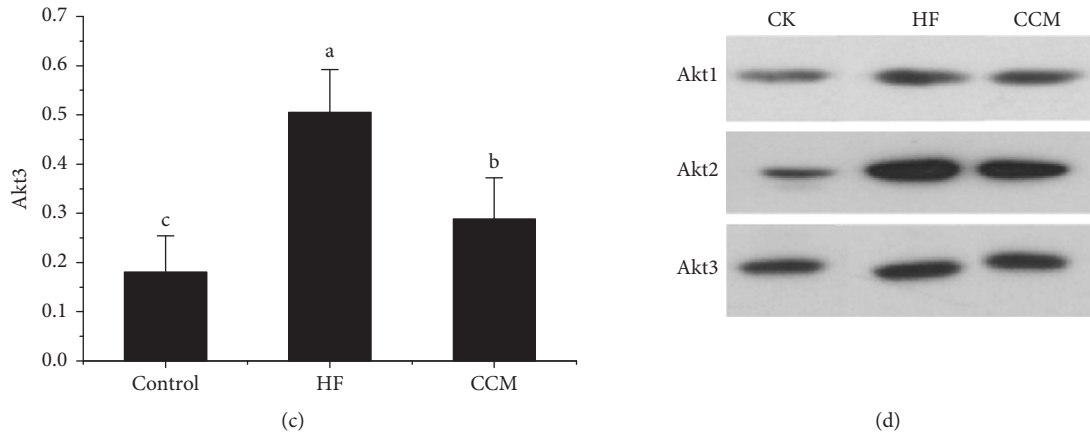


FIGURE 2: Effects of cardiac contractility modulation (CCM) on Akt1, Akt2, and Akt3 expression in different rabbit myocardial tissues under different treatments. (a) Akt1 expression; (b) Akt2 expression; (c) Akt3 expression; and (d) western blot images of Akt1, Akt2, and Akt3. CK, control group; HF, heart failure. Different lower letters above each boxplot showed the significant differences at $p < 0.05$.

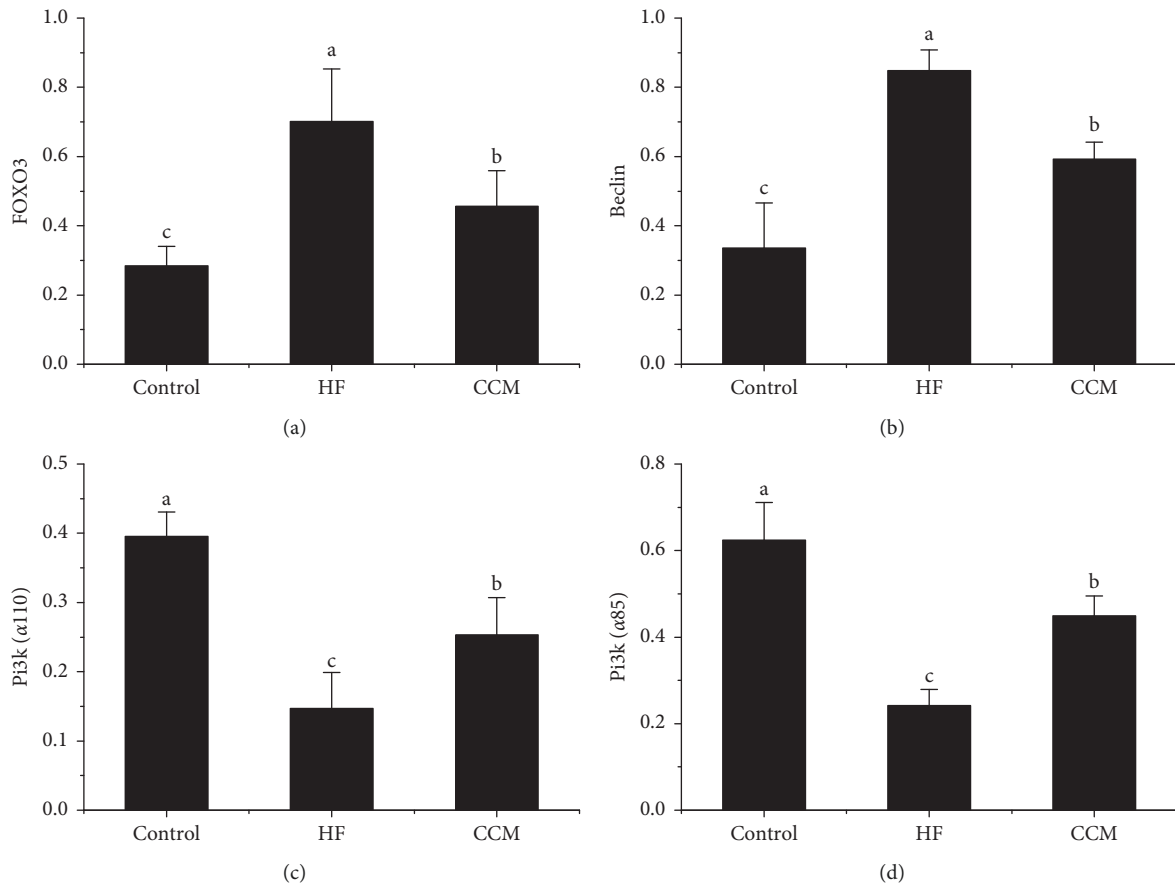


FIGURE 3: Continued.

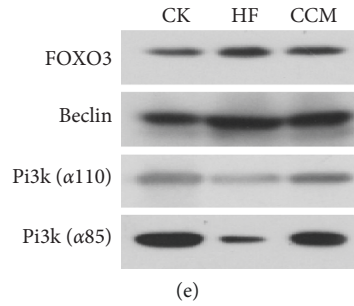


FIGURE 3: Effects of cardiac contractility modulation (CCM) on FOXO3, Beclin, Pi3k(α 110), and Pi3k(α 85) expression in different rabbit myocardial tissues under different treatments. (a) FOXO3 expression; (b) Beclin expression; (c) Pi3k(α 110) expression; (d) Pi3k(α 85) expression; and (e) western blot images of FOXO3, Beclin, Pi3k(α 110), and Pi3k(α 85). CK, control group; HF, heart failure. Different lower letters above each boxplot showed the significant differences at $p < 0.05$.

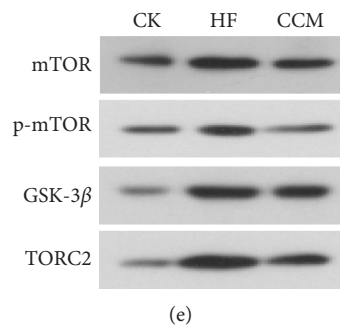
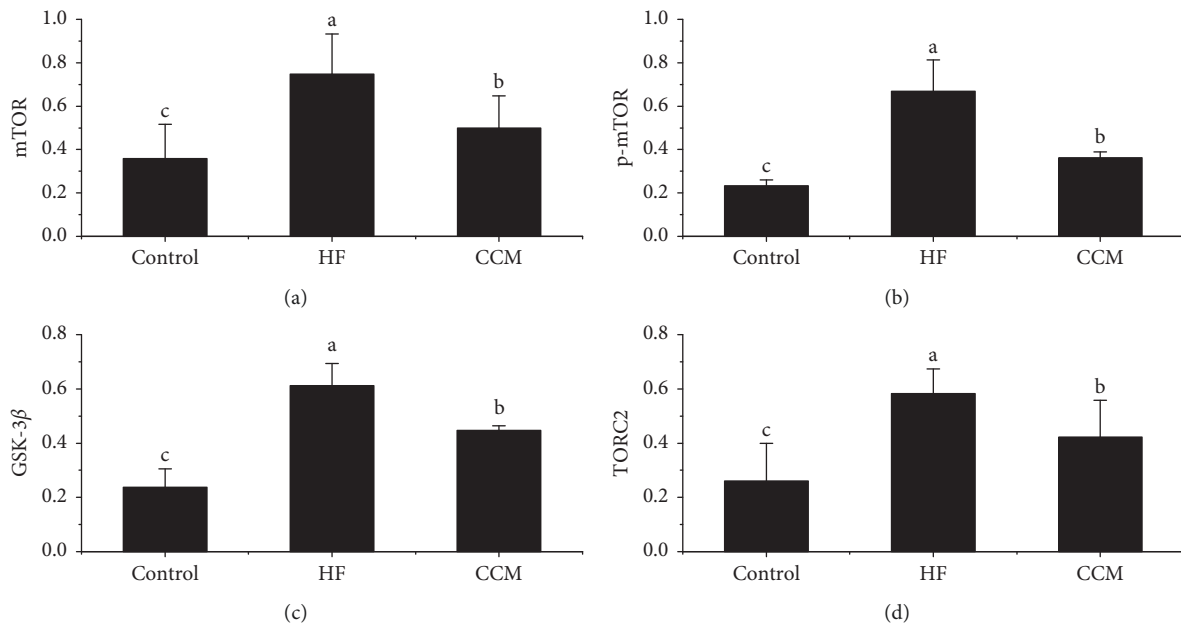


FIGURE 4: Effects of cardiac contractility modulation (CCM) on mTOR, p-mTOR, GSK-3 β , and TORC2 expression in different rabbit myocardial tissues under different treatments. (a) mTOR expression; (b) p-mTOR expression; (c) GSK-3 β expression; (d) TORC2 expression; and (e) western blot images of mTOR, p-mTOR, GSK-3 β , and TORC2. CK, control group; HF, heart failure. Different lower letters above each boxplot showed the significant differences at $p < 0.05$.

autophagy and exacerbates cardiac dysfunction and pathological remodeling [25]. In our study, higher FOXO3 and Beclin expressions were observed in rabbits with HF compared with those in the control group, and CCM signals application significantly decreased their expressions

(Figure 3). Wu et al. [26] reported that the activation of Pi3k expressions in the mouse heart could prevent cardiac remodeling. In this study, lower Pi3k expressions were observed in the HF group than in the control group, and their concentrations significantly increased in the CCM

group (Figures 3(c) and 3(d)). Combining the results of FOXOs mainly plays a detrimental role [24], and Beclin expression causes the heart dysfunction; it was concluded that CCM is a potential method to attenuate HF by adjusting FOXO3, beclin, and Pi3k expressions in cardiac cardiomyocytes.

As reported from the previous literature, the anabolic effects of Akt are mediated, in part, through activation of mammalian target of rapamycin (mTOR) [27] and inhibition of glycogen synthase kinase-3 β (GSK-3 β). Activation of mTOR stimulates protein translation through its effects on p70 ribosomal S6 kinase (p70 S6K) and eukaryotic translation initiation factor 4E binding protein-1 (eIF4E-BP) [28]. However, Akt-mediated phosphorylation of GSK-3 β [29] stimulates protein translation [30] by diminishing its inhibitory phosphorylation of eIF2B [31]. AKT (Ser473) is the downstream effector of mTORC2 [32], which means that while AKT (Ser473) is activated, suggesting that CCM could activate mTORC2 signaling. In the present study, we observed that CCM application significantly decreased the mTOR, GSK-3 β , and TORC2 expression in myocardial cells in rabbits while compared with those in the HF group (Figure 4). Based on these findings, it was concluded that CCM therapy could prevent myocardial fibrosis in heart failure which is possibly related to the change in the PI3K/AKT signaling pathway in a rabbit model.

Data Availability

The original data used to support the findings of this study are available from the corresponding author upon request.

Conflicts of Interest

The authors declare that they have no conflicts of interest.

Acknowledgments

This study was supported by the Key Project of Hebei Health Department, China (no. 20180072).

References

- [1] F. Zhang, X. Qi, Y. Li et al., "Cardiac contractility modulation improves cardiac function in a rabbit model of chronic heart failure," *BioMed Research*, vol. 28, pp. 1894–1899, 2017.
- [2] K. D. Aaronson, J. S. Schwartz, T.-M. Chen, K.-L. Wong, J. E. Goin, and D. M. Mancini, "Development and prospective validation of a clinical index to predict survival in ambulatory patients referred for cardiac transplant evaluation," *Circulation*, vol. 95, no. 12, pp. 2660–2667, 1997.
- [3] D. Farwell, N. R. Patel, A. Hall, S. Ralph, and A. N. Sulke, "How many people with heart failure are appropriate for biventricular resynchronization?," *European Heart Journal*, vol. 21, no. 15, pp. 1246–1250, 2000.
- [4] F. A. McAlister, "Meta-analysis: β -blocker dose, heart rate reduction, and death in patients with heart failure," *Annals of Internal Medicine*, vol. 150, no. 11, p. 784, 2009.
- [5] M. Packer, M. R. Bristow, J. N. Cohn et al., "The effect of carvedilol on morbidity and mortality in patients with chronic heart failure," *New England Journal of Medicine*, vol. 334, no. 21, pp. 1349–1355, 1996.
- [6] W. T. Abraham, W. G. Fisher, A. L. Smith et al., "Cardiac resynchronization in chronic heart failure," *New England Journal of Medicine*, vol. 346, no. 24, pp. 1845–1853, 2002.
- [7] R. García, J. F. Nistal, D. Merino et al., "P-SMAD2/3 and DICER promote pre-miR-21 processing during pressure overload-associated myocardial remodeling," *Biochimica et Biophysica Acta (BBA)—Molecular Basis of Disease*, vol. 1852, no. 7, pp. 1520–1530, 2015.
- [8] A. H. Chaanine and R. J. Hajjar, "AKT signalling in the failing heart," *European Journal of Heart Failure*, vol. 13, no. 8, pp. 825–829, 2011.
- [9] I. Shiojima and K. Walsh, "Regulation of cardiac growth and coronary angiogenesis by the Akt/PKB signaling pathway," *Genes & Development*, vol. 20, no. 24, pp. 3347–3365, 2006.
- [10] P. K. Majumder and W. R. Sellers, "Akt-regulated pathways in prostate cancer," *Oncogene*, vol. 24, no. 50, pp. 7465–7474, 2005.
- [11] W. T. Abraham, J. Lindenfeld, V. Y. Reddy et al., "A randomized controlled trial to evaluate the safety and efficacy of cardiac contractility modulation in patients with moderately reduced left ventricular ejection fraction and a narrow QRS duration: study rationale and design," *Journal of Cardiac Failure*, vol. 21, no. 1, pp. 16–23, 2015.
- [12] M. Borggrefe and D. Burkhoff, "Clinical effects of cardiac contractility modulation (CCM) as a treatment for chronic heart failure," *European Journal of Heart Failure*, vol. 14, no. 7, pp. 703–712, 2012.
- [13] R. C. Gupta, S. Mishra, M. Wang et al., "Cardiac contractility modulation electrical signals normalize activity, expression, and phosphorylation of the Na⁺-Ca²⁺ exchanger in heart failure," *Journal of Cardiac Failure*, vol. 15, no. 1, pp. 48–56, 2009.
- [14] S. Rastogi, S. Mishra, V. Zacà, Y. Mika, B. Rousso, and H. N. Sabbah, "Effects of chronic therapy with cardiac contractility modulation electrical signals on cytoskeletal proteins and matrix metalloproteinases in dogs with heart failure," *Cardiology*, vol. 110, no. 4, pp. 230–237, 2008.
- [15] C. Wei, J. Qiu, Y. Zhou et al., "Repression of the central splicing regulator RBFOX2 is functionally linked to pressure overload-induced heart failure," *Cell Reports*, vol. 10, no. 9, pp. 1521–1533, 2015.
- [16] B. Ning, X. Qi, Y. Li, H. Liu, F. Zhang, and C. Qin, "Biventricular pacing cardiac contractility modulation improves cardiac contractile function via upregulating SERCA2 and miR-133 in a rabbit model of congestive heart failure," *Cellular Physiology and Biochemistry*, vol. 33, no. 5, pp. 1389–1399, 2014.
- [17] F. Zhang, Y. Dang, Y. Li, Q. Hao, R. Li, and X. Qi, "Cardiac contractility modulation attenuate myocardial fibrosis by inhibiting TGF- β 1/smad3 signaling pathway in a rabbit model of chronic heart failure," *Cellular Physiology and Biochemistry*, vol. 39, no. 1, pp. 294–302, 2016.
- [18] I. Shiojima, M. Yefremashvili, Z. Luo et al., "Akt signaling mediates postnatal heart growth in response to insulin and nutritional status," *Journal of Biological Chemistry*, vol. 277, no. 40, pp. 37670–37677, 2002.
- [19] O. J. Kemi, M. Ceci, U. Wisloff et al., "Activation or inactivation of cardiac Akt/mTOR signaling diverges physiological from pathological hypertrophy," *Journal of Cellular Physiology*, vol. 214, no. 2, pp. 316–321, 2008.
- [20] I. Shiojima, K. Sato, Y. Izumiya et al., "Disruption of coordinated cardiac hypertrophy and angiogenesis contributes to

- the transition to heart failure,” *Journal of Clinical Investigation*, vol. 115, no. 8, pp. 2108–2118, 2005.
- [21] Y. Taniyama, M. Ito, K. Sato et al., “Akt3 overexpression in the heart results in progression to adaptive to maladaptive hypertrophy,” *Journal of Molecular and Cellular Cardiology*, vol. 38, no. 2, pp. 375–385, 2005.
- [22] B. DeBosch, N. Sambandam, C. Weinheimer, M. Courtois, and A. J. Muslin, “Akt2 regulates cardiac metabolism and cardiomyocyte survival,” *Journal of Biological Chemistry*, vol. 281, no. 43, pp. 32841–32851, 2006.
- [23] K. Wang, F. Liu, L. Y. Zhou et al., “MiR-874 regulates myocardial necrosis by targeting caspase-8,” *Cell Death & Disease*, vol. 4, no. 7, p. e709, 2013.
- [24] Z. Xin, Z. Ma, S. Jiang et al., “FOXOs in the impaired heart: new therapeutic targets for cardiac diseases,” *Biochimica et Biophysica Acta (BBA)—Molecular Basis of Disease*, vol. 1863, no. 2, pp. 486–498, 2017.
- [25] H. Zhu, P. Tannous, J. L. Johnstone et al., “Cardiac autophagy is a maladaptive response to hemodynamic stress,” *Journal of Clinical Investigation*, vol. 117, no. 7, pp. 1782–1793, 2007.
- [26] J. Wu, D. Li, L. Du et al., “Ouabain prevents pathological cardiac hypertrophy and heart failure through activation of phosphoinositide 3-kinase α in mouse,” *Cell & Bioscience*, vol. 5, no. 1, pp. 1–15, 2015.
- [27] B. D. Manning and L. C. Cantley, “AKT/PKB signaling: navigating downstream,” *Cell*, vol. 129, no. 7, pp. 1261–1274, 2007.
- [28] D. C. Fingar, S. Salama, C. Tsou, E. Harlow, and J. Blenis, “Mammalian cell size is controlled by mTOR and its downstream targets S6K1 and 4EBP1/eIF4E,” *Genes & Development*, vol. 16, no. 12, pp. 1472–1487, 2002.
- [29] D. A. E. Cross, D. R. Alessi, P. Cohen, M. Andjelkovich, and B. A. Hemmings, “Inhibition of glycogen synthase kinase-3 by insulin mediated by protein kinase B,” *Nature*, vol. 378, no. 6559, pp. 785–789, 1995.
- [30] C. Rommel, S. C. Bodine, B. A. Clarke et al., “Mediation of IGF-1-induced skeletal myotube hypertrophy by PI(3)K/Akt/mTOR and PI(3)K/Akt/GSK3 pathways,” *Nature Cell Biology*, vol. 3, no. 11, pp. 1009–1013, 2001.
- [31] G. I. Welsh, C. M. Miller, A. J. Loughlin, N. T. Price, and C. G. Proud, “Regulation of eukaryotic initiation factor eIF2B: glycogen synthase kinase-3 phosphorylates a conserved serine which undergoes dephosphorylation in response to insulin,” *FEBS Letters*, vol. 421, no. 2, pp. 125–130, 1998.
- [32] Y. Li, Y. Wang, M. Zou et al., “AMPK blunts chronic heart failure by inhibiting autophagy,” *Bioscience Reports*, vol. 38, no. 4, pp. 1–8, 2018.

Research Article

Effect of Metformin on a Preeclampsia-Like Mouse Model Induced by High-Fat Diet

Fuchuan Wang ¹, Guangming Cao,² Wei Yi,¹ Li Li,¹ and Xiuzhen Cao¹

¹Department of Obstetrics and Gynecology, Beijing Di-Tan Hospital, Capital Medical University, Beijing 100015, China

²Department of Obstetrics and Gynecology, Beijing Chao-Yang Hospital, Capital Medical University, Beijing 100020, China

Correspondence should be addressed to Fuchuan Wang; wangfuchuan001@126.com

Received 6 August 2019; Revised 3 October 2019; Accepted 18 October 2019; Published 7 December 2019

Guest Editor: Peng Bao

Copyright © 2019 Fuchuan Wang et al. This is an open access article distributed under the Creative Commons Attribution License, which permits unrestricted use, distribution, and reproduction in any medium, provided the original work is properly cited.

Background. Metformin has been reported to decrease insulin resistance and is associated with a lower risk of pregnancy-induced hypertension and preeclampsia. It is widely accepted that the placenta plays a crucial role in the development of preeclampsia. Our aim is to explore the effect of metformin on preeclampsia. **Study Design.** We examined control diet-fed (isocaloric diet) pregnant mice (CTRL group), pregnant mice fed a high-fat diet (HF group), and high-fat-diet-fed pregnant mice treated with metformin (HF-M group). The HF mice were fed a high-fat diet six weeks before pregnancy to establish a preeclampsia-like model; then, the group was randomly divided into a HF group and a HF-M group after pregnancy. Blood pressure, urine protein, pregnancy outcomes, protein expression, and histopathological changes in the placentas of all groups were examined and statistically analysed. **Results.** We observed that metformin significantly improved high blood pressure, proteinuria, and foetal and placental weights in the HF-M group compared with the HF group. Metformin significantly improved placental labyrinth and foetal vascular development in preeclampsia. In addition, metformin effectively increased matrix metalloproteinase-2 (MMP-2) and vascular endothelial growth factor (VEGF) levels in the placenta. **Conclusions.** Our results suggest that metformin can improve preeclamptic symptoms and pregnancy outcomes.

1. Introduction

Preeclampsia is characterized by the onset of high blood pressure and proteinuria and results in substantial maternal and neonatal morbidity and mortality [1–3]. Type 1 and type 2 diabetes (T2DM), gestational diabetes (GDM), and polycystic ovarian syndrome (PCOS) are also risk factors for preeclampsia [4]. Specifically, women with T2DM have high rates of maternal morbidity, including gestational hypertension and preeclampsia (17–19%) [5–8]. Moreover, some reports have demonstrated that an increased body mass index (BMI) increases the risk of preeclampsia and that obesity is an important risk factor for preeclampsia [9, 10].

Metformin (1,1-dimethylbiguanide hydrochloride), an oral biguanide insulin sensitizer, is a low-cost, low-risk, effective and approved oral hypoglycaemic agent for T2DM and is an important treatment option for patients with GDM [11, 12]. An increasing number of patients with PCOS or

diabetes have used metformin during pregnancy, and researchers have found that metformin is associated with a lower risk of pregnancy-induced hypertension [11, 13]. Importantly, metformin is associated with a lower risk of neonatal hypoglycaemia and neonatal intensive care admission [14]. The available data also suggest that metformin exposure during the first trimester is not associated with major congenital malformations but reduces the risks of early pregnancy loss, preeclampsia, preterm delivery, and GDM, prevents or attenuates antipsychotic-associated weight gain, and improves conception chances and pregnancy outcomes in the presence of PCOS [14–20].

It is widely accepted that preeclampsia is associated with the two-stage model of the placenta. Extravillous cytotrophoblast invasion (EVT) of the uterine spiral arteries is limited to the superficial decidua and does not reach the myometrium, which is believed to lead to shallow implantation and hypoperfusion of the placenta during the first

stage of pregnancy. In the second and third trimesters, hypoperfusion of the placenta results in placental hypoxia and ischaemia, and the maternal-foetal interface is subjected to relatively strong oxidative stress. Subsequently, cytokines and cell debris are secreted into the circulation of the maternal blood system by the placenta, eventually leading to maternal preeclamptic symptoms and injuries to other important organs [21–25].

Although researchers have investigated the use of metformin during pregnancy, the precise role of metformin in the placenta of preeclampsia remains unknown. Moreover, it has been demonstrated that insulin resistance together with adipocyte dysfunction might be involved in the pathophysiology of preeclampsia in obese women [26–28]. A literature search revealed a study in which high-fat-diet-fed pregnant mice exhibited significantly worse glucose tolerance and insulin sensitivity than control diet-fed pregnant mice, as shown by their elevated blood glucose levels, fasting serum insulin levels, and HOMA-IR, which were also increased in the HF group compared with the CTRL group; moreover, researchers have successfully fed mice a high-fat diet to induce preeclampsia [29–31].

Increasing attention has been paid to the application of metformin during pregnancy, and many studies have been carried out; however, to our knowledge, there is no study on the effect of metformin on the placenta during preeclampsia. The mechanism of metformin in reducing the incidence of preeclampsia is still unclear. Therefore, we employed a high-fat-diet-induced mouse model of preeclampsia and administered metformin to investigate the pregnancy outcomes of preeclampsia and the histological changes in the placenta during preeclampsia. We also examined the protein levels of matrix metalloproteinase (MMP)-2 and vascular endothelial growth factor (VEGF) to confirm the possible mechanism of metformin in preeclampsia. We further explored the effect of metformin on preeclampsia and provide evidence for the use of metformin during pregnancy.

2. Materials and Methods

2.1. Establishment of Animal Model. This study was approved by the Animal Ethics Committee of the Capital Medical University Beijing Chao-Yang Hospital. Animals were given humane care in accordance with the guide for the care and use of experimental animals. Thirty-eight female, 4-week-old CD-1 mice were obtained from Weitong Lihua Experimental Animal Technology Co., Ltd. (Beijing, China) and randomly divided into the CTRL group ($n = 13$), which was fed an isocaloric stock diet (energy ratio: 12% fat, 28% protein and 60% carbohydrates), and the HF group ($n = 25$), which was fed a high-fat diet (energy ratio: 62% fat, 18% protein, 20% carbohydrates) purchased from Research Diets, Inc. (New Brunswick, USA). All animals were housed in groups of 4–6 mice per cage, under an ambient temperature of 22–26°C, a relative humidity of 50–60%, and a 12 h-12 h light-dark cycle and fed their respective diets (ad libitum). After 6 weeks, the mice were weighed and mated. Females were checked daily for postcopulatory plugs, and the presence of a plug represented day 0.5 of pregnancy. The

twenty-five HF mice were randomly divided into 2 groups, namely, the HF group and the HF-M group, starting at day 0.5 of pregnancy. Metformin was administered to the HF-M group at a daily dose of 20 mg/kg. Blood pressure was measured via the tail-cuff method using a softron BP-98A tail-cuff haemodynamometer (Softron, Tokyo, Japan) after the behaviour and heart rate of the mice had stabilized. The blood pressure is reported as the mean of at least three measurements recorded during the same session that exhibited <5% variation. Most blood pressure values were within the required range once the mice had stabilized. Urine samples were collected by the reflex voiding method at day 18.5 of pregnancy; the urinary protein level was measured using a mouse albumin ELISA quantitation set (Bethyl Corp USA); urinary creatinine was detected using mouse urine creatinine detection kits (Cayman Corp USA), according to the manufacturer's instructions. All mice were sacrificed by vertebral dislocation at day 18.5 of pregnancy. The foetal and placental weights were measured, and the placentas were removed immediately. Part of the placenta was immediately frozen and stored at –80°C, and the other part of the placenta was fixed in 10% formaldehyde.

2.2. Histological Analyses. The placental specimens were dehydrated in a graded alcohol series and embedded in paraffin. Sections were deparaffinized and stained with haematoxylin-eosin (HE) for histological examination. Twenty microscopic fields (400x) were examined using a microscope (Olympus Corp, Japan).

2.3. Immunohistochemical Analysis. Paraffin sections of the placenta were deparaffinized, rehydrated, and subjected to antigen retrieval in 0.01 M sodium citrate buffer (pH 6.0) in a microwave oven. Then, the sections were treated with 3% hydrogen peroxide to block endogenous peroxidase activity. The placental sections were subsequently incubated with primary polyclonal antibodies against laminin (Santa Cruz Biotechnology, Santa Cruz, CA, USA), diluted 1 : 100 and 1 : 50. After washing with tris-buffered saline (TBS), specific secondary antibodies were applied, and then, the sections were incubated with an avidin-biotin-peroxidase complex according to the manufacturer's instructions (ABC-peroxidase kit, Vector Labs, Burlingame, CA, USA). Finally, the sections were incubated in a solution of 0.05% 3–3'-diaminobenzidine tetrahydrochloride (Sigma Aldrich, St. Louis, MO, USA) and 0.33% hydrogen peroxide. All sections were counterstained with Harris haematoxylin, dehydrated in a graded alcohol series and in xylene, and coverslipped.

2.4. Western Blotting. The proteins of the placentas were extracted, and the protein concentration was determined with the bicinchoninic acid protein quantification method. Then, 30 µg of total protein was separated by SDS-PAGE and electrotransferred onto nitrocellulose membranes (Millipore, Bedford, MA, USA) using a semidry western blot transfer system (Bio-Rad Laboratories, Inc., Hercules, CA, USA). The membranes were incubated with primary rabbit

anti-MMP-2 monoclonal antibody (1 : 1,000 dilution), rabbit anti-VEGF monoclonal antibody (1 : 1,000 dilution) (Abcam, Cambridge, MA, USA), and anti-GAPDH (loading control, 1 : 3,000 dilution) at 4°C overnight. After washing with PBST three times, the membranes were incubated with secondary HRP-conjugated goat anti-rabbit antibody (1 : 10,000 dilution; Cell Signalling Technology, Inc.) for 2 h at room temperature. Finally, the signals were developed with a chemiluminescent ECL reagent (Millipore), and the membrane was exposed to X-ray film. The strips were analysed by scanning using Image Lab software. The ratio of the protein band density to the reference GAPDH band density was determined as the relative expression level of the target protein.

2.5. Statistical Analysis. Statistical analyses were performed by two-way ANOVA for comparisons among the 3 pregnant mouse groups, and unpaired *t* tests were used for comparisons between two groups. GraphPad Prism software, version 4.0 (GraphPad Software, Inc., San Diego, CA, USA), was used for data analysis and plotting. Data are presented as the mean \pm SD. Values of $P < 0.05$ were considered to indicate significant differences.

3. Results

3.1. Effects of Metformin on Maternal Symptoms of Preeclampsia. The blood pressure and urinary protein levels in the HF group were significantly elevated compared to those in the CTRL and HF-M groups. The blood pressure in the HF-M group began to decrease on the 12th day, compared with that in the HF group; there was a significant difference on days 12, 14, 16, and 18. Metformin improved blood pressure and urinary protein levels in the HF-M group (both $P < 0.05$) (Figure 1).

3.2. Subject Characteristics. The characteristics of the mice are summarized in Table 1.

3.3. Effects of Metformin on Maternal, Foetal, and Placental Weights. A significant difference in body weight before pregnancy was observed between the model group and the CTRL group mice ($P < 0.05$). No significant differences in body weight at day 18.5 of pregnancy were found among the three groups ($P > 0.05$). The effect of metformin on the foetoplacental unit was also examined. The foetal and placental weights of the HF group were significantly lower than those of the CTRL and HF-M groups ($P < 0.05$), but no significant difference in foetal weight was observed between the CTRL and HF-M groups ($P > 0.05$). Metformin treatment enhanced the placental and foetal weights of the HF group ($P < 0.05$). No significant difference in the average litter size was observed among the three groups (12.9 ± 0.4) (see Figure 2).

3.4. Analysis of the Placental Structure of the Pregnant Mice. We analysed the tissue structure of the placentas. HE staining of placental tissue sections showed that the overall

cross-sectional area of the placenta was obviously decreased in the HF group but was improved after metformin treatment, which is consistent with the decrease in placental weight (Figure 3(a)). We also analysed the labyrinth and sponge of the placenta. The labyrinth of the placenta in the HF group was significantly smaller (Figure 3(b)). There was no significant difference in the sponge of the placenta (Figure 3(c)). The ratio of the labyrinth to the sponge of the placenta in the HF group was significantly smaller than that in the CTRL group (Figure 3(d)). Furthermore, laminin labelling of foetal blood vessels in the foetal vascular branches of the HF group was significantly affected (Figure 3(e)). The foetal blood vessels and the maternal blood sinusoids in the labyrinth layer were marked (Figure 3(e), red indicates foetal blood vessels, and blue indicates the maternal sinusoids). Statistical analysis of the foetal blood vessel area and maternal blood sinuses showed that the maternal blood sinus area was not affected in HF mice (Figure 3(f)) but that the foetal vascular area in the labyrinth layer of the preeclamptic group was decreased to 15% of that in the CTRL group (Figure 3(g)).

3.5. Effect of Metformin on Placental Proteins. We further analysed the expression of proteins in the placenta by western blotting. Our results showed that the levels of VEGF and MMP-2 were significantly decreased in the HF group ($P < 0.05$). However, after metformin treatment, the levels of VEGF and MMP-2 in the placentas of preeclamptic mice were significantly increased ($P < 0.05$) (see Figure 4).

4. Discussion

Metformin can increase the insulin sensitivity. Studies have indicated that insulin resistance is one of the causes of preeclampsia [32]. Among studies in the literature, there is no study on metformin in preeclampsia patients. In one *in vitro* study on the prevention and treatment of preeclampsia with metformin, trophoblasts and omental vessels, isolated from the placentas of 23 pregnant women with severe preeclampsia and 25 women with normal pregnancies, were co-cultured with metformin, and researchers found that metformin could significantly improve the dysfunction in placental endothelial cells in preeclampsia, dilate and ameliorate injured vessels, and promote angiogenesis [17, 32].

Our study successfully established the signs of preeclampsia, including hypertension and proteinuria, in pregnant rats in the HF group. This is similar to the methods reported in the literature [29–31]. We also observed that the foetal weights of the preeclamptic mice were significantly lower than those of the CTRL mice, suggesting that foetal development in the preeclamptic pregnant mice was obviously delayed. This finding is completely consistent with the symptoms that we observed in patients with preeclampsia. We also found that the embryonic weight in the HF-M group increased significantly compared with that in the HF group. The weight of a new-born is an important biological parameter and reflects the growth and nutritional status of the

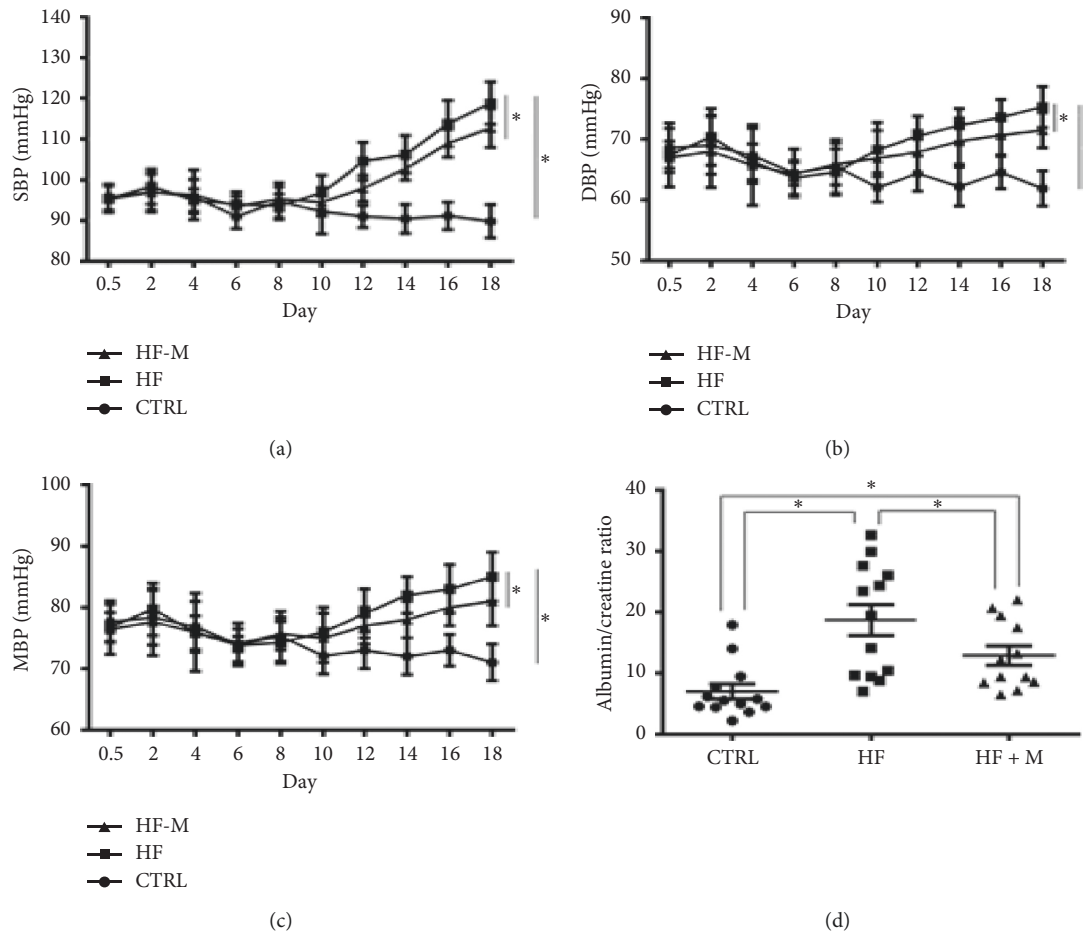


FIGURE 1: Effects of treatment with metformin on maternal signs of preeclampsia. (a) Systolic blood pressure. (b) Diastolic blood pressure. (c) Mean arterial blood pressure. (d) Urinary protein. The results are presented in mean \pm SD. * $P < 0.05$.

TABLE 1: Characteristics of the mice.

Characteristics	CTRL ($n = 13$)	HF ($n = 13$)	HF-M ($n = 12$)
Body weight before pregnancy (g)	29.38 \pm 1.44	32.92 \pm 2.50	32.50 \pm 2.24
Body weight before delivery (g)	56.08 \pm 4.29	56.30 \pm 4.33	55.08 \pm 3.53
Litter size of each group	174	175	164
Foetal weight (g)	1.06 \pm 0.19	0.95 \pm 0.17	1.02 \pm 0.16
Placental weight (g)	0.11 \pm 0.02	0.09 \pm 0.01	0.10 \pm 0.02

Data indicate the mean \pm SD.

foetus in utero. This suggests that metformin can significantly improve foetal development in preeclamptic pregnant mice.

It is well known that the majority of foetuses from preeclamptic patients show intrauterine growth restriction, and preeclampsia originates from abnormal placental development. Now, people are convinced that the placenta plays a crucial, causative role in the potential mechanism of preeclampsia. Therefore, it is now clear that preeclampsia is a placental disease. We also found that the placental weight of the HF group was significantly lower than that of the CTRL group, and the placentas of preeclamptic pregnant mice appeared retarded. The placental weight of the HF-M group dramatically increased. Nutrients are exchanged in the

labyrinth of the mouse placenta, and the maternal-foetal barrier includes two layers of syncytiotrophoblasts and foetal vascular endothelial cells.

Therefore, we analysed the placental structures of the three groups. Our results show that the area of the labyrinth and the area of the foetal blood vessels in the placenta of the HF group were significantly reduced compared with those of the normal CTRL group, but those of the HF-M group increased significantly compared with those in the HF group. These results suggest that metformin can improve the development of the labyrinth, the foetal blood vessels, and the shallow implantation of the placentas of preeclamptic mice.

It is important that further efforts be made to study the possible mechanism of metformin in preeclampsia. Therefore,

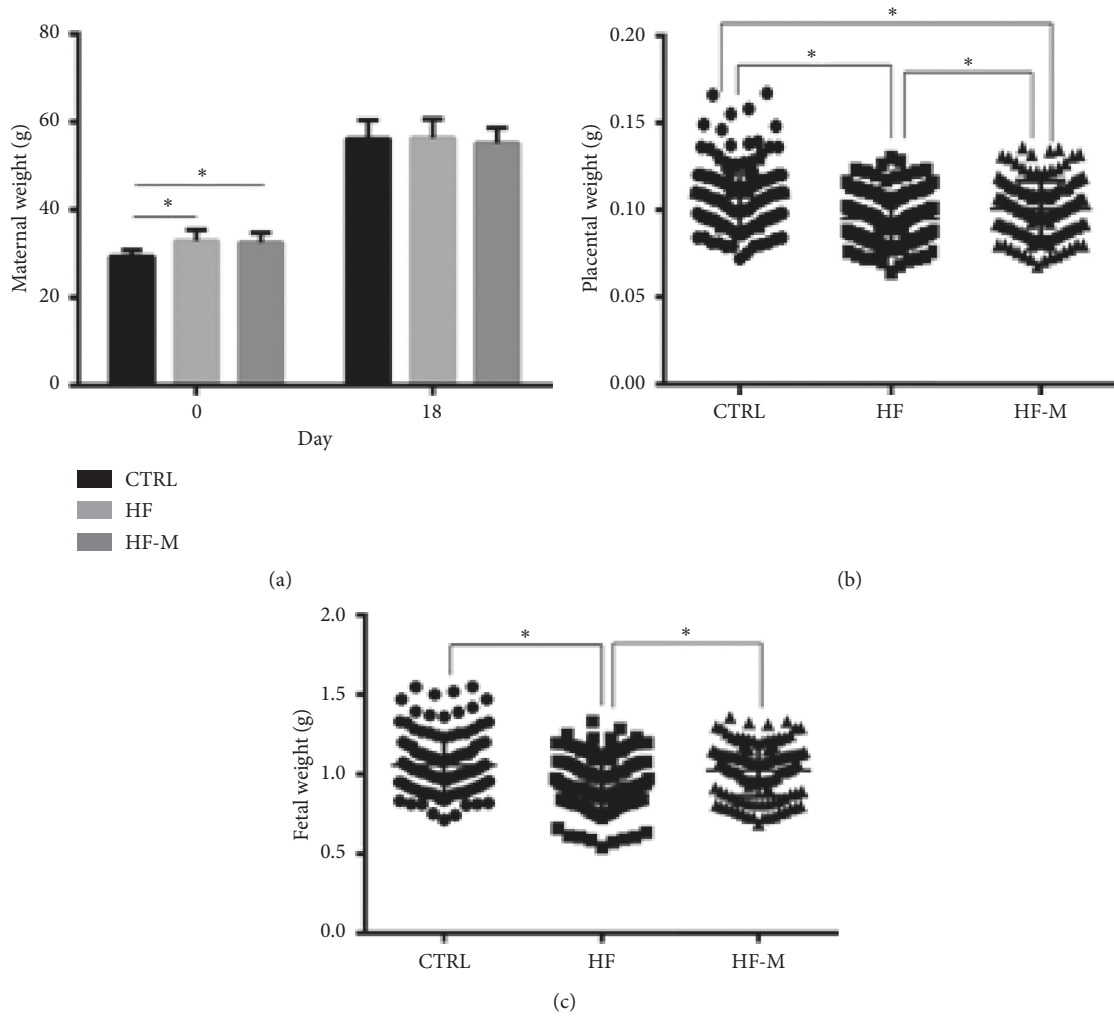


FIGURE 2: The weights of (a) the pregnant mice, (b) the placenta, and (c) the foetus at day 18.5 of pregnancy. Data are expressed as the mean \pm SD. * $P < 0.05$ between two groups.

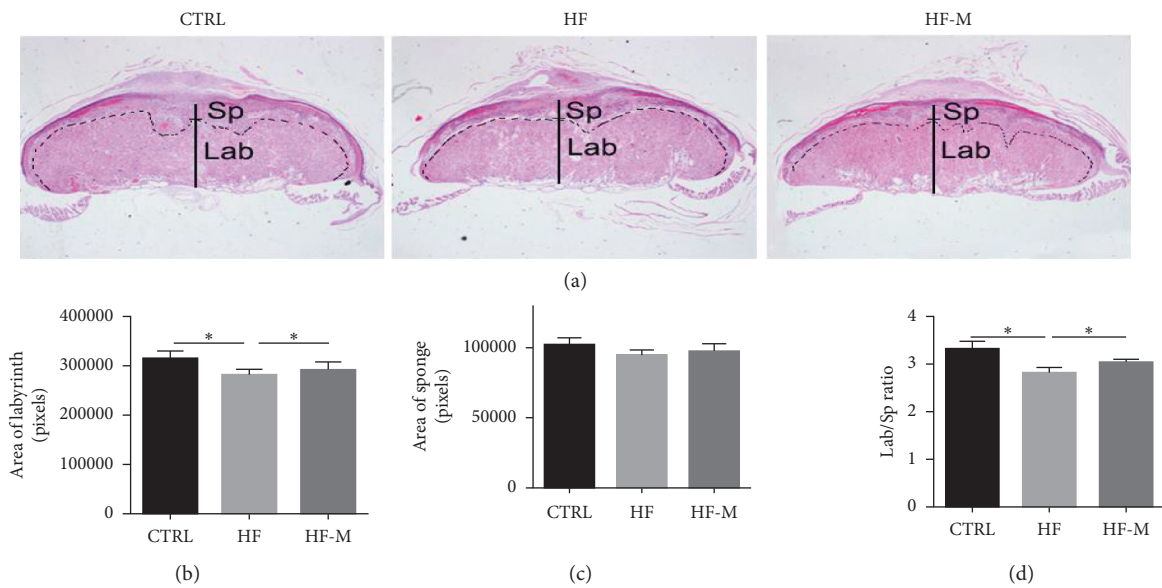


FIGURE 3: Continued.

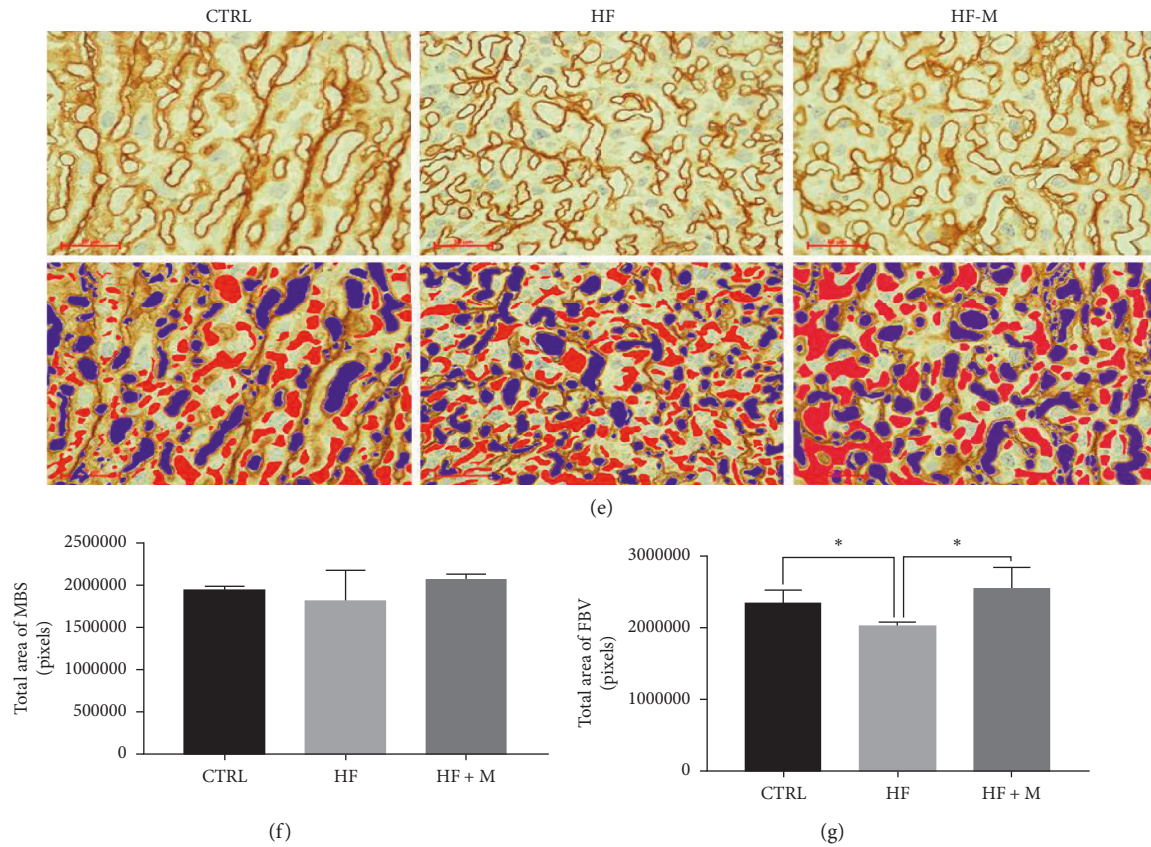


FIGURE 3: Analysis of placental structure. (a) Placental HE staining results of the three groups. The magnification is 20x in the upper panels. (b-d) Bar charts show the labyrinth and sponge of the placenta. (e) An immunohistochemical analysis of laminin in the placenta. The magnification is 400x in the panels. Pseudocolour is used to indicate foetal blood vessels (red) and the maternal blood sinusoid (blue) in the placental labyrinth. (f-g) Bar graphs show the quantitative results of the red and blue areas of all placentas in each group, indicating the area of the maternal blood sinusoid (MBS) and foetal blood vessels (FBV). The statistical analysis was based on the results of all placentas in each group. Data are expressed as the mean \pm SD. * $P < 0.05$ between two groups.

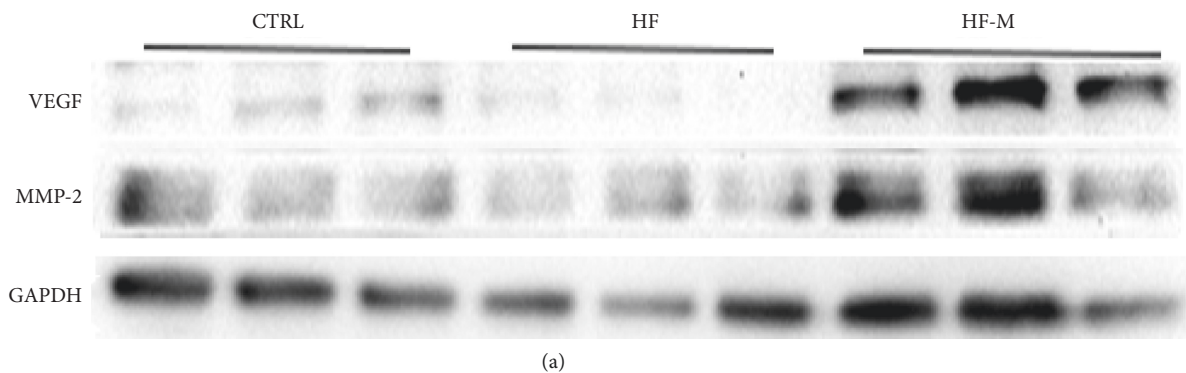


FIGURE 4: Continued.

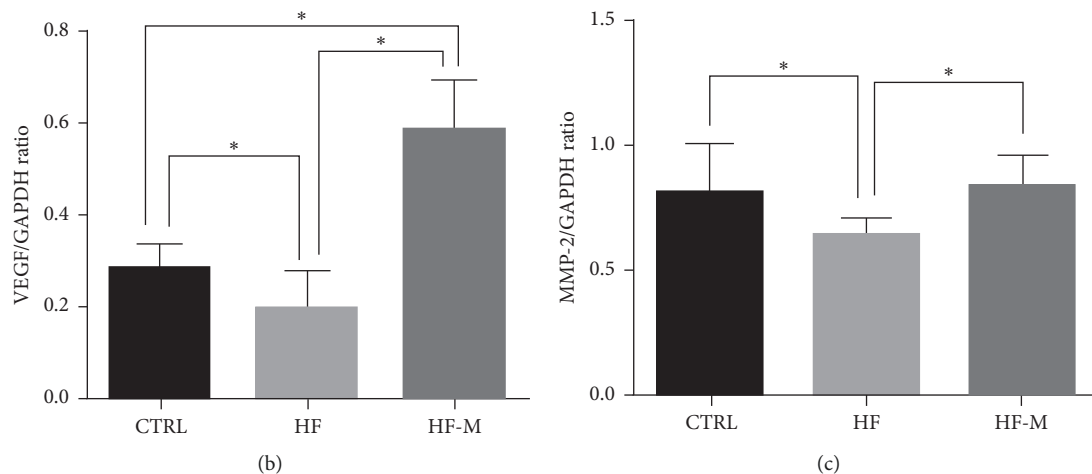


FIGURE 4: The protein expression of the placenta by western blotting. (a) Western blotting shows the relative expression of VEGF and MMP-2 in the placentas. (b-c) Bar graphs show the relative protein levels of VEGF and MMP-2 based on the statistical analysis of the western blotting results. Data are expressed as the mean \pm SD. * $P < 0.05$ between two groups.

we examined the protein levels of the cytokines VEGF and MMP-2, which have been shown to be closely related to the development of the placenta in preeclampsia, in the placental tissues of mice by western blotting [33–36]. MMP-2, also known as gelatinase A, is the most common MMP and is thought to play important roles in trophoblast invasion.

VEGF, which is indispensable for normal pregnancy, is the most important growth factor in promoting angiogenesis. First, VEGF participates in angiogenesis and placental vascular recasting. Second, VEGF plays an important role in regulating the infiltration, proliferation, and differentiation of trophoblast cells [35, 36].

We observed that the expression of VEGF and MMP-2 in the HF group was significantly decreased compared to that in the CTRL group but that the expression levels of VEGF and MMP-2 in the HF-M group were significantly enhanced compared to those in the HF group. Therefore, we speculated that metformin might promote the expression of the VEGF and MMP-2 proteins, further improve shallow placental implantation in preeclamptic mice, and eventually ameliorate the maternal and foetal outcomes of preeclamptic mice.

Our research suggests that metformin plays an important role in the regulation of placental implantation in preeclampsia. These results will provide important information on the prediction and treatment of preeclampsia.

5. Conclusion

Metformin can significantly improve placental development in preeclamptic mice, thereby improving the related symptoms of preeclampsia and maternal and foetal outcomes, including hypertension, proteinuria, and foetal birth weight.

Data Availability

The data used to support the findings of this study are available from the corresponding author upon request.

Ethical Approval

This study was approved by the Animal Ethics Committee of the Capital Medical University Beijing Chao-Yang Hospital (Beijing, China).

Conflicts of Interest

The authors declare that there are no conflicts of interest regarding the publication of this article.

Acknowledgments

The study was supported by the Sino-RUS Cooperation Funds (no. 2015DFR31070) and by the National Natural Science Funds (no. 81571455).

References

- [1] J. Uzan, M. Carbonnel, O. Piconne, R. Asmar, and J. M. Ayoubi, "Pre-eclampsia: pathophysiology, diagnosis, and management," *Vascular Health and Risk Management*, vol. 2011, no. 7, pp. 467–474, 2011.
- [2] M. L. Rosser and N. T. Katz, "Preeclampsia: an obstetrician's perspective," *Advances in Chronic Kidney Disease*, vol. 20, no. 3, pp. 287–296, 2013.
- [3] L. C. Poon and K. H. Nicolaides, "Early prediction of preeclampsia," *Obstetrics and Gynecology International*, vol. 2014, Article ID 297397, 11 pages, 2014.
- [4] J. Z. Qin, L. H. Pang, M. J. Li et al., "Obstetric complications in women with polycystic ovary syndrome: a systematic review and meta-analysis," *Reproductive Biology and Endocrinology*, vol. 11, no. 1, p. 56, 2013.
- [5] N. Anim-Nyame, S. R. Sooranna, P. J. Steer et al., "Longitudinal analysis of maternal plasma leptin concentrations during normal pregnancy and pre-eclampsia," *Human Reproduction*, vol. 15, no. 9, pp. 2033–2036, 2000.
- [6] H. R. Murphy, S. A. Steel, J. M. Roland et al., "Obstetric and perinatal outcomes in pregnancies complicated by Type 1 and Type 2 diabetes: influences of glycaemic control, obesity and

- social disadvantage," *Diabetic Medicine*, vol. 28, no. 9, pp. 1060–1067, 2011.
- [7] N. Holman, N. Lewis-Barned, R. Bell et al., "Development and evaluation of a standardized registry for diabetes in pregnancy using data from the Northern, North West and East Anglia regional audits1," *Diabetic Medicine*, vol. 28, no. 7, pp. 797–804, 2011.
- [8] K. M. Knight, E. K. Pressman, D. N. Hackney, and L. L. Thornburg, "Perinatal outcomes in type 2 diabetic patients compared with non-diabetic patients matched by body mass index," *The Journal of Maternal-Fetal & Neonatal Medicine*, vol. 25, no. 6, pp. 611–615, 2012.
- [9] R. P. Thornburg, A. Morani, A. Moriscot, U. F. Machado et al., "Insulin resistance of pregnancy involves estrogen-induced repression of muscle GLUT4," *Molecular and Cellular Endocrinology*, vol. 295, no. 1-2, pp. 24–31, 2008.
- [10] C. M. Boney, A. Verma, R. Tucker, and B. R. Vohr, "Metabolic syndrome in childhood: association with birth weight, maternal obesity, and gestational diabetes mellitus," *Pediatrics*, vol. 115, no. 3, pp. e290–e296, 2005.
- [11] S. A. Brietzke, "Oral antihyperglycemic treatment options for type 2 diabetes mellitus," *Medical Clinics of North America*, vol. 99, no. 1, pp. 87–106, 2015.
- [12] T. A. Woudes, M. Battin, S. Coat et al., "Neurodevelopmental outcome at 2 years in offspring of women randomised to metformin or insulin treatment for gestational diabetes," *The Journal of Maternal-Fetal & Neonatal Medicine*, vol. 101, no. 6, pp. F488–F493, 2016.
- [13] L.-P. Zhao, X.-Y. Sheng, S. Zhou et al., "Metformin versus insulin for gestational diabetes mellitus: a meta-analysis," *British Journal of Clinical Pharmacology*, vol. 80, no. 5, pp. 1224–1234, 2015.
- [14] P. Kitwitee, S. Limwattananon, C. Limwattananon et al., "Metformin for the treatment of gestational diabetes: an updated meta-analysis," *Diabetes Research and Clinical Practice*, vol. 109, no. 3, pp. 521–532, 2015.
- [15] M. Cassina, M. Donà, E. Di Gianantonio, P. Litta, and M. Clementi, "First-trimester exposure to metformin and risk of birth defects: a systematic review and meta-analysis," *Human Reproduction Update*, vol. 20, no. 5, pp. 656–669, 2014.
- [16] J. Kulkarni, A. Storch, A. Baraniuk, H. Gilbert, E. Gavrilidis, and R. Worsley, "Antipsychotic use in pregnancy," *Expert Opinion on Pharmacotherapy*, vol. 16, no. 9, pp. 1335–1345, 2015.
- [17] F. C. Brownfoot, R. Hastie, N. J. Hannan et al., "Metformin as a prevention and treatment for preeclampsia: effects on soluble fms-like tyrosine kinase 1 and soluble endoglin secretion and endothelial dysfunction," *American Journal of Obstetrics and Gynecology*, vol. 214, no. 3, pp. 356.e1–356.e15, 2016.
- [18] R. L. Barbieri, "Metformin for the treatment of polycystic ovary syndrome," *Obstetrics and Gynecology*, vol. 101, no. 4, pp. 785–793, 2013.
- [19] R. S. Legro, H. X. Barnhart, W. D. Schlaff et al., "Clomiphene, metformin, or both for infertility in the polycystic ovary syndrome," *New England Journal of Medicine*, vol. 356, no. 6, pp. 551–566, 2007.
- [20] J. Zheng, P. F. Shan, and W. Gu, "The efficacy of metformin in pregnant women with polycystic ovary syndrome: a meta-analysis of clinical trials," *Journal of Endocrinological Investigation*, vol. 36, no. 10, pp. 797–802, 2013.
- [21] D. Goldman-Wohl and S. Yagel, "Regulation of trophoblast invasion: from normal implantation to pre-eclampsia," *Molecular and Cellular Endocrinology*, vol. 187, no. 1-2, pp. 233–238, 2002.
- [22] C. Lam, K.-H. Lim, and S. A. Karumanchi, "Circulating angiogenic factors in the pathogenesis and prediction of preeclampsia," *Hypertension*, vol. 46, no. 5, pp. 1077–1085, 2005.
- [23] J. M. Roberts and C. A. Hubel, "The two stage model of preeclampsia: variations on the theme," *Placenta*, vol. 30, no. Suppl A, pp. 32–37, 2009.
- [24] E. S. Vashukova, A. S. Glotov, P. V. Fedotov et al., "Placental microRNA expression in pregnancies complicated by superimposed pre-eclampsia on chronic hypertension," *Molecular Medicine Reports*, vol. 14, no. 1, pp. 22–32, 2016.
- [25] J. M. Roberts and C. Escudero, "The placenta in pre-eclampsia," *Pregnancy Hypertension: An International Journal of Women's Cardiovascular Health*, vol. 2, no. 2, pp. 72–83, 2012.
- [26] K. Duckitt and D. Harrington, "Risk factors for pre-eclampsia at antenatal booking: systematic review of controlled studies," *BMJ*, vol. 330, no. 7491, p. 565, 2005.
- [27] H. Masuyama, S. Inoue, and Y. Hiramatsu, "Retinol-binding protein 4 and insulin resistance in preeclampsia," *Endocrine Journal*, vol. 58, no. 1, pp. 47–53, 2011.
- [28] H. Masuyama, T. Segawa, Y. Sumida et al., "Different profiles of circulating angiogenic factors and adipocytokines between early- and late-onset pre-eclampsia," *BJOG: An International Journal of Obstetrics & Gynaecology*, vol. 117, no. 3, pp. 314–320, 2010.
- [29] H. Masuyama and Y. Hiramatsu, "Treatment with a constitutive androstane receptor ligand ameliorates the signs of preeclampsia in high-fat diet-induced obese pregnant mice," *Molecular and Cellular Endocrinology*, vol. 348, no. 1, pp. 120–127, 2012.
- [30] M. N. Sun, Z. Yang, and R. Q. Ma, "Effect of high-fat diet on liver and placenta fatty infiltration in early onset pre-eclampsia-like mouse model," *Chinese Medical Journal*, vol. 125, no. 19, pp. 3532–3538, 2012.
- [31] H. Masuyama, T. Mitsui, J. Maki et al., "Dimethylsulfonamide ameliorates maternal glucose intolerance and fetal overgrowth in high-fat diet-fed pregnant mice via constitutive androstane receptor," *Molecular and Cellular Biochemistry*, vol. 419, no. 1-2, pp. 185–192, 2016.
- [32] M. J. Bertoldo, M. Faure, and J. Dupont, "Impact of metformin on reproductive tissues: an overview from gametogenesis to gestation," *Annals of Translational Medicine*, vol. 2, no. 6, p. 55, 2014.
- [33] O. M. Froment, M. Shokry, H. Ismail et al., "Expression of matrix metalloproteinases 2 and 9 in human trophoblasts of normal and preeclamptic placentas," *International Journal of Health Sciences (Qassim)*, vol. 5, no. 2 Suppl 1, pp. 21–23, 2011.
- [34] J. V. Cockle, N. Gopichandran, J. J. Walker, M. I. Levene, and N. M. Orsi, "Matrix metalloproteinases and their tissue inhibitors in preterm perinatal complications," *Reproductive Sciences*, vol. 14, no. 7, pp. 629–645, 2007.
- [35] S. N. Cross, E. Ratner, T. J. Rutherford et al., "Bevacizumab-mediated interference with VEGF signaling is sufficient to induce a preeclampsia-like syndrome in nonpregnant women," *Reviews in Obstetrics & Gynecology*, vol. 5, no. 1, pp. 2–8, 2012.
- [36] S. Brouillet, P. Hoffmann, J.-J. Feige, and N. Alfaidy, "EG-VEGF: a key endocrine factor in placental development," *Trends in Endocrinology & Metabolism*, vol. 23, no. 10, pp. 501–508, 2012.